Second Series *August, 1927* *Vol. 30, No. 2*

THE

PHYSICAL REVIEW

TOTAL REFLECTION OF X-RAYS AND THE INDEX OF REFRACTION OF CERTAIN METALS

By Hiram W. Edwards

Abstract

Total reflection of a beam of x-rays ($\lambda = 0.7078$A) is obtained from mirrors of glass, tin, silver, selenium, and zinc. The deviations of the reflected rays at the critical positions were measured on photographic films placed 312.5 cm from the mirrors. The index of refraction was calculated from the measured critical angle in each case, with the following results: crown glass $\delta \times 10^6 = 1.711$; tin 3.97; silver 5.78; selenium (vitreous) 2.67; and zinc 4.59. The experimental values of δ agree with those calculated by the Drude Lorentz dispersion formula to about 0.5%. It is shown in the case of the metals that there are undoubtedly in each atom 2 electrons which have the critical K absorption frequency.

THE specular reflection of x-rays from flat polished surfaces was shown by Compton[1] to take place provided the glancing angle of incidence was less than the critical angle. His observations were made on glass and speculum metal and were used to determine the index of refraction for several wavelengths. He also shows that these results are in accord with the usual electron theory of dispersion as first developed by Drude[2] and Lorentz.[3]

Other investigators have determined the index of refraction for a few substances. Webster and Clark[4] obtained a deviation of the K lines from rhodium by means of a rhodium prism. Stentrom[5] and Siegbahn[6] employed a method which depends upon the effect of refraction in producing a small deviation from Bragg's law. Von Nardroff,[7] Davis and Hatley[8] used crystal wedges which were ground and polished in such a way that the surface made a small angle with the reflecting planes. By this device they were able considerably to increase the amount of the refraction. Von Nardroff applied his results to a determination of the number of K electrons of iron and finds that for $K = 2$ the dispersion formula gives a close check upon his experimental determination of the index of refraction.

[1] Compton, Phil. Mag. **45**, 1121 (1923).
[2] Drude, "Theory of Optics" (transl.) p. 388.
[3] Lorentz, "The Theory of Electrons" 2nd. Ed. p. 149.
[4] Webster and Clark, Phys. Rev. **8**, 528 (1916).
[5] Stentrom, Dissertations, Lund (1919).
[6] Siegbahn, Comptes rendus **173**, 1350 (1921) and **174** (1922).
[7] Von Nardroff, Phys. Rev. **24**, 143 (1924).
[8] Davis and Hatley, Phys. Rev. **23**, 290 (1923) and **24**, 486 (1924).

Linnick and Lascharew[9] have described a visual method for observing the reflected beam from polished surfaces and made photographs for measuring the critical angles from glass, alum, iron, mica and quartz, using the K lines from copper ($\lambda = 1.537$A). Their optical path was too short (about 40 cm) to permit accurate determinations of the index of refraction.

The present work makes use of the total reflection method and was undertaken with the purpose of determining (1) how closely the Drude-Lorentz dispersion formula for the index of refraction would check the experimental values, (2) whether the critical absorption K frequencies of some of the metals as determined otherwise might be used in the total reflection formulas and (3) whether the number of K electrons per atom having these frequencies was 2 or some other number.

Apparatus and Experimental Procedure

The $K\alpha$ radiation from a molybdenum tube was excited in the usual manner. No attempt was made to produce a monochromatic radiation, for the shorter rays from the tube fall off before the critical angle of the $K\alpha$ lines is reached. The longer rays, only, are reflected through angles larger than the critical angle of $K\alpha$, and these are relatively so weak that no difficulty was experienced by having them present.

The reflection apparatus consisted of a 2 inch (5.1 cm) brass tube about 600 cm long, near the center of which was placed the reflecting surface. The end of the tube nearer the x-ray tube carried a narrow lead slit. Another slit was placed very close to the mirror. The mirror was mounted on the

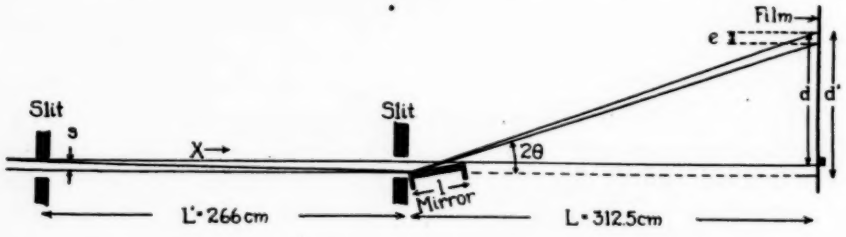

Fig. 1. Reflection of x-rays at critical position.

axis of a spectrometer table and could be rotated by a fine tangent screw through very small angles. The film was placed at the far end of the tube. Its distance from the front edge of the mirror was 312.5 cm. The whole apparatus could be operated at a reduced air pressure or filled with a light gas such as hydrogen, if desired, but it was found unnecessary to do either with the large amount of energy available. A satisfactory exposure from the best surfaces required only four minutes for a fixed position of the mirror. The approximate position of the critical angle was determined and then a longer exposure was made during which the mirror was turned successively by small amounts through the critical position.

[9] Linnik and Lascharew, Zeits. f. Physik. **38**, 659 (1926).

Measurements were made on the film from the edge of the shadow cast by the mirror in the path of the direct rays to the position in the reflected ray at which the intensity decreases abruptly. The measured distance is a little too large because the rays of the x-ray beam are not strictly parallel.

An inspection of the diagram (Fig. 1) will readily show how the following relations are obtained, from which the critical angle θ may be calculated. Since $e=sL/L'$, $d'=d+s$, $s=l \sin \theta=l\theta$, and $2\theta=(d'-e)/L$, it follows that $\theta=d/[2L-l(1-L/L')]$ when d is the deviation measured on the film and l is the length of the mirror. It is obvious that had L' been equal to L no correction would have been necessary. The second slit serves only to reduce the amount of secondary radiation produced in the long tube and hence lessens the undesirable fogging of the film.

Some of the photographic results are reproduced in Fig. 2. The sharp character of the reflected ray from an optically flat piece of glass is shown in (*a*). The mirror was moved but once in this photograph and then to another position which was slightly greater than the critical position. The decrease in intensity is prominent. This is also clearly shown in (*b*) in which case the glass mirror was turned about 3 seconds every minute.

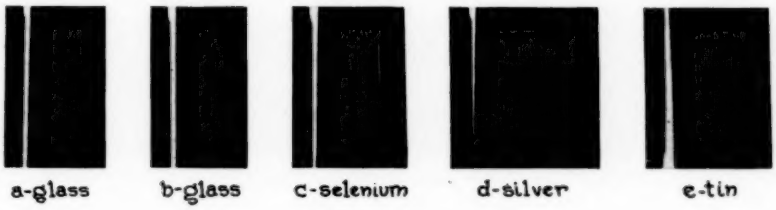

Fig. 2.

The selenium mirror was made by simply pouring hot melted selenium upon a thick piece of plate glass. The sudden cooling produces the vitreous form. The surface was very smooth except for a few small scattered pits due to gas pockets. The reproduction in Fig. 2*c* shows the trace of the reflected beam upon turning the mirror through a sufficient angle to pass through the critical position. A front surface silvered mirror was used for measuring the critical angle for silver with the result shown in Fig. 2*d*.

Considerable difficulty was encountered in producing satisfactory mirrors with tin and zinc. The final specimens were planed very carefully in a precision planing machine and then burnished or polished by hand. The surfaces obtained were not accurately flat but were highly polished. The critical edge in the reflection from tin (Fig. 2*e*) was not sharp enough to reproduce well but permitted the measurement of the deviation to a little better than 0.01 cm. The lack of sharpness is explained as due to a double reflection of some of the rays which would cause them to be reflected through angles greater than the critical angle. The final result from zinc was a little better than that from tin.

Experimental and Theoretical Results

In Table I the measured deviations are listed together with the critical angles. The index of refraction was determined from the measured critical

TABLE I

Measured values of the critical angles.

Substance	Density gm/cc	l (cm)	Measured deviation (cm)	Critical angle (rad.)
Glass (crown)	2.58	5.0	1.155 ±.003	.00185
Tin	7.30	4.5	1.76 ±.01	.00282
Silver	10.5	3.5	2.124 ±.003	.00340
Selenium (vitreous)	4.25	5.0	1.444 ±.005	.00231
Zinc	7.10	5.0	1.89 ±.01	.00303

angle by using the relation $\delta = 1 - \mu = \frac{1}{2}\theta^2$ where μ is the index of refraction. The values of δ are tabulated below in Table II.

Making use of the Drude-Lorentz dispersion formula

$$\delta = \frac{e^2 n}{2\pi m}\left[\frac{K}{\nu_0^2 - \nu_K^2} + \frac{Z-K}{\nu_0^2}\right]$$

we may calculate δ. Here e and m are the charge and mass of the electron, with n the number of atoms per cc, Z the atomic number, and K the number of K electrons per atom.

The K critical absorption wave-lengths as determined by Blake, Duane and Hu[10] were used for determining ν_K. The frequencies of all the other electrons are so small in comparison with that of the incident radiation that they may be neglected. In the case of glass the K frequencies of the constituent elements are also small enough to be neglected, except for those of barium, zinc and arsenic, which elements occur in relatively small quantities and hence the effects of their K electrons are negligible. The values of δ were calculated for $K = 1$, 2 and 3. Each result is tabulated below.

TABLE II

Values of $\delta \times 10^6$.

Substance	Experimental value	Calculated values $K=1$	$K=2$	$K=3$
Glass	1.711	1.717	(K frequencies neglected)	
Tin	3.97	4.07	3.95	3.81
Silver	5.78	5.990	5.749	5.496
Selenium	2.67	2.573	2.654	2.734
Zinc	4.59	4.52	4.58	4.65

It is readily seen upon comparing these results with the experimental value of δ in the case of each of the metals that K is undoubtedly equal to 2. It is also to be concluded that the K critical absorption frequencies function in the phenomenon of reflection.

Appreciation of the skill and patience of Mr. Thomas Watson, University mechanic, in preparing the metal mirrors is gratefully acknowledged.

UNIVERSITY OF CALIFORNIA AT LOS ANGELES,
April 15, 1927.

[10] Blake, Duane and Hu, Phys. Rev., July and Dec. 1917; June 1918 and Dec. 1919.

ELECTRICAL PROPERTIES AND NATURE OF ACTIVE NITROGEN

By Philip A. Constantinides

Abstract

Source of currents between electrodes in active nitrogen.—Glowing active nitrogen from an electrodeless discharge tube was drawn in succession through two sets of coaxial cylindrical electrodes. The current between the electrodes of the second set was found to remain constant when the potential between the electrodes of the first set was varied from 0 to 250 volts. This indicates that the conductivity is not due to ions drawn from the discharge chamber. By varying the ratio of the areas of the second set of electrodes it was established that the saturation currents were proportional to the area of the negative electrode. It is concluded that the current between electrodes in active nitrogen is due to electrons emitted from the surfaces of the electrodes either photoelectrically or by direct action of the active nitrogen on the metal. The form of the current-potential curves indicates that the electrons are emitted with relatively high velocities.

Effect of He, N_2, H_2, O_2 on the duration of the afterglow.—Helium did not affect the afterglow up to pressures ten times that of the nitrogen. The other gases shortened the afterglow in the order named.

Ionization of foreign gases by active nitrogen.—It was found that active nitrogen did not ionize hydrogen or mercury vapor. Indications of ionization of iodine vapor were obtained. This suggests that the molecule of active nitrogen is N_2 in a metastable state with energy between 9.4 and 10.4 volts.

Introduction

IN THE year 1900, E. P. Lewis[1] described an afterglow obtained in nitrogen when a condensed discharge with spark gap was used. It is to R. J. Strutt,[2] however, that we owe perhaps the most systematic study of the physical and chemical properties of what he calls "the active modification of nitrogen" or, simply, "active nitrogen" produced when nitrogen is subjected to a condensed discharge. Nitrogen, whatever the source or method of its production, under the proper conditions emits an afterglow, the intensity and duration of which is governed by factors whose exact determination has been the subject of long discussions and tedious experiments. One question of interest was that of the degree of purity of the nitrogen necessary for the production of the afterglow. At first it was thought that the afterglow could be produced in very pure nitrogen as well as in nitrogen containing a certain amount of impurities. However, Compte,[3] Tiede,[4] Domcke, and Pirani,[5] showed that it is impossible to produce the glow in very pure

[1] E. P. Lewis, Astrophys. J. **12**, 219 (1900); Ann. d. Physik **2**, 249 (1900); Astrophys. J. **20**, 49 (1904); Phys. Rev. **1**, 469 (1913); Nature **111**, 599 (1923).

[2] R. J. Strutt (now Lord Rayleigh), Proc. Roy. Soc. **A85**, 219 (1911); ibid, **A86**, 56 (1911–12); ibid, **A86**, 262 (1911–12); ibid, **A87**, 179 (1912); ibid, **A88**, 539 (1913).

[3] F. Compte, Phys. Zeits. **14**, 74 (1913).

[4] Tiede, Ber. d. D. Phys. Ges. **46**, 4065 (1913).

[5] Pirani, Chemical Abstracts, 157 (1923).

nitrogen. The remarkable conductivity of active nitrogen is also of interest. Strutt, in a series of papers, describes a number of experiments conducted in connection with the determination of the electrical conductivity of glowing nitrogen. He does not, however, arrive at a definite conclusion concerning the cause of the ionization or nature of the conductivity. It was thought that this question demanded further investigation; furthermore, the determination of the mechanism of ionization in active nitrogen could possibly be of assistance in the better understanding of its physical and chemical properties.

I. Electrical Properties of Active Nitrogen

(A) *Method of activation.* It is possible to activate nitrogen in several ways,[6] but the simplest and best recognized of all are those of the condensed electric discharge with spark gap, and the electrodeless discharge. By the first method the active nitrogen is produced by introducing nitrogen at low pressure into a discharge tube whose electrodes, made of aluminum, platinum or tungsten, are attached to the secondary terminals of a large induction

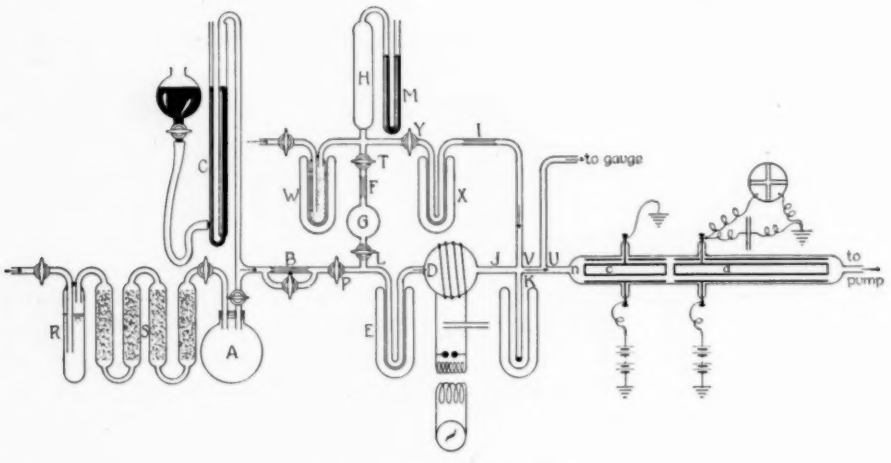

Fig. 1. Diagram of apparatus.

coil or to the terminals of a 2200 volt alternating current transformer. By the second method, nitrogen is introduced at low pressure into a glass bulb around which are wound a few turns of well insulated wire connected in series with a condenser of suitable capacity and then to the secondary terminals of a high tension transformer. The spark gap is connected in parallel with the coil.

In the experiments to be described below, the second method was used. The Pyrex glass bulb *D* (see Fig. 1) was 8 cm in diameter. The Thordarson transformer was rated at 24000 volts, 60 cycles, 1 K.W. The coil had four turns and the capacity consisted of nine 12 by 14 in. glass plates of $\frac{1}{4}$ in.

[6] Nitrogen in the proximity of radioactive substances presents the chemical activity characteristic of active nitrogen.

thickness, the sides of which were coated with 10 by 12 in. tin-foil sheets. The condenser plates were connected in parallel and immersed in transformer oil. The nitrogen used was supplied from a compressed nitrogen gas tank (manufactured by Tilden Air Products). At first it was freed from traces of oxygen by passing through five bottles *R* containing alkaline pyrogallol solution (22% aqueous solution of pyrogallol mixed with five or six times as much potassium hydroxide solution (3:2)) through drying tubes *S* containing phosphorous pentoxide, potassium hydroxide and calcium chloride. Later it was found that the commercially prepared nitrogen was sufficiently free from oxygen and could be used without passing through the pyrogallol solution without any perceptible dimunition of the intensity and duration of the afterglow. The uniform flow of the gas through the bulb was regulated by introducing the gas into a reservoir *A* of considerable size and then through a capillary tube *B* to the bulb *D*. The reservoir *A* was connected to a graduate manometer *C* which kept the pressure within *A* constant. Changes in volume could be measured with a precision of 0.1 cc. The pressure within *A* was kept at 80 cm of mercury. The intensity of the afterglow in the bulb was found to be greatest at a pressure of 0. 7 mm. The color of the afterglow at that pressure was deep yellow. The range of pressures between which the activation was satisfactory was from 1 mm to 0.5 mm. With pressure above 1 mm the nature of the discharge changed and no afterglow or ionization could be observed. Below 0.5 mm pressure the glow was a faint yellow and of shorter duration, due, apparently, to the faster diffusion of the active gas to the walls of the vessel.

(B) *Electrical properties*. In order to determine directly that the ionization is not due to the survival of ions produced during the discharge, the active nitrogen was drawn through two sets of electrodes (see Fig. 1), each one consisting of two coaxial cylinders. The *c* electrodes were used as an ion trap and were 50 cm long, the diameters of the coaxial cylinders being respectively 3.34 cm and 2.25 cm. They were placed 50 cm from the source of activation. The *d* electrodes were 36.5 cm long, the diameters of the coaxial cylinders being 1.9 and 1.27 cm and were placed 50 cm from the end of the ion trap. One of the ion trap electrodes was connected with the ground, the other to a battery whose maximum potential was 135 volts so that the field between the electrodes could be varied from zero to 250 volts per cm. One of the *d* electrodes was connected to a Dolezalek electrometer and the other to a 16 volt battery. It was observed that the ionization current in *d* was not affected more than two percent when the field between the ion trap electrodes was varied from zero to 250 volts per cm. Now any preexisting ionization due to the disruptive discharge or to any other cause could not pass through the strong field between the ion trap electrodes. Therefore one may conclude that the ionization observed in *d* was produced by changes taking place after the passage of active nitrogen through the ion trap. The slight changes observed can be explained in the light of what follows.

Before going further it is necessary to say a few words about the method of measuring the ionization and the determination of the conductivity of

active nitrogen. In this determination great difficulty is experienced in view of the fact that the energy of discharge for the production of active nitrogen is so great that despite the precautions taken to screen the electrometer, the electrodes and the connecting leads, the electrometer needle oscillated violently during the discharge. The disturbing effects were due to the existence of the small opening *n* (Fig. 1) through which the gas flowed from the activation chamber to the electrodes. When the passage *n* was closed with a stop cock the electrometer was unaffected by the discharge. A high resistance galvanometer is not so much affected but it is not sensitive enough to measure ionization unless the activation is very strong and the electrodes are very near to the place where activation is produced. Moreover, with a continuous discharge it is difficult to have uniform temperature on the walls of the bulb *D* and, consequently, uniform activation, since the destructive effect of the walls increases with their temperature.

For the above reasons the discharge was made intermittent, lasting one second every two minutes. The electrometer readings were made at some definite time after the discharge had been interrupted. The points of the conductivity curves (see Fig. 2) were obtained by connecting the electrometer to the electrodes twenty-five seconds after each discharge and measuring the total deflection (i.e. total charge instead of rate of charging). In order to obtain conductivity curves whose saturation point was below the ionization potential of nitrogen, it was necessary to use comparatively long electrodes.

In the experiment described above, it was shown that the conductivity observed in active nitrogen is not due to the survival of ionization produced during the disruptive discharge. If the conductivity observed is due to the presence in the gas of ions, these ions must have been spontaneously produced. Such spontaneous ionization is conceivable with the help of a simple hypothesis concerning the nature of active nitrogen. Assuming that active nitrogen is an ordinary molecule of N_2 whose valence electrons have been transferred to higher energy levels, then spontaneous ionization could be produced after an elastic collision of the second type between two excited molecules. In that case all the energy in one of the molecules is transferred during the collision to the other with possible ionization of the latter. However, as will be seen from the experiments to be described below, the conductivity in active nitrogen is not due to spontaneous ionization but to electrons apparently emitted by the electrodes either by photo-electric action when active nitrogen reverts to the normal state, or by the direct action of impinging atoms as observed by Holst and Oosterhuis,[7] Webb,[8] Messenger.[9]

A second series of experiments was carried out to test this point by a method analogous to those that have been employed to distinguish between radiating and ionization potentials in gases. If the conductivity were due

[7] Oosterhuis and Holst, Phil. Mag. **46**, 1117 (1923).
[8] H. W. Webb, Phys. Rev. **24**, 113 (1923).
[9] H. A. Messenger, Phys. Rev. **28**, 962 (1926).

to spontaneous ionization, the number of positive and negative ions present would be equal, and the saturation positive or negative currents would be equal irrespectively of the relative size of the coaxial cylinders between which the active nitrogen flowed. If, however, the conductivity were due entirely to electrons from the walls, since the number of the emitted electrons is proportional to the surface exposed, the number of electrons emitted from the outer cylinder will be to that emitted from the inner cylinder exactly in the ratio of their respective exposed surfaces. That is, the negative charges must be proportional to the areas of the negative electrodes or, what amounts to the same thing, the ratio K between the positive and negative saturation currents must be equal to the ratio of the surfaces of their respective electrodes. Besides the above two cases which represent extreme conditions we have a third possibility in which the conductivity is due at the same time to spontaneous ionization and to electron emission.

In the determination of the ratio K of the value of negative and positive saturation currents certain precautions are necessary, which, if omitted, may lead to considerable error in the determination of that value. From the analysis of the spectrum emitted by the afterglow it appears that the first positive band, to which the α-group bands characteristic of the afterglow belong, corresponds to a high excitation potential. It is possible, therefore, that the active nitrogen might ionize any impurity whose ionization potential is below the potential corresponding to the α-group bands. Such impurities might be the hydrocarbon vapors due to stop-cock grease, mercury vapor, etc. All these vapors were condensed by using a liquid air trap E through which the nitrogen gas passed before going to the activation chamber. Moreover, all the connections from that point to the pump were of glass. Incondensable impurities that are in the gas, such as oxygen, helium, or argon, have ionization potentials above the resonance potentials of active nitrogen and consequently no ionization can take place by collision.

In preparing the surfaces of the electrodes particular care was taken to give them similar finishing and not to touch them with the hands or any substances which would affect the electron emission from the surfaces. These surfaces were also polished several times during the experiments. The electrodes used were of brass and the ratios of the surface of the outer cylinder to the inner changeable cylinder were 1.7, 1.5, and 3. The readings were taken by applying alternately positive and negative potentials to the outer cylinder so that, in determining the values of positive and negative ionization currents corresponding to a given field, any change that could take place, such as diminution of photo-electric emission, would affect equally both values. It was essential during definite intervals of time to observe the conductivity corresponding to a field taken as standard in order to be sure that the general conditions determining the conductivity corresponding to other potentials were identical. Factors that could influence most effectively the conductivity were variations in the energy of the disruptive discharge and slight changes in the density of the flowing gas since, under these influences, the amount of activated nitrogen would vary and consequently

the observed ionization. The curves of Fig. 2 represent the conductivity obtained using electrodes whose ratio of surfaces were 3:1 and 1.5:1. It will be observed that in the neighborhood of 4 volts the ratio between the negative and positive currents is about 3 to 1 in the one case and 1.5 to 1 in the other, these ratios remaining constant for saturation currents obtained in the neighborhood of 14 volts. For potentials above the ionization potential of nitrogen we have a slow increase of conductivity, the ratios, however, remaining constant. The observed slight discrepancies in the ratios must be attributed to the cumulative ionization of active nitrogen, or to the possible ionization of slight impurities present. Greater ratios between the surfaces of the electrodes have been used and analogous results have been obtained.

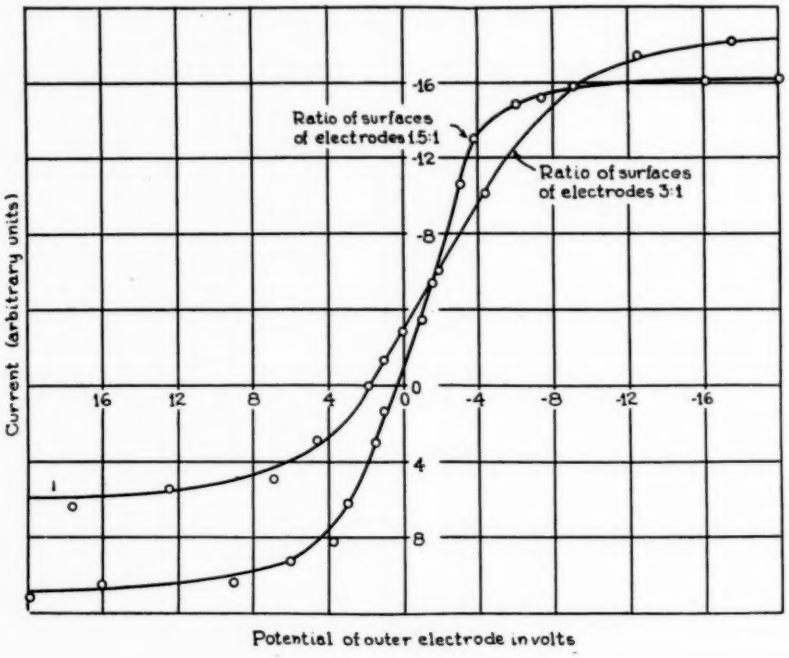

Fig. 2. Saturation curves with electrodes of different areas.

However, in using as an inner electrode a cylinder of small diameter, it was impossible to obtain saturation below the ionization potential of nitrogen. This equality of the ratios of the surfaces of the electrodes and of the saturation currents indicates that the conductivity of active nitrogen is due to electrons emitted from the surfaces of the electrodes. In the curve of Fig. 2, where the ratio of the surfaces is 3:1, a positive potential of 1.8 volts on the outer cylinder was necessary to obtain zero current. This may be interpreted as due to the electrons leaving the surfaces with considerable velocity so that a retarding potential must be applied to the larger surface to prevent a charging of the inner electrode. The slow saturation may also be interpreted as due to the electrons emitted having a high velocity.

In this connection experiments were also carried out in which a hot oxycathode arc in nitrogen served as a source of active nitrogen in place of the disruptive discharge. A steady arc was maintained with approximately 50 volts while the gas was allowed to flow past into the cylindrical electrodes. The characteristic yellowish glow of active nitrogen could be observed in the neighborhood of the arc. Between the electrodes the same type of conductivity curve was observed as with the methods described in the last paragraph. However, when an ion trap was introduced to prevent any possible ions reaching the electrodes, the active nitrogen was so weakened as to make measurements unreliable.

Experiments were carried out with the pressure adjusted to be above that at which active nitrogen is formed. Here the ion trap was adjusted so

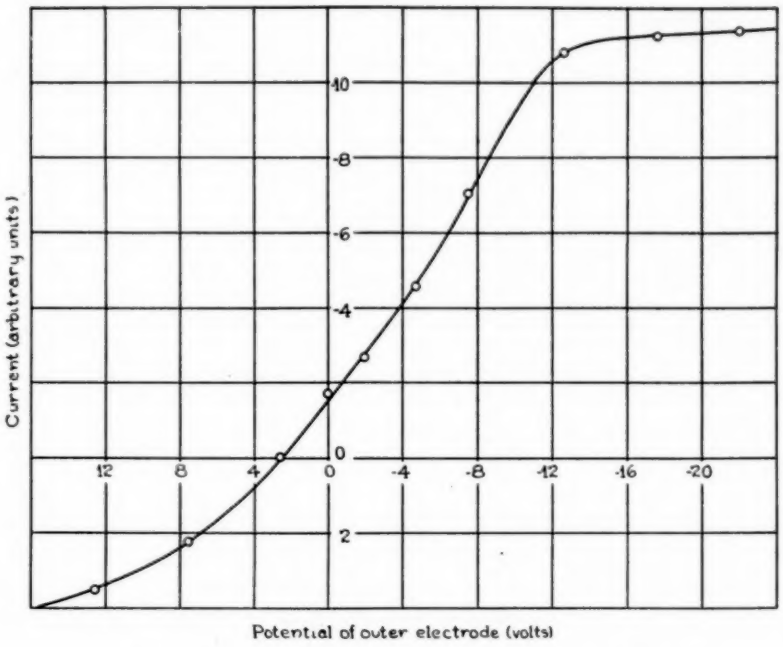

Fig. 3. Saturation curve of photoelectrons from electrodes.

that the radiation from the arc could pass through and cause photo-electric emission directly from the surfaces of the electrodes. It was found that the same type of ionization curve with saturation at about 14 volts (see Fig. 3) was obtained in this case. This confirmation of the interpretation of the conductivity as due to the emission of electrons from the electrodes with high velocity was repeated with three other gases, oxygen, helium and hydrogen. The gas in each case was allowed to flow past the arc at about the same pressure as the active nitrogen.

We may conclude then from the first part of this investigation that the conductivity between two electrodes in active nitrogen is due to electrons emitted from the surfaces of the electrodes. There is no direct ionization of the gas and the electrons have a relatively high velocity.

II. Molecular Nature of Active Nitrogen

The second part of this investigation is concerned with experiments bearing on the molecular nature of active nitrogen and particularly with the determination of the energy possessed by the molecule in this state. Two methods have been used. In one the rate of extinction of the luminous glow when various gases were added showed the degree to which the added gases could take up the energy of the excited active nitrogen. In the second method the transfer or absence of transfer of energy to various added gases was observed by the production of ionization in some and the absence of ionization in others. Most of the previous experimental observation can be interpreted by assuming that active nitrogen is either atomic or molecular in structure. Saha[10] assumes the active nitrogen to be an excited molecule with energy corresponding to 8.5 volts, while Birge[11] calculates the maximum molecular energy to be 11.5 volts, at which level he considers a metastable state to be possible. Foote, Ruark and Chenault[12] conclude that a metastable state of N_2 exists between 9.5 and 9.6 volts while Strutt and Sponer[13] consider that active nitrogen is atomic. We shall see later that the present observations fit in well with the excited molecule theory, and we shall use that theory in discussing the effects to be expected in these experiments.

(A) *Experiments on the effect of foreign gases on the duration of the afterglow.* The study of the effect on the glow due to the introduction of foreign gases can be made with two different arrangements. In the first arrangement the nitrogen from the reservoir A (Fig. 1) flows through the capillary tube B to the activation chamber D. At the point L it meets the stream of gas whose effect on the glow is to be studied. The amount of flow of this gas is regulated by the capillary tube F and the manometer M connected to the reservoir H. With this arrangement, when the activation takes place, we have in D a thorough mixture of the two gases. In the second arrangement the stop cock T is closed and the vessels are cleaned by letting nitrogen flow for a considerable time. Then P is closed, and the pressure in D is reduced to 0.07 cm. The next step consists in closing L and introducing the gas whose effect on the glow is to be studied into the bulb G, the amount of gas being regulated by keeping the pressure in H constant and the stop cock T open for a definite length of time. Under this arrangement, soon after the activation of the pure nitrogen, a definite quantity of the foreign gas is introduced by opening the stop cock L. It is to be noted that with the last method, possible activation of the foreign gas during the discharge is avoided, while on the other hand, a complicated manipulation with its concomitant disadvantages is introduced. The gases used were oxygen, hydrogen and helium. Readings were also taken by introducing nitrogen through L at

[10] Saha and Sur, Phil. Mag. **48,** 421 (1924).

[11] Birge, Nature **114,** 642 (1924).

[12] Foote, Ruark and Chenault, Phys. Rev. **25,** 24 (1925). In a later paper Foote, Ruark, Chenault and Rudnik, J.O.S.A. **14,** 17 (1927) give the value of the energy of active nitrogen as greater than 10 volts and consider the probability that active nitrogen is atomic.

[13] H. Sponer, Zeits. f. Physik, **38,** 622 (1925).

various rates in addition to the nitrogen constantly flowing through *B*. The curve so obtained serves as a control to which the other curves can be referred. Helium and hydrogen were purified by passing slowly through a tube filled with charcoal and immersed in liquid air. The curves of Fig. 4 represent the results obtained by the first method. The abscissas represent rate of inflow of foreign gas taking as a unit the rate of flow of nitrogen through *B*. The ordinates give the corresponding duration of the afterglow, observed by a stop-watch from the instant of cutting off the exciting current to the time when no more luminosity could be observed.

The nitrogen-oxygen mixture afterglow presents, perhaps, the most interesting features since, besides changes in duration, we have changes in

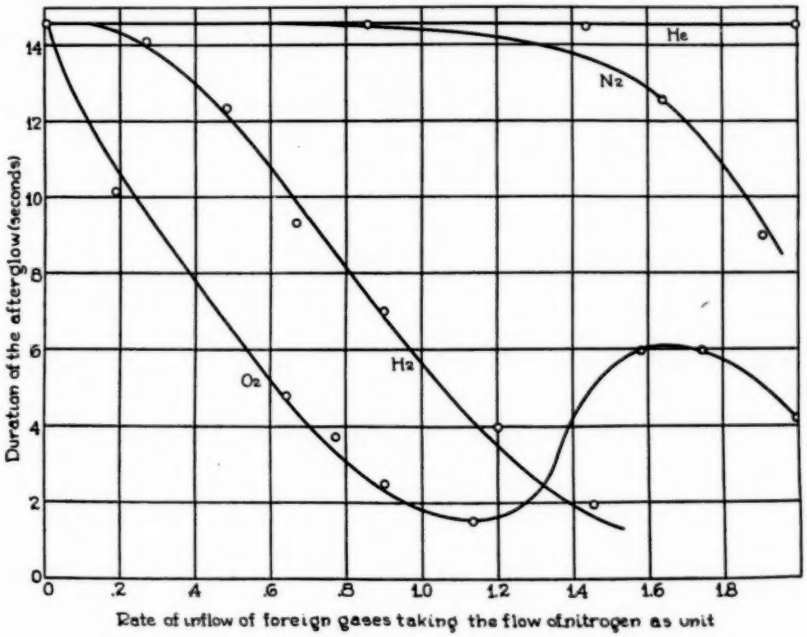

Fig. 4. Effect of foreign gases on the duration of the afterglow

the color of the afterglow. With increasing rates of inflow of oxygen the glow changes from deep yellow to greenish-yellow, then to greenish-blue and attains a minimum intensity and duration when the inflow of oxygen is about equal to that of nitrogen, the color of the glow being deep blue. With further increases in the amount of oxygen, the duration and intensity of the glow increases, reaching a maximum when the rate of flow of oxygen is about 1.7 times that of nitrogen. So far as I am aware the existence of this maximum in the afterglow of nitrogen-oxygen mixtures has not been observed before. The color of the afterglow is then a brilliant green. With a still further increase of oxygen the glow becomes a dark green, diminishing gradually in intensity and duration. Strutt[14] studied the afterglow of rarified air and

[14] Strutt, Proc. Roy. Soc. **A85,** 533 (1911).

attributed the greenish-yellow glow to the conbination of ozone and nitrogen oxides formed during the discharge. His observations correspond to the glow observed in the present experiments when the amount of oxygen was about two-tenths that of nitrogen. It seems to me, however, that the afterglow under the above conditions is due mostly to active nitrogen if we judge by its color which, during the first six seconds is yellow and very similar to that of active nitrogen, the greenish yellow becoming prominent only during the last four seconds. The curve for the duration of the afterglow in nitrogen-hydrogen mixtures does not present the anomalies of the oxygen curve. The duration diminishes gradually with increasing amounts of hydrogen and the glow remains a deep yellow. Apparently the energy is not transferred as easily to hydrogen molecules as to those of oxygen. The nitro-

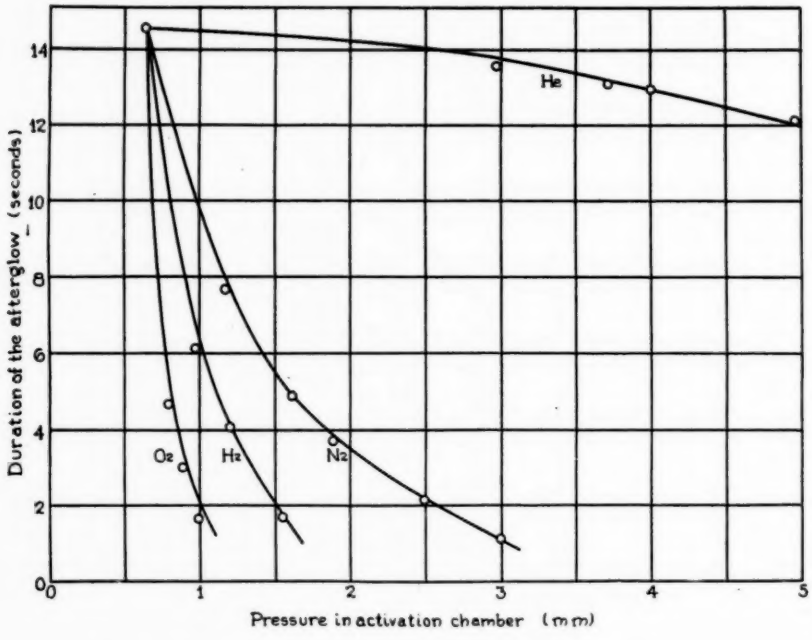

Fig. 5. Effect of foreign gases on the duration of the afterglow.

gen curve serves to show the effect of increase in pressure (increase of molecular collisions) on the duration of the afterglow and serves as a convenient standard of comparison with the other mixtures since the abscissas are proportional to the pressure of the mixtures. The nitrogen-helium curve is of special interest since no decrease in the duration of the afterglow is observed when helium is introduced. When the ratio becomes one part of nitrogen to ten of helium, the only change observed is that in the color of the glow which becomes reddish-yellow. From the study of the nitrogen-helium mixture we derive the important conclusion that not only is no energy transferred in increasing the internal energy of helium molecules, but that even the energy transferred in increasing the translational energy of helium molecules

must be small. The high resonance potential of helium (20.5 volts) would lead us to expect that no energy would go to increasing the internal energy of the helium atom.

The curves of Fig. 5, obtained by the second method give the same general results. The ordinates represent duration of glow and the abscissas the pressure in the bulb after the introduction of the foreign gas. The nitrogen was always activated when at a pressure of 0.07 cm, so that the conditions of the discharge remained identical. The other gases were introduced immediately after the nitrogen had been excited.

(B) *Ionization in foreign gases produced by active nitrogen.* One more avenue to the study of active nitrogen is opened by the knowledge that its conductivity is due to electrons emitted from the electrodes. In a previously described experiment it was shown that the ratio between the negative and positive saturation currents was three to one, that is, exactly the ratio of the exposed surfaces of the electrodes. Now if by the introduction of a certain vapor this ratio becomes smaller, it will indicate that the vapor is ionized by collision. Furthermore, the knowledge of the ionization potential of the introduced vapors will help to place the excitation potential of active nitrogen.

The vapors used were hydrogen (ionization potential 15.9), mercury (ionization potential 10.4), and iodine (ionization potential 9.4[15]). Hydrogen was introduced in a continuous stream and in various amounts at a point V between the activation chamber and the electrodes. No change was observed either in the conductivity or in the ratio between the two saturation currents. This is an indication that ionization by collision does not take place. Mercury vapor was introduced by placing mercury in a tube K where it could be cooled by liquid air or heated by a Bunsen flame. No change was observed either in the conductivity or in the ratio, even when the mercury was heated to the point of active evaporation. Iodine, like mercury, was placed in a tube K where its evaporation could be controlled by suitable changes of temperature. When a small iodine crystal was placed in K and the tube immersed in liquid air no effect was produced either in the color of the glow or in the ratio. When the tube K was directly above the liquid air flask and so kept quite cool, the glow in the activation chamber remained a deep yellow, while in the tube J the color changed to a bright, light blue due to the excitation of iodine vapor. The conductivity decreased and the ratio changed to about 2.5:1. Finally, when the temperature in K was that of the room, the evaporation was greater and the light blue fluorescence due to iodine turned to dark blue, while the conductivity became very small and the ratio decreased to 2:1, indicating a considerable amount of ionization by collision.

(C) *Theoretical inferences.* The experiments above point towards the hypothesis that active nitrogen is an excited molecule of nitrogen having a metastable state between 9.4[16] and 10.4[17] volts if we can judge by the ioniza-

[15] Smyth and Compton, Phys. Rev. **10**, 501 (1920).

[16] This is the nearest to that determined by Foote, Ruark and Chenault which is between 9.5 and 9.6 volts.

[17] Ionization potential of mercury is 10.4 volts.

tion by collision effects. The metastable hypothesis presents certain obvious difficulties in view of the long duration of the glow. It is, however, theoretically conceivable that an atom might remain for an arbitrary length of time in an excited state provided only that the pressure and temperature are kept sufficiently low. Low pressure and low temperature mean few and less violent collisions. Another external influence that we should expect to be much more destructive to the metastable state than the simple collision between two molecules, is the collision between a metastable molecule and a freely moving electron because of the unneutralized electromagnetic field associated with the electron. The absence of free electrons in active nitrogen as demonstrated in the present investigation adds significance to this view.

The hypothesis that active nitrogen is a metastable state of nitrogen reverting to nitrogen after a collision and that, as was supposed above, collisions with electrons are especially effective in reverting active nitrogen to the normal state, finds additional support in certain exceedingly interesting results obtained by Strutt.[18] He succeeded in making his nitrogen so pure that the afterglow became very dim. Strong restoration of the afterglow was obtained by introducing such impurities as methane, oxygen, chlorine, hydrogen[19] and other electro-negative gases, while the introduction of argon, helium or of nitrogen itself does not restore the glow. We may interpret these observations as follows. During the disruptive discharge the gas is ionized, and in the case of pure nitrogen gas, the electrons move freely and with great translational velocities so that we might expect the number of successful collisions to be great and the reversion of metastable nitrogen to normal nitrogen to be rapid. In the case of the presence of electro-negative impurities such as oxygen, Franck[20] showed that the electrons served as nuclei for the formation of slowly moving ions, in that way decreasing the number of effective collisions.

Strutt gave to the above results an almost diametrically opposite explanation which in brief is as follows. He assumes that active nitrogen consists of monatomic nitrogen which is produced only by the impact of a negative ion in the discharge, while free electrons are not effective in administering the right kind of blow. Experiments by Hogness and Lunn[21] on the ionization of nitrogen by electron impacts have shown that atoms are formed along with charged molecules except with very low pressures where the charged molecules make no collisions. Thus we would expect nitrogen atoms to be present even when the gas was very pure.

H. Sponer has also assumed that active nitrogen is monatomic nitrogen, the afterglow appearing when two atoms of nitrogen collide simultaneously with a neutral nitrogen molecule. In the collision they could excite the nitrogen molecule by transferring to it their dissociation energy, at the same

[18] Strutt, Proc. Roy. Soc. **A91,** 303 (1914–15).

[19] J. J. Thomson, Proc. Roy. Soc. **A89,** 10 (1910) established the existence of negatively charged atoms of carbon, oxygen, chlorine and hydrogen.

[20] Franck, Verh. d. D. Phys. Ges. **12,** 613 (1910).

[21] Hogness and Lunn, Phys. Rev. **26,** 786 (1925).

time recombining to form a neutral molecule. With this hypothesis one could explain satisfactorily the long duration of the afterglow since collisions such as are described above are rare in comparison with bimolecular collisions. However this hypothesis requires the energy of dissociation of nitrogen to be between 11.4 volts (260,000 cal.) and 13.0 volts (296,000 cal.) or, more specifically as it appears from a later paper,[22] the dissociation potential to be placed at 11.4 volts. This value is very different from Eucken's[23] revised value (16.5) volts and also from A. Grimm's[24] value, obtained from positive ray analysis, which is 15.9 volts. The present investigation also shows that the energy set free in the reversion of active nitrogen to the normal form is not able to ionize mercury (10.4 volts). Moreover, with Sponer's hypothesis it is difficult to explain the lack of afterglow when the nitrogen is free of impurities without making the additional hypothesis that these impurities serve as a protection against the catalytic action of the walls of the vessel.

Wood showed that hydrogen can be dissociated under the influence of an electric discharge and that if this gas in its atomic form is drawn over metals or any other substances having catalytic properties, they can be brought into incandescence by the heat liberated during the process of recombination into molecular form. In the present experiments it had been found that the active nitrogen was much weakened after passing through a metal ion trap and an attempt was made to see if this destruction was accompanied by a heating of the metal. A coil of nichrome wire was placed in the path of the active nitrogen and connected to a Wheatstone bridge. Any change in temperature of the wire greater than 0.1°C could be easily determined from the change in the resistance of the wire. No change in resistance was observed. This suggests that the phenomena in nitrogen are not similar to those in atomic hydrogen, as would be expected if active nitrogen is atomic. On the excited molecule theory the energy can go into the kinetic energy of the ejected electron.

The view that active nitrogen is of a more complex atomic grouping cannot be advanced with any great advantage. Strutt's attempt at condensation of active nitrogen by liquid air was repeated with negative results. A bulb containing nitrogen was immersed in liquid air and the appearance and duration of the afterglow was observed when the duration of the electrodeless discharge was varied from one second to fifteen minutes. The appearance and duration of the afterglow remained the same irrespectively of the changes in the duration of discharge which indicates that no change of pressure took place within the bulb due to condensation of active nitrogen. Since ozone is condensed at liquid air temperature we might expect a complex molecule such as N_3 to be condensed also. This result by analogy, is unfavorable to the idea that active nitrogen is of the form N_3.

[22] Birge and Sponer, Phys. Rev. **28,** 259 (1926).

[23] A. Eucken, Ann. d. Chemie, **440,** 111 (1924) originally gave the dissociation potential of N_2 obtained from the specific heat calculation as about 19 volts (430,000 calories).

[24] A. Grimm, Zeits. f. Electrochemie **31,** 474 (1925).

The observed increase in the intensity of the glow when active nitrogen is locally cooled can be interpreted as due to an increase in the number of collisions with the active molecule. By locally cooling a closed vessel we obtain a greater density in the part cooled and it can be shown that the number of collisions varies as $T^{-3/2}$ where T is the absolute temperature. For instance, if one part of the vessel is kept at a temperature of 20°C and another at that of liquid air, then the number of collisions in the two parts will be in the ratio of 1:5.5. An experiment was performed in which active nitrogen was produced by an electrodeless discharge inside a closed bulb with a wide, short tube which could be immersed in liquid air.[25] When the bulb was at room temperature the afterglow lasted about 28 seconds. When the lower end of the tube was immersed in liquid air the glow was concentrated in the lower part and lasted about 4 seconds, which gives a 7:1 rate of decay instead of 5.5:1 as predicted by theory.[26] It must be added, however, that it was difficult to make accurate observations on the duration of the afterglow when the tube was immersed in liquid air because of the vapors that condensed on the surface of the bulb. The observations are thus seen to be in good agreement with the hypothesis that the phenomena associated with active nitrogen are due to a metastable form of the molecule.

The author wishes to express his thanks and indebtedness to Professor A. J. Dempster, under whose direction the above investigation has been carried out, for his suggestions and criticisms on all phases of this work.

RYERSON PHYSICAL LABORATORY,
UNIVERSITY OF CHICAGO,
March 25, 1927.

[25] This experiment has been suggested by a similar experiment conducted by Strutt in which, however, he observed the intensity instead of the duration of the glow.

[26] In the light of the above considerations we should expect a decrease in the duration of the afterglow with accompanying increase in intensity when the density of the gas in the bulb is kept constant while its temperature is increased in view of the fact that the number of collisions is proportional to the square root of the absolute temperature. The observed decrease in intensity when the gas is heated at constant density, which is in disagreement with the above considerations, may be due to the liberation of water vapor and other gases from the heated bulb which have a great influence in decreasing the intensity of active nitrogen and in that way altering greatly the pure temperature effects.

IONIZATION EFFICIENCY OF ULTRA-VIOLET LIGHT IN CAESIUM VAPOR

By Edward Milton Little

Abstract

Efficiency of photo-ionization in caesium vapor at 166°C as a function of wave-length.—Light from a quartz mercury arc after being resolved by a quartz spectrograph was passed through a tube containing caesium vapor. The energy of the radiation was measured with a Coblentz thermopile. The photo-ionization of the vapor was determined by drawing out the positive ions to a plate and measuring their number with an electrometer. The vapor pressure of the caesium was obtained by interpolation between existing data. The pressure at 166°C was taken as 0.027 mm which corresponded to an atomic concentration of 5.96×10^{14} atoms per cc. The efficiency of ionization B (the Einstein probability of absorption coefficient) was found to increase from 0.17×10^{-10} ions per atom per erg at 3345A to 3.4×10^{-10} at 3135A. The theoretical threshold is at 3184A. For shorter wave-lengths B diminished to a minimum of 1.2×10^{-10} at 2800A and then increased slowly for still shorter wave-lengths. The estimated possible error in B is 5 percent in relative values and 25 percent in absolute values.

Photoelectric efficiency from a caesium-gold alloy surface.—It was incidentally observed that caesium alloyed readily with a gold electrode and that the resulting surface was very active photo-electrically. The photo-sensitivity varied from 0.5×10^{8} electrons per erg at 6100A to 2.0×10^{8} at 2800A.

Introduction

IN THE last five years a very determined effort has been made to measure quantitatively the photo-ionization in alkali vapors as a function of the wave-length of the radiation. Kunz and Williams[1] were the first to detect electrically the ionization of a vapor by ultra-violet light. They found that radiation of wave-length greater than 3180A did not ionize caesium vapor at 140°–200°C but that wave-lengths shorter ionized it readily. It may be recalled that 3184A is the convergence wave-length of the caesium arc spectrum. Williamson[2] found for potassium vapor a critical wave-length of 2800–3100A in good agreement with the theoretical limit 2856A. He used graded filters to analyse the light, and to avoid surface effects, passed the light through a jet of the vapor. Lawrence[3] using the same form of tube but with a Pfund iron arc and monochromatic illuminator as a source, found 2610A as the limit and claimed that Williamson's data when corrected gave a similar value. He accounted for the discrepancy of 246A between his value and the theoretical one by supposing that in the jet many of the atoms were grouped into diatomic molecules which required 0.4 volts, corresponding to 246A, to separate them into atoms. Harrison and Slater[4] show that with

[1] Kunz and Williams, Phys. Rev. **15**, 550 (1920); **22**, 456 (1923).
[2] Williamson, Phys. Rev. **21**, 107 (1923).
[3] Lawrence, Phil. Mag. **50**, 345 (1925).
[4] Harrison and Slater, Phys. Rev. **26**, 176 (1925).

rapidly distilling sodium vapor at about 800°C there are about fifty times as many diatomic molecules as atoms.

More recently Mohler, Foote and Chenault[5] have applied to the problem the very sensitive method of detecting positive ions which had been developed by Kingdon[6] and Hertz[7] independently. By this method they were able to show that in caesium vapor the ionization efficiency in ultra-violet light is a maximum at about 3184A, the theoretical threshold, and that it decreases for shorter wave-lengths to about one-eighth of the maximum value at 2700A. They also found ionization at the resonance potentials corresponding to wave-lengths longer than 3184A, although close to 3184A the resolution was insufficient for separation of the peaks. We doubt whether ionization of such amount would take place in the normal vapor at the resonance wave-lengths without the heavy stream of electrons passing through. Mohler, Foote and Chenault's explanation of this ionization is that the light raises an electron to an outer orbit and a collision due to thermal agitation will lift it the rest of the way. The electrons in their tube had a velocity of about one volt—sufficient to ionize from the 4370A level. This velocity is 300 times the thermal velocity of the atoms, so most of the ionization was probably completed by electronic rather than by atomic impact. In Lawrence's work referred to above no such ionization at the resonance wave-lengths was found.

The photo-ionization of vapors by radiation of wave-length shorter than the arc spectrum limit is correlated with the absorption by the vapor of such radiation. Recently Harrison[8] by photographic and densitometer methods has quantitatively measured the absorption of light in Na vapor. His results on the variation of absorption with wave-length beyond the series limit closely resemble in general trend those of Mohler, Foote and Chenault on the variation with wave-length of photo-ionization.

The method used by Mohler, Foote and Chenault though very sensitive, did not lend itself to a quantitative determination of the photo-ionization as a function of the energy of the radiation. Moreover the presence of the slowly moving electrons was likely to confuse the measurements in the vicinity of the threshold wave-length because of their ability to complete the ionization by impact. The purpose of the present investigation is (1) a redetermination of the threshold wave-length, and (2) a determination of the absolute values of the ionization efficiency for various wave-lengths beyond the threshold.

Method

The general arrangement of the apparatus is shown in Fig. 1, A. A 110 volt D. C. Cooper-Hewitt mercury arc is the source. The current when it

[5] Foote and Mohler, Phys. Rev. **26,** 195 (1925); Mohler, Foote and Chenault, Phys. Rev. **27,** 37 (1926).

[6] Kingdon, Phys. Rev. **21,** 408 (1923).

[7] Hertz, Phys. Zeits. **18,** 307 (1923).

[8] Harrison, Phys. Rev. **24,** 466 (1924).

became steady after about thirty minutes, was 4.50 ± 0.05 amperes and the potential drop across the arc was about 50 volts. The current rose about 4 percent if the asbestos in front was removed, thus cooling the arc. The Hilger quartz spectrograph was fitted at the farther end with a slit a trifle larger, both vertically and horizontally, than the image of the first slit which was kept 10.1 by 0.75 mm in size. A system of screens, tubes, a lens and a sliding screen controlled by a string hung over glass rods, led the light to the furnace.

What was desired in illumination was a uniform cylinder of light, but as this was impossible (a point source would mean too little energy) the convergence of light to two images, one at each end of the tube, was deemed best. The objects for these two images were approximately 50 cm apart.

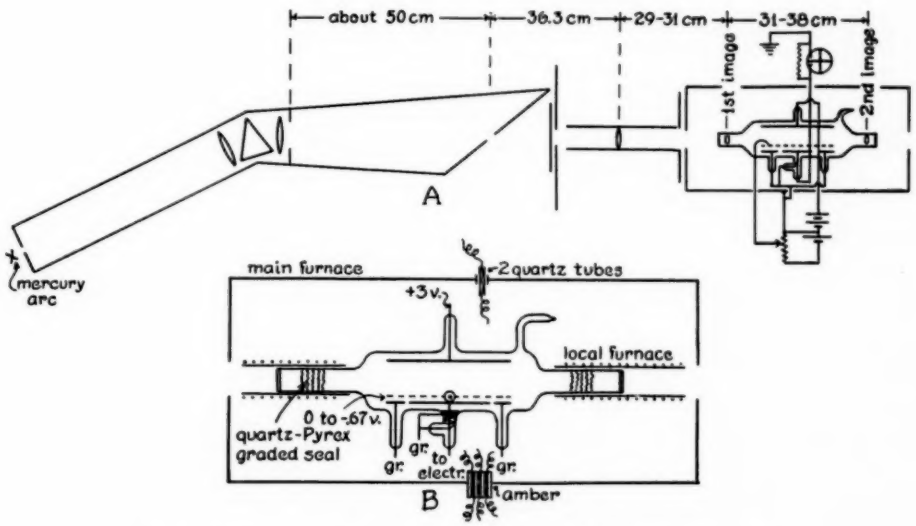

Fig. 1. A, arrangement of apparatus; B, detail of ionization tube.

One was an elliptical diaphragm (major axis 4.3 cm) just behind the second spectrograph lens, and the other was the image (1.3 cm high) of the first spectrograph slit. The light could not stray beyond the envelope of lines connecting the peripheries of the two images (except for aberrations). The shape and dimensions of the beam opposite the ends and at two intermediate points of the collecting plate were measured to determine the average cross section illuminated. This was done for two wave-lengths and a straight line graph was drawn to determine it at other wave-lengths. The average cross-section multiplied by the effective length of the collecting plate gave the volume from which the positive ions were collected.

The furnace was non-inductively wound. It had holes about 3.5 cm in diameter at each end, together with openings for a thermometer, and the electrical connections. The furnace, its accompanying lens, etc., were capable of being moved bodily with respect to the spectrograph.

The tube was made of quartz and Pyrex glass and is shown in Fig. 1. B The plane parallel quartz plates attached to quartz-Pyrex seals were furnished by the Cooper-Hewitt Company. The grid consisted of 0.105 mm platinum wire with a spacing of 0.51 mm. Thus the fractional area between the wires was 0.628. The quantity of electricity collected on the plate was divided by this fraction to correct for loss to the grid. The mesh was pressed against a framework of stiff platinum wire in a hot flame at almost the melting point to fasten it firmly. The other electrodes were similarly made but with platinum foil substituted for the mesh. The framework was arc welded to a platinum hub into which the substantial tungsten leads were screwed. The length over all was 36.5 cm and the diameter of the main part was 6.2 cm. The quartz plates were 1.8 mm thick. To intercept surface currents, a grounded platinum spiral touched the glass all around the inside of the glass bell of the collecting electrode. Lead foil was wrapped around outside and grounded for the same reason. The guard electrodes at the ends of the collecting plate collected ions produced in the ends of the tube not opposite the collecting plate and made the region of production of the ions collected on the plate definitely calculable. The positive ions, rather than the electrons, were collected because thermal electrons from the walls and electrodes were always present. The grid was for the purpose of making the net current to the collecting plate zero in total darkness. If it were absent thermal electrons would usually make a troublesome current although in the second of the two runs, to give best results, the grid was kept grounded. The opposite plate was kept at three volts (less than ionizing potential) to drive positive ions to the collecting plate. Potentials as high as 10.5 volts, however, when tried after the last run, failed to produce any noticeable ionization by collision.

The electrometer had a sensitivity of 1500 mm per volt at 1 meter. A scale distance of 2.83 meters was used. A pencil resistance on hard rubber was used as a shunt. When best adjusted for our experiment its resistance was 1.173×10^9 ohms.

The spectrum was calibrated with a Coblentz thermopile of 26 hot junctions totalling 20 by 2 mm in area. The thermopile resistance was 11.2 ohms. The galvanometer had a resistance of 12 ohms and a figure of merit of 1.71×10^{-9} amp./mm at 1 meter. A scale distance of 3.33 meters was used. The thermopile was calibrated by placing it one meter from a Hefner lamp in a light-tight box. According to Coblentz[9] an unshielded Hefner lamp gives out 26 microcalories (± 6 percent) per sq. cm. per sec. at a distance of 1 meter. The slit of the thermopile was cut down to 1.45×0.18 cm (0.261 sq. cm) so as to make sure that all the light entering it reached the junctions. The energy entering the slit for 1 mm deflection of the galvanometer was found to be 0.637 ergs/sec.

Another thermopile tested was a stellar vacuum thermocouple of 1 pair of junctions made by Pettit and Nicholson[10] of the Mount Wilson Observa-

[9] Coblentz, Bull. Bur. Standards **11**, 95 (1914).

[10] Pettit and Nicholson, Astrophys. J. **56**, 295 (1922).

tory. On account of the difficulty of obtaining a sharply defined image of the slit on a target 1 mm square, it was no more sensitve than the Coblentz thermopile and was less reliable for this kind of work. Still another instrument experimented with was a coil thermopile studied by Wilson and Epps[11] and suggested to us by Dr. J. P. Cooley. It is a high resistance thermopile (700 ohms) with 100 pairs of junctions in a space of 1.5 cm. Thus it can be used with a galvanometer of high resistance and consequent high sensitivity. Although it gave twice the sensitivity of the Coblentz thermopile when used at atmospheric pressure, and six times when in an evacuated chamber with a quartz window, it was quite sluggish and required four minutes to reach half its final deflection. For this reason the Coblentz thermopile was finally used. It was sensitive enough and responded almost instantly.

Vapor pressure of caesium. There have been several determinations of the vapor pressure of caesium but unfortunately these were not made near

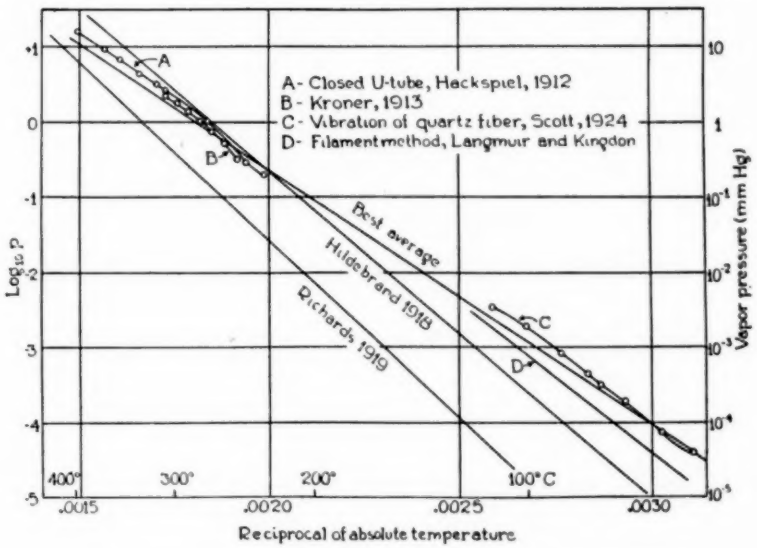

Fig. 2. Vapor pressure of caseium as a function of temperature.

166° and 204°C, the temperatures at which we worked. They have been made at 230°C and up by Hackspiel,[12] who used a closed U-tube method, and also at 120°C and down by Langmuir and Kingdon,[13] who measured the number of atoms striking an incandescent tungsten filament over 1100°C (all atoms then leave the filament as positive ions). Other determinations were made by Kroner[14] and by Scott[15] who used a vibrating quartz fibre method. These determinations are all shown in Fig. 2 where log p is plotted against the reciprocal of the absolute temperature of the vapor.

[11] Wilson and Epps, Proc. Phys. Soc. London **32**, 326 (1920).
[12] Hackspiel, Comptes rendus **154**, 877 (1912).
[13] Langmuir and Kingdon, Proc. Roy. Soc. **107A**, 61 (1925).
[14] Kroner, Ann. d. Physik **40**, 448 (1913).
[15] Scott, Phil. Mag. **47**, 49 (1924).

If we assume, with Hildebrand,[16] and others that such a plot should give a straight line, we obtain the most probable value of the vapor pressure by drawing the straight line which best fits the four sets of experimental data. For a temperature of 166°C we thus find that $p=0.027$ mm Hg and at 203.9°C it is 0.107 mm Hg. The corresponding numbers of atoms per cc are 5.96 and 21.70×10^{14}.

Results

(a) *Energy distribution in the mercury spectrum.* In measuring the photo-ionization of the caesium vapor the light was passed straight through the tube so that account must be taken of both transmission losses at the first quartz window and of the gain by reflection at the second window. In some incidental measurements of the photoelectric effect from a caesium-gold alloy surface the light was passed obliquely through the tube. In this case only transmission losses at the first plate need to be considered. Actual transmissions for our fused quartz plate 1.8 mm thick were taken at two wave-lengths (2540 and 3130A) by means of a thermopile. A smooth curve was constructed which passed through these two points and coincided in the visible region with the transmission curve as calculated from the index of refraction of fused quartz. It was assumed that in the visible region there was no true absorption. The values taken from the curve so constructed are given in Table I.

Table I

Energy calibration of the spectrum.

t denotes the fraction of the energy transmitted by the first quartz plate; t' the energy in the tube per unit energy outside when the light goes straight through the tube.

λ (angstroms)	t	t'	Energy (in ergs/sec.) outside	after traversing quartz plate	after reflection from 2nd plate
2399	.805	.869	9.4	7.6	8.16
scattered			6.9	5.6	
2525, -35, -37, -39	.823 (obs.)	.887	33.4	27.4	29.67
2804	.857	.920	17.9	15.3	16.47
2967	.874	.940	23.4	20.4	22.00
3022, -8	.880	.946	41.3	36.3	39.1
scattered			5.2	4.6	
3126, -32, -45	.887 (obs.)	.953	82.3	73.0	78.3
scattered			5.0	4.4	
3342, -52	.900	.963	15.8	14.2	15.2
3650, -56, -63, -80	.916	.979	127.6	116.7	124.8
4047, -78	.927		47.2	43.7	
4348, -59	.930		71.9	66.7	
5461	.931		73.7	68.6	
5769, -90	.931		93.7	87.2	
5804, -19					
6152, 6232	.932		4.3	4.0	

When the light goes straight through the tube and is partially reflected at the second plate the flux of energy through the tube is $t(1+r+ra^2)$,

[16] Hildebrand, J. Amer. Chem. Soc. **40**, 45 (1918).

where t is the fraction transmitted by the first plate (taken from the curve already constructed), r is the reflection coefficient and a is the fraction transmitted at each face. This second series of values is also given in Table I, which in addition contains calibration of the spectrum taken from Fig. 3.

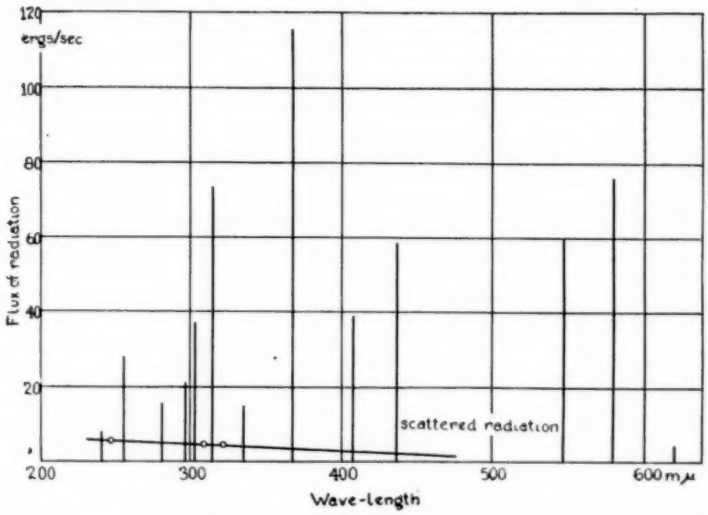

Fig. 3. Flux of radiation from a 225 watt quartz mercury arc 25 mm from a 10.1 by 0.75 mm entrance slit of the spectrograph, after passing through spectrograph. The slant line near the bottom of the figure refers to the scattered radiation.

The last five values in the next to the last column of Table I have been corrected by multiplying by 0.9 to take account of the fact that a different second slit was used in the last part of the experiment which did not cut off the stray light at the top and bottom and a little of the image itself, while it did in the calibration. This column is the one used for the calculation of the efficiency of the photoelectric effect of the caesium-gold alloy. The last column was used in calculating the efficiency of photo-ionization in the caesium vapor.

TABLE II

Ionization of caesium vapor.

Average temperature 166°C; potential of opposite plate = +3.0 volts.

Wave-length (Angstroms)	Grid potential (volts)	Current (amp.)	Ions/cc/sec.	Ions/cc/erg	Ions/atom/erg $=B$	Temp. (°C.)
2399	−.67	$.88\times10^{-12}$	10.87×10^{5}	13.32×10^{4}	22.35×10^{-11}	166
2525–35–37–39	−.67	2.98	35.4	11.94	20.10	167
2804	−.67	1.09	12.08	7.34	12.33	166
2967	−.50	3.12	33.65	15.27	25.00	
3022–8	−.43	4.68	49.8	12.74	21.40	
3126–32–45	−.19	15.37	158.5	20.25	34.10	166
3342–52	−.19	.16	1.57	1.03	1.73	166
3650–56–63–80	−.19	.84	7.77	.62	1.04	

(b) *Ionization of caesium vapor.* In Table II are shown the results for caesium vapor at 166°C. A run was also made at 203.9°C which gave similar results. These results are not given because of the possibility that the vapor was not saturated. The ionization current in Table II is corrected for the estimated fraction of the light cut off by condensation of caesium on the front quartz plate. In a second run at 203.9°C condensation was eliminated by placing special non-inductively wound heating coils over the two ends of the tube and keeping them about 10° warmer than the body of the tube. The number of ions per cc per sec. is corrected for the grid aperture by dividing by 0.628. The deflections due to the ionization currents ran as high as 103 mm. The number of ions per atom per erg is of course the ionization efficiency or the Einstein probability coefficient of absorption B. The values of B in Table II are estimated to be in error by not more than 5 percent when

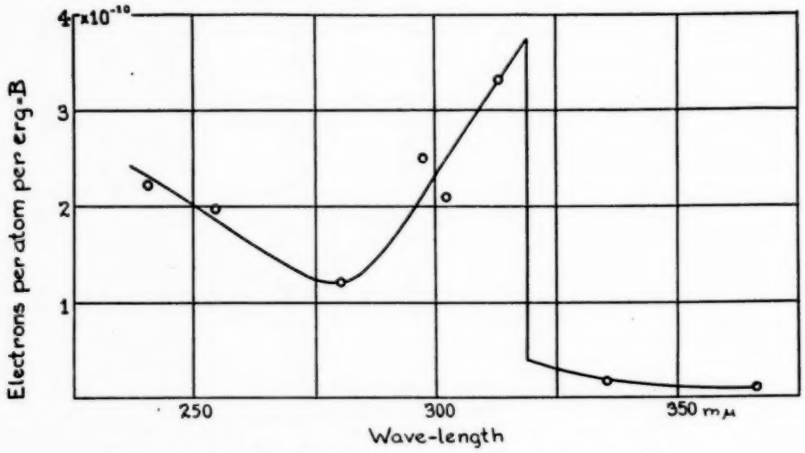

Fig. 4. Ionization efficiency, B, for caesium vapor at 166°C.

relative values are considered, but the possible error in absolute value is probably about 25 percent.

The values of B are plotted in Fig. 4. We have drawn the line vertical at 3184A as we believe it to be. The ionization for wave-lengths greater than this threshold rises slightly to meet the foot of the line. Had it been possible to obtain more points in this region it is probable that the curve would not have been smooth but would have consisted of a succession of peaks gradually rising in height and number as 3184A is approached. This would be accounted for by the completion of ionization of excited atoms by thermal impact. From Fig. 3 it is seen that the spectrograph scattering at 3350A is 5.5 percent of the energy at 3130A. If all the scattered light came from this wave-length all the ionization apparently due to 3350A would be accounted for by the spectrograph scattering. Scattering at 3660A is 4.9 percent of the energy at 3130A and this would account for more than the observed ionization. Of course all the scattered light does not come from 3130A.

The shape of the curve is rather uncertain because this and only one other successful run were obtained before the tube cracked. However, for wave-lengths less than 3184A the shape of the curve checks qualitatively with those of the curves obtained by Mohler, Foote and Chenault and also with the shape of the absorption curves of Harrison. The absolute values of the efficiency are here given for the first time. At 3184A it is seen that the Einstein probability coefficient is about 4×10^{-10} electrons per atom per erg. The minimum occurs at 2800A and is about one-third of the above maximum. Our run at 204°C gave one-fifth and Mohler, Foote and Chenault's results give one-eighth for this ratio of minimum to maximum. Their results were for higher temperatures. This seems to show that the ratio of minimum to maximum decreases with increasing temperature. They also found the minimum to be at about 2800A although at 230°C it seems to be shifted toward shorter wave-lengths. If this is a true minimum and the curve rises

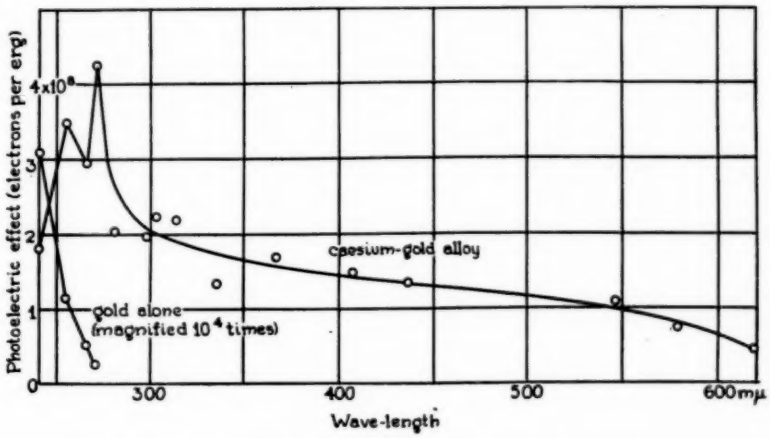

Fig. 5. Photoelectric effect of a caesium gold alloy surface.

again for shorter wave-lengths as our results indicate, then neither a λ^4 nor a λ^3 law could possibly fit.

(c) *Photoelectric effect for caesium-gold alloy.* The first tube made had gold plated electrodes. Because we had trouble with copper chloride fogging the quartz plates when heated after cleaning with HCl, we changed to electrodes made of solid coin gold from Baker. When we finally filled the tube with caesium a drop that had lodged between an electrode and the glass disappeared within a few hours, covering the whole electrode with a light colored alloy. This was at room temperature. When the tube was raised to 200°C very large thermionic currents were observed first in one direction and then another. Upon cooling, the glass was perfectly clean everywhere with no excess caesium in a drop anywhere. The gold was very light colored, indicating that the caesium had readily formed an alloy with it. Since no data on the photoelectric effect of caesium-gold alloys were to be found in any tables a test was run to determine the photoelectric effect, per unit light intensity, of the alloy. The light went slightly obliquely through the

first quartz plate and was carefully directed to the grid. The ionization before the caesium was introduced and then after is plotted in Fig. 5. It will be seen that the current from the gold is about one ten-thousandth of that from the caesium-gold alloy. It seems that despite the precaution of using a liquid air trap, enough mercury vapor got through to make its presence felt. Before the caesium was introduced the current seemed to be entirely due to mercury for it approached zero at the limit determined by Kazda[17] for liquid mercury, namely 2735A. On the other hand it is possible that the limit for gold is about the same as that for mercury. The large hump at short wave-lengths for the caesium-gold alloy is probably due to mercury or gold. The photo-currents from the alloy are about 1000 times the current from 1 cc of vapor at about 200°C. This means that 1 sq. cm of liquid caesium is equivalent to 1000 cc of caesium vapor at 200°C in its absorbing power. The sensitivity of the alloy is rather uniform except near the mercury threshold and thus it could be used as an ultra-violet photometer.

The writer wishes to express his thanks to Professor A. P. Carman who has been so especially generous in the obtaining of equipment and material. He is particularly indebted to Professor Jakob Kunz who suggested the problem and whose advice and inspiration were invaluable. The glass blower, Mr. Anders and the head mechanician, Mr. Tornquist are to be commended for their skill and perseverance.

LABORATORY OF PHYSICS,
UNIVERSITY OF ILLINOIS,
June, 1926.

[17] Kazda, Phys. Rev. **26**, 648 (1925).

MOTION OF STRIAE IN DISCHARGE TUBES*

By L. H. Dawson

Abstract

Curves of the variation with pressure of the position of the striae of the positive column of a discharge tube have been obtained for tubes of 16, 34, and 80 mm diameter with hydrogen, helium, nitrogen, air, carbon monoxide, carbon dioxide and oxygen for pressures from 0.8 to 0.05 mm of mercury. As the pressure is reduced the striae move away from the cathode. The magnitude of the shift for a given pressure change increases rapidly with diameter of the tube. For the 80 mm tube it is about 10 cm for a pressure change of 0.1 mm. Such a discharge tube may be used as a *sensitive and quickly responding pressure gauge*. The shift of the striae is unaffected by variation of the distance between electrodes, or by variation in the current up to 10 m.a. On the other hand increasing the current from 10 to 30 m.a. shifts the striae about 1 cm toward the anode.

Variation with pressure of the length of the cathode dark space. Curves are presented showing the variation in length of the cathode dark space in H_2, He, N_2, CO, O_2, CO_2, and air with pressures from about 0.07 to 0.8 mm. The increase in length is of the order of 1 cm for a decrease of pressure of 0.1 mm in H_2 and He, and about half that amount for the other gases. The change in length is not greatly affected by the diameter of the tube, shape of the electrodes, or current up to 10 m.a.

IN EXPERIMENTS on the discharge of electricity through gases at reduced pressure, apparently little attention has been given to the steady march away from the cathode of the striated positive column as the pressure in the discharge tube is reduced. In the present investigation curves giving the rate of this march with the variation of pressure have been obtained for helium, hydrogen, nitrogen, oxygen, carbon dioxide, carbon monoxide and air. By means of these curves a discharge tube may be conveniently used for the measurement of rapid changes in pressure for the range from about 0.05 mm to 0.8 mm of mercury. At the same time the length of the Crooke's dark space with the different pressures has been measured. Four cylindrical glass discharge tubes connected to a McLeod gauge and the pumps, were used in turn, and were excited by a rectified 500 cycle alternating current. The tubes were 8, 16, 34 and 80 mm in internal diameter with aluminum disk electrodes of diameters approximately those of the respective tubes. The distance between the electrodes was adjustable and for the 80 mm tube this adjustment was made by means of an external electromagnet. All the gases, except helium, were generated chemically, purified and dried when necessary; the helium, however, was taken from a standard Navy tank and contained about 3% of nitrogen. The experiment was pointed out to me by Dr. E. O. Hulburt.

We may recall certain well known phenomena of a discharge tube excited by direct current. When the pressure is around 5 mm of mercury a uniform

* Published by permission of the Navy Department.

glow fills the tube throughout its length. Reducing the pressure, to about 1 mm causes the positive column to appear, as yet unstriated, with the end toward the cathode sharply marked; at the same time the Crooke's dark space with the attendant negative glow and Faraday dark space become visible. With further decrease in pressure the positive column breaks up into striae which, with continuing reduction of pressure, march steadily towards the anode, and finally cease their march and remain stationary until the pressure reaches a point at which the tube becomes non-discharging. When the distance between the cathode and anode is small enough the striae march right into the anode and disappear. The end of the positive column is especially well defined and the position of the striae can be determined in most cases to well within 1 mm. Hydrogen presents peculiarities which the

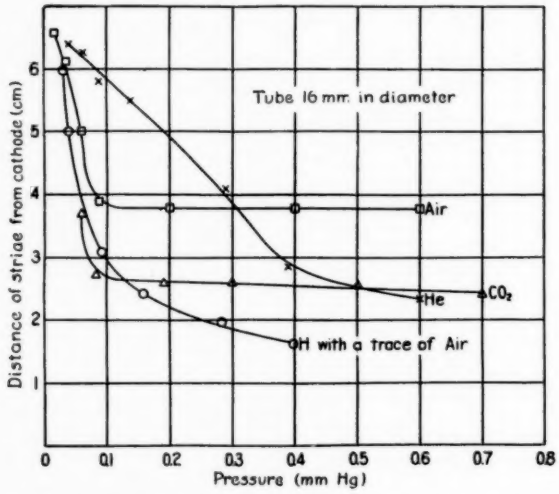

Fig. 1. Motion of striae in a discharge tube of 16 mm diameter.

other gases do not show. At pressures around 1 mm of mercury a set of thin blue convex striae fill the entire tube; and as the pressure decreases this set of striae gradually dissolves and is replaced by a set which is much thicker and farther apart and appear similar to the striae of other gases. This set persists down to the point at which measurements are impossible.

With the 8 mm diameter tube, the striae, although sharply enough defined, did not move very much with change in pressure the total travel being approximately 3 mm for pressures from 0.8 to 0.05 mm of mercury. This smallness of motion was curious for one often sees rather extensive motions of the striae in complex discharge systems of tubes of this size. With the 16 mm diameter tube the character of the striae march is shown in the curves of Fig. 1, where the abscissas are the pressures in the discharge tube in mm of mercury and the ordinates are the distances of the first striation of the positive column from the cathode. The striations in pure hydrogen were found to flicker about in an erratic manner and no exact measurements could be made. With a trace of air in the hydrogen the striae were steadier and the curve for this case is shown in Fig. 1.

Fig. 2. shows the behavior of the striae in the 34 mm diameter tube; as in Fig. 1, the ordinates are the distances of the first striation from the cathode. It is seen that the curves for hydrogen and helium lie apart from those of the heavier gases. Whether the curve for pure helium would be the same as for the helium of Fig. 2 which contained about 3% of nitrogen cannot be stated. The curves come to an end at both the lower and higher pressures because of the disappearance of the striae. The displacements of the second, third and fourth striation were slightly greater than those of the first. With a

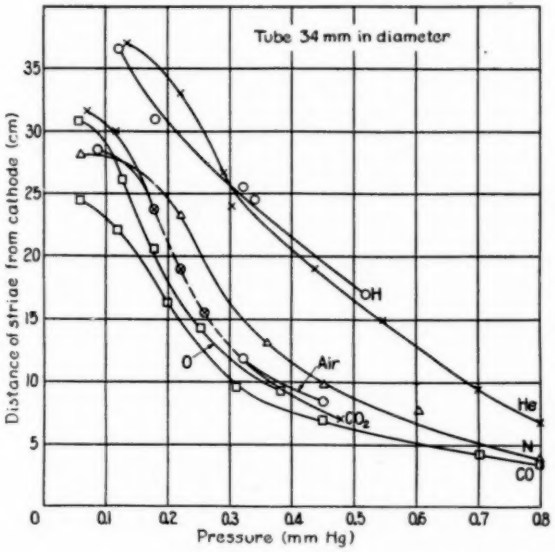

Fig. 2. Motion of striae in a discharge tube of 34 mm diameter.

tube 80 mm in diameter the striae were very steady and the character of the march to the anode similar to that in the smaller tubes as Fig. 3 shows. The total motion was so great that the distance between the anode and cathode, which was 75 cm, could not be made great enough to prevent the striae from marching into the anode. The distance between the electrodes had no effect upon the character of the march of the striae in any of the tubes. Increases of current up to 10 milliamperes produced no effect upon the position of the striae, but an increase from 10 to 30 milliamperes made them move toward the anode about 1 cm.

The striation distance however, is hardly suitable for an absolute measurement of the pressure. This may be determined by an observation of the length of the cathode dark space. Accurate measurements of the cathode dark space as a function of the pressure, the type of gas, etc., are available[1]; but data of the various observations are none too consistent and of any particular observer often have been confined to a rather small pressure range. It was thought, therefore, worth while to repeat the cathode dark space

[1] Aston and Watson, Proc. Roy. Soc., **A84,** 168 (1912), et infra.

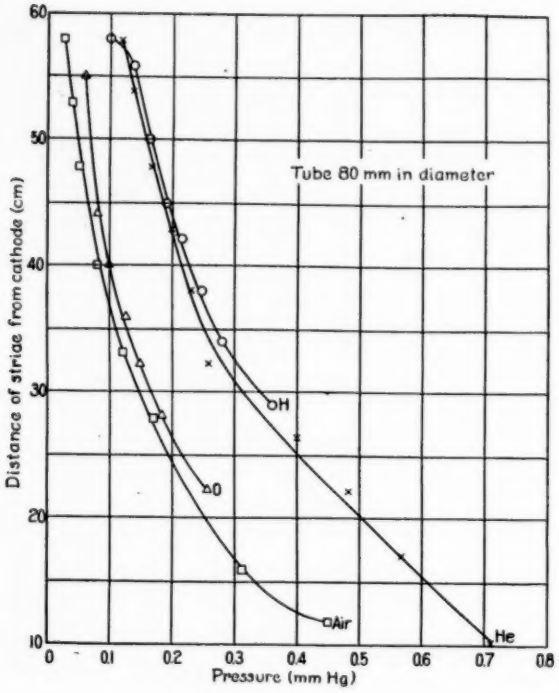

Fig. 3. Motion of striae in a discharge tube of 80 mm diameter.

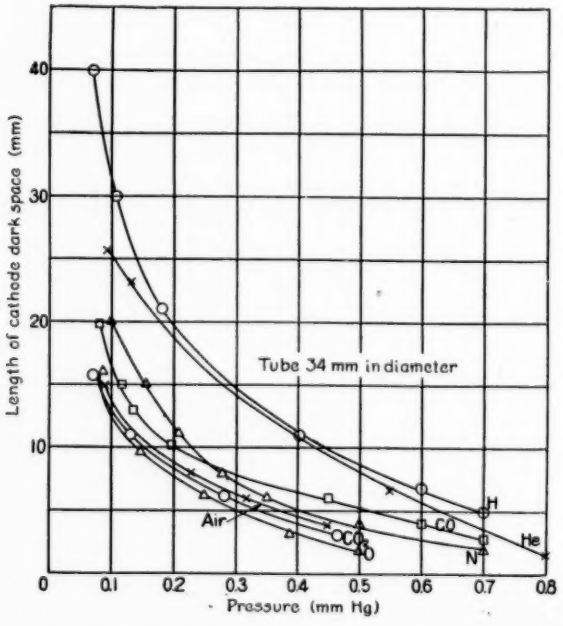

Fig. 4. Dark space pressure curves for a 34 mm diameter discharge tube.

measurements and to present them in a single figure. The results are given in the curves of Fig. 4 for aluminum electrodes and for a current of 10 milliamperes. These curves will serve for a quick determination of the pressures in a discharge tube. The cathode dark space is not greatly affected by the diameter of the discharge tube or the shape of the electrodes, disk or wire for example and by changes in current from 0 to 10 milliamperes. The data of Fig. 4 are in fair agreement with previous measurements.

HEAT AND LIGHT DIVISION,
NAVAL RESEARCH LABORATORY,
April 15, 1927.

PRESSURES IN DISCHARGE TUBES*

By W. H. Crew and E. O. Hulburt

Abstract

Temperature and percentage dissociation of He, H_2, O_2, N_2, air, CO and CO_2 as functions of pressure and power input in discharge tubes.—The increase in pressure of a gas in a discharge tube due to the discharge has been measured for pressures from about 0.1 to 20 mm of mercury for helium, hydrogen, oxygen, nitrogen, air, carbon monoxide and carbon dioxide. The pressure increase is regarded as due to two chief causes, one, the increase in temperature of the gas, and another, the dissociation of the molecules of the gas into atoms or less complex molecules, and has been used to determine the temperature and the dissociation. Two discharge tubes were used in turn, one 300 cm in length and 9 mm in internal diameter, the other 80 cm x 34 mm. Pressures below 1 mm of mercury were measured by a striation gauge, which was a second discharge tube (joined to the main tube) excited by direct current calibrated so that the shift of the striations of the positive column with pressure was known. Pressures from 2 to 20 mm were measured with an oil manometer. With helium the temperature increment above the temperature with no discharge, about 300°K, calculated from the pressure increased linearly with the power in the discharge tube, being about 11° and 22°C with 500 and 1000 watts, respectively, in the long tube, and 14° with 500 watts in the shorter tube. With moist hydrogen the pressure increments, corrected for temperature, gave for γ, the concentration of the hydrogen atoms (i.e. the number of atoms divided by the number of atoms plus molecules) values which increased rapidly with the power to about 400 watts for the long tube and pressures below 1 mm of mercury, being thereafter appreciably constant; the values of γ for 150 watts were 50 to 70% and for powers above 400 watts were close to 100%. For the shorter, larger diameter tube γ was not so great as in the long tube, due to the fact that the power per unit area was less. With dry hydrogen γ was less. All in all, the atomic concentrations were in exact accord with spectroscopic inferences. For oxygen γ rose to values as high as 60% at pressures below 0.25. For nitrogen, carbon monoxide and carbon dioxide γ was close to zero. These conclusions are based on the assumption that few complex molecules were formed, such as H_3, N_3, O_3, etc. The results with condensed discharges were roughly the same as with uncondensed currents. The higher pressure measurements, from 2 to 20 mm, indicated discharge temperatures as high as 300°C, but could not be used to determine γ becuse of uncertain temperature corrections. A new striation phenomenon with condensed discharges at these pressures is described.

WHEN an electric current is passed through a gas in a discharge tube one would naturally expect the pressure of the gas to increase, and it actually does increase, but to our knowledge no one has troubled to observe even this simple fact or to investigate the question in a systematic way. In the present experiments the increase of pressure in a discharge tube due to the discharge has been measured for those pressures normally occurring in discharge tubes, from about 0.1 to 20 mm of mercury, for seven gases, helium, hydrogen, oxygen, nitrogen, air, carbon monoxide and carbon dioxide. The pressure increase is regarded as due to two chief causes, one, the increase

*Published with the permission of the Navy Department. Read before the National Academy of Sciences, April 26, 1927.

in temperature of the gas, and the other, the dissociation of the molecules of the gas into atoms or less complex molecules. The observed pressure increments have therefore been used to determine the temperatures and the amounts of dissociation of the gas in the discharge. The main interest of the present investigation is found in the pressure range below 1 mm of mercury, where it has been possible to draw conclusions as to the amount of dissociation, for it has turned out that, although the pressures have been measured without difficulty for the higher pressures, the temperature calculations, and hence the dissociation percentages, in this range are uncertain.

We adopt the view that it is entirely proper to speak of the "temperature" of a gas in the electrical discharge, although this has been questioned because of a possible lack of, or perhaps an unusual sort of, thermodynamic equilibrium. Certainly one can observe and measure the pressure definitely enough, and this implies a definite temperature, or a definite average temperature, of the molecules or the atoms of the gas. Further, there need be no confusion caused by the possibility of the presence of groups of high velocity electrons to which have been ascribed very high temperatures in some cases.[1]

Experimental details. A long slim discharge tube, 300 cm in length and 9 mm in internal diameter, and a large tube, 80 cm in length and 34 mm in internal diameter, were used in turn. These will be referred to as "tube *A*" and "tube *B*," respectively. The discharge tube was connected to the pumps, the supply of gas, the pressure gauge, and the source of electrical power; aluminum electrodes were used. For uncondensed currents the energy was supplied directly to the tube from a 1 KW, 30 KV, 25 cycle transformer, the power in the tube being taken to be the product of the current and voltage at the electrodes. The correctness of this was verified to within about 10%, over the range of powers, pressures and gases of the experiments for both tubes *A* and *B*, by simultaneous observations of the power with the ammeter and voltmeter and with a potential transformer (Weston, Model 311, ratio of transformation 60 to 1) and a wattmeter (Weston, Model 810). For condensed discharges a 0.012 microfarad condenser, charged by the 25 cycle transformer, was allowed to discharge through the tube, a quenched gap being in series with the tube to insure abrupt discharges. Since the condensed discharges were oscillatory, although heavily damped, the power in the tube could not be determined by simple electrical measurements.

For the measurements of pressures below 0.8 mm of mercury a second discharge tube joined to the main discharge tube served as a pressure gauge. This was a tube 34 mm in internal diameter, with disc aluminum electrodes 40 cm apart and excited by rectified current (500 cycle) of strength about 8 milliamperes. The shift of the striations of the positive column along the tube and the length of the cathode dark space as functions of the pressure for the gases in question have recently been measured in this laboratory

[1] Langmuir, Phys. Rev. **26**, 285 (1925).

by L. H. Dawson.[2] Therefore, observations of the cathode dark space and the striations in the gauge tube could be translated into pressures by means of Dawson's curves. Fig. 1 shows the arrangement of tube *B* and the pressure gauge tube. The length of the dark space was generally used to give the pressure with no discharge in the main tube, and the shift in the position of the first striation (the striation nearest the cathode) of the positive column to give the change in pressure when the discharge was turned on. Occasionally the electric fields of powerful condensed discharges in the main tube obliterated the striations of the gauge tube. When this occurred the pressure and pressure changes were observed entirely by means of the cathode dark space in the gauge tube. All pressures have been recorded in millimeters of mercury.

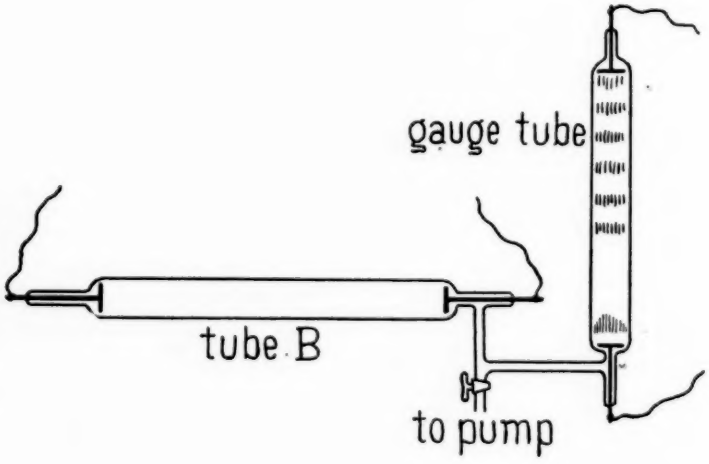

Fig. 1. Arrangement of tube *B* and the pressure gauge tube.

The measurement of pressure changes by means of the striations in the gauge tube deserves a brief description. The method is visible, quick, and one which does not contaminate the main discharge tube with a foreign gas; all of these advantages are not shared by a mercury gauge, for example. Upon reducing the pressure in the gauge tube to about 10 mm of mercury the Crookes dark space, negative glow, Faraday dark space, and positive column appear. At this pressure the positive column is either uniform or broken up into narrow striations, usually rather ill defined, which are often tilted or V-shaped. Upon reducing the pressure below 1 mm these striations change to, or make way for, another set of wider striations, usually symmetrically curved with respect to the axis of the tube, but well defined, particularly those nearest the cathode. It is these which are used to indicate changes in pressure, for with a further reduction in the pressure they move away from the cathode along the tube. They become indistinct and some-

[2] Dawson, Phys. Rev. **30**, 119 (1927).

times jump about[3] when the pressure falls below about 0.05 mm of mercury. Therefore the method is only useful for a limited range of pressures, from about 0.8 to 0.05 mm of mercury, the exact range varying somewhat with each gas. The striations move roughly linearly with the pressure in the central portion of the useful range, for example being displaced from the cathode by 30 mm for a pressure change from 0.330 to 0.250 mm of mercury in helium and 0.285 to 0.250 in oxygen, for a gauge tube 3.4 cm in diameter (the striation shift increases with the diameter of the tube). The shift, if it is not too large, is about the same for any of the first three or four striations. Since the shift could be observed to within 1 mm, pressure changes of 0.005 mm of mercury were measurable with fair accuracy; observed shifts from 2 to 40 mm were met with. When the pressure was changed and a striation shift occurred the current through the gauge tube changed as well. This introduced an error, for the striations moved with changes in current. This error, however, was negligible as long as the current was small, below 10 milliamperes; it could be avoided, if necessary, by adjusting the current through the gauge to a constant value at all times.

An oil manometer was used to measure the pressures from about 2 to 20 mm of mercury. There was thus a region of pressures from 0.8 to 2 mm of mercury, between the upper limit of the striation gauge and the lower limit of the oil manometer, in which no observations could be made. However, as will appear later, the higher pressure observations have been uncertain of interpretation. The high pressure observations were made only with tube B, none were possible with tube A, the tube being so long that no discharge occured at these pressures with the potentials available.

Formulas. Denote by v' the volume of that portion of the main discharge tube which was filled with the discharge; its temperature is T_1 degrees Kelvin when the discharge is off and T_2 when it is on. The remaining volume of the system, comprised by the gauge, connecting tubes, etc., is denoted by v; its temperature is taken to be T_1 at all times. The pressures in the system with and without the discharge are p_2 and p_1, respectively. We assume the gas to be diatomic and that in the discharge a certain proportion of the molecules of the volume v' are dissociated into atoms. This causes an increase in pressure which forces some of the molecules and atoms from v' to v. Those atoms which pass from v' to v, being no longer in the discharge, are assumed to recombine. So that after a steady state has been reached with the discharge running, the pressure of the system is increased, there are only molecules in v and there are (or may be) both molecules and atoms in v'.

Let n_1 and n_1' be the number of molecules in v and v', respectively, with no discharge in v', and n_2 and n_2' the respective numbers of molecules with the discharge. Let n_2'' be the number of atoms in v' when the discharge is going. Then

$$n_1+n_1'=n_2+n_2'+n_2''/2. \tag{1}$$

[3] Terroux, Phys. Rev. **28,** 1242 (1926).

From the general gas equation,

$$\left.\begin{aligned} p_1 v &= R n_1 T_1, \qquad p_1 v' = R n_1' T_1, \\ p_2 v &= R n_2 T_1, \quad p_2 v' = R(n_2' + n_2'') T_2. \end{aligned}\right\} \tag{2}$$

The concentration γ of the atoms in the volume v' is defined by

$$\gamma = n_2''/(n_2' + n_2''). \tag{3}$$

From (1), (2) and (3), we find

$$\gamma = 2\left\{1 - \frac{T_2}{T_1}\left[\frac{p_1}{p_2}\left(\frac{v}{v'} + 1\right) - \frac{v}{v'}\right]\right\}. \tag{4}$$

For no dissociation $\gamma = 0$ and (4) gives

$$T_2 = T_1\left[\frac{p_1}{p_2}\left(\frac{v}{v'} + 1\right) - \frac{v}{v'}\right]^{-1}. \tag{5}$$

For the long slim tube, tube A, v and v' were 535 and 243 cc, respectively; then $v/v' = 2.20$. For the large tube, tube B, with the striation gauge v and v' were 386 and 715 cc, respectively; and $v/v' = 0.54$. For tube B with the oil manometer $v/v' = 0.52$. The accuracy of the measurement of p_2 would be improved by making v as small as possible compared with v'; this would mean making the volume of the gauge tube small. However, the shift of the striations was small in a tube of small diameter, the shift in a tube 30 mm in diameter being roughly ten times that in a tube 10 mm in diameter, and for this reason a rather large gauge tube was selected.

Method of the determination of the temperature in the discharge. The concentration of the atoms γ has been determined from (4) with a knowledge of p_1, p_2, v, v', T_1 and T_2. All of these have been measured directly except T_2, which has been determined directly only in the case of helium. For the other gases T_2, the average temperature in the discharge, has been found by calculation from the value of T_2 for helium at the same power and pressure. The values of γ which have been obtained depend upon the correctness of this calculation, but not seriously, all the values of γ for hydrogen, and the high values of γ for the other gases being hardly affected at all by allowable uncertainties in T_2.

When the discharge is running the gas in the discharge tube is receiving electrical energy and is dispensing this energy to the walls of the tube. A steady thermal state is assumed and the energy lost by the gas in the form of radiation is assumed to be negligible compared with that transmitted to the walls by conduction and convection. At the lower pressures, below 1 mm of mercury, the discharge filled the entire tube and the gas therefore received energy uniformly across a cross-section of the tube. The gas is probably thoroughly circulated about the tube by forced convection due to the discharge. Further, the process of convection is much faster than that of conduction. For all these reasons the temperature T_2 is taken to be constant across the cross-section of the tube except in a film, relatively thin,

lying next to the glass walls, which owes its existence to the viscosity of the gas. In this film the temperature descends to T_1 that of interior surface of the wall; and it is in this film that the energy passes to the wall by conduction.[4] T_1 is approximately the average temperature of the glass wall, since the thermal conductivity of glass is great compared with that of a gas. Upon putting the electrical energy q supplied per second to 1 cm length of the tube equal to that lost by conduction across the film, we obtain

$$q=2\pi r\theta(T_2-T_1)/\Delta z, \tag{6}$$

where r is the radius of the tube, θ the thermal conductivity of the gas and Δz the thickness of the film. Δz is assumed to vary directly with the viscosity κ of the gas and inversely with the momentum of the convection currents. Thus,

$$\Delta z \sim \kappa/\rho u, \tag{7}$$

where ρ is the density of the gas and u the mass velocity of the convection currents. κ is independent of the density and the temperature of the gas.[5]

We may now compare the discharge temperatures T_2-T_1 and $T_2'-T_1$ for two different gases in the same discharge tube at the same pressure excited with equal electrical powers. Denoting the two gases by primed and unprimed quantities, respectively, we have from (6) and (7) that

$$(T_2-T_1)/(T_2'-T_1)=\kappa\theta'\rho'u'/\kappa'\theta\rho u.$$

This relation holds equally well for the discharge temperatures of the same gas at two different pressures in the same discharge tube with the same electrical power. Into this expression we put $\theta=1.6027\ \kappa C_v$, where C_v is the specific heat at constant volume,[6] and obtain

$$(T_2-T_1)/(T_2'-T_1)=C_v'\rho'u'/C_v\rho u. \tag{8}$$

Since the energy flow into and out of the gas is the same in the two cases we may assume equal kinetic energies of the convection currents. Hence $\rho u^2=\rho' u'^2$, and (8) becomes

$$(T_2-T_1)/(T_2'-T_1)=(C_v'/C_v)(\rho'/\rho)^{1/2}. \tag{9}$$

By means of (9) the average temperature T_2 of any gas, for example, oxygen, in the discharge tube at a given pressure and power was calculated from the observed temperature T_2' for helium at the same pressure and power. The value of T_2 was then used in (4) to calculate γ. In the case of condensed discharges T_2 was calculated from T_2' for helium at the same pressure and current; a procedure somewhat questionable, but probably not conducive to serious error.

Formula (9) is based on assumptions admittedly imperfect. If, instead of assuming (7), we assume that the thickness Δz of the film varies inversely

[4] Cf. Langmuir, Phys. Rev. **34**, 401 (1912).

[5] Jeans, "The Dynamical Theory of Gases," page 252, 1904.

[6] Jeans, loc. cit., page 266.

with the kinetic energy $\rho u^2/2$ of the convection currents, then instead of (9) we obtain

$$(T_2-T_1)/(T_2'-T_1)=C_v'/C_v. \tag{10}$$

Neither (9) or (10) is exact. We have written both merely to illustrate that they, or some closely similar formula, may be regarded as workable approximations. The derivation of the true expression must await more precise knowledge of the temperature distribution in the discharge than is available at the present time. For all values of γ for hydrogen and for γ greater than 50% in the case of the heavier gases, there is a difference of only a few percent in γ determined from (9) and (10). For low values of γ with the heavier gases there is a greater difference. For example, with carbon dioxide in tube B at 300 watts, p_1 was 0.360 and p_2 0.374 mm of mercury; γ was +2% when (9) was used and −14% when (10) was used. Again, with nitrogen at 510 watts, $p_1=0.510$, $p_2=0.565$, and γ was +16 and −5% with (9) and (10), respectively. In these cases γ was considered to be close to zero. On the other hand, with oxygen in tube A at 150 watts, $p_1=0.118$, $p_2=0.133$ and γ was 72 and 68% from (9) and (10), respectively.

Certain further difficulties of an experimental nature in dealing with the temperature effects must be mentioned. When the discharge was started in the main tube the pressure increased quickly for the first third of a second, (as shown by the shift of the gauge striations) and thereafter crept up more slowly. The first quick change was ascribed to the heating and the dissociation of the gas and the later slow small change to the warming of the tube walls. Approximate equilibrium was reached in a few seconds. For this reason the measurement of p_1 and p_2 was repeated several times, and an average taken after fairly steady temperature conditions were attained, with a pause between readings neither too long nor too short. At pressures below 1 mm of mercury the temperature of the glass walls was usually about 10 to 30°C above that of the room, but near the electrodes the glass was hotter than this. In the lower pressure calculations T_1 has been taken to be 300°K; however, small errors in its value do not affect the values of γ appreciably.

In the higher range of pressures the assumptions underlying (9) break down because of the fact that the discharge no longer filled the entire cross-section of the tube as it did at the lower pressures, but was confined to the central region of the tube. For example, in tube B with internal diameter 34 mm, the diameters of the path of the discharge were 34, 34, 25, 20, 16, 13, 12, 11 and 10 mm for pressures 0.2, 0.6, 2, 3.5, 5, 8, 10, 13 and 18 mm of mercury, respectively, for a constant current of 100 milliamperes and an uncondensed discharge. Since this was the case it was not correct to assume that the temperature was uniform across the tube; the temperature was manifestly higher in the center, and no certain estimates may be made as to the character of the convection and conduction of the energy across the tube. The observations at the higher pressures are described in the last section.

Helium. The helium was taken from a Navy cylinder and was passed through drying bottles without further purification; it contained about 3% of nitrogen. The values of $T_2' - T_1$ (the prime denotes helium in accord with the notation of (9)), calculated from the observed pressures by means of (5) with $T_1 = 300°K$, are plotted in degrees Centigrade as ordinates against the powers as abscissas in curves 1 and 2, Fig. 2, which refer to tubes A and B, respectively. The curves are for uncondensed discharges. It is seen that $T_2' - T_1$ increased linearly with the power in the tube. The increase was found to be about the same for the pressures from $p_1 = 0.2$ to 0.7 mm of mercury, although the observations indicated that the increase was less at the higher pressures. This would be in agreement with (9) rather than (10). However, the error of experiment was too great to permit a decision in favor of one or the other of these formulas. In illustration, with helium in tube A at 1014 watts, $T_2' - T_1$ was $20° \pm 4°C$ for $p_1 = 0.70$ and $25° \pm 4°C$ for $p_1 = 0.318$; and (9) would have it that $T_2' - T_1$ varied inversely with the

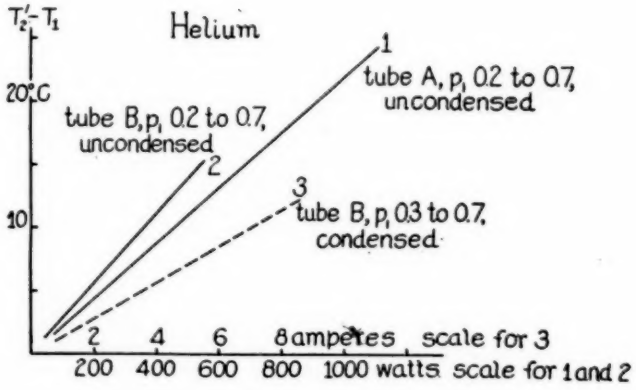

Fig. 2. Temperature increase in a helium discharge tube as a function of the power input.

square root of the pressure, whereas (10) that $T_2' - T_1$ was independent of the pressure. The values of $T_2' - T_1$ from curves 1 and 2 have been used in the calculations for the other gases. The values are of the order of magnitude of those observed by Seeliger[7] with a thermocouple. It is hardly necessary to remark that in this experiment we are dealing essentially with a constant volume helium thermometer. Curve 3, Fig. 2, gives the temperatures of the helium in tube B excited by condensed discharges.

From the data of curves 1 and 2, Fig. 2, the thickness Δz of the conducting film of gas may be calculated. We assume that the electrical power is expended uniformly along the tube; this is an approximation, for the potential gradient along the tube is probably not uniform, but greater close to the electrodes and with minor variations along the positive column. For tube A with 400 watts, $T_2' - T_1$ from curve 1 is 8.7°C, $q = 400/300$ watts, $r = 0.45$ cm and $\theta = 34 \times 10^{-5}$ calories. These numbers in equation (6) give $\Delta z = 0.025$

[7] Seeliger, Phys. Zeits. **27**, 732 (1926).

cm. Similarly, for tube B with 400 watts, $T_2' - T_1$ from curve 2 is 11.3°C, and $\Delta z = 0.026$ cm. This shows that Δz is independent of the radius of the tube, which is as it should be. The film thickness is seen to be small; this is in keeping with the conditions assumed in the discharge, i.e. convection currents which produce a constant temperature across the tube except for the thin film next to the walls where conduction holds sway.

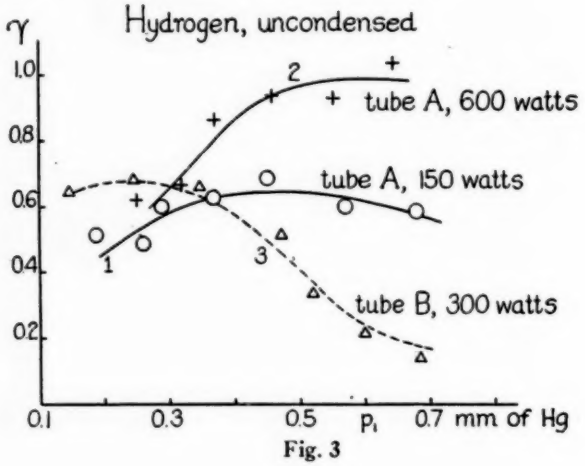

Fig. 3

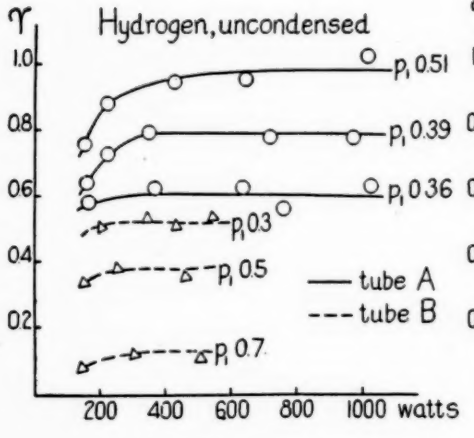

Fig. 4

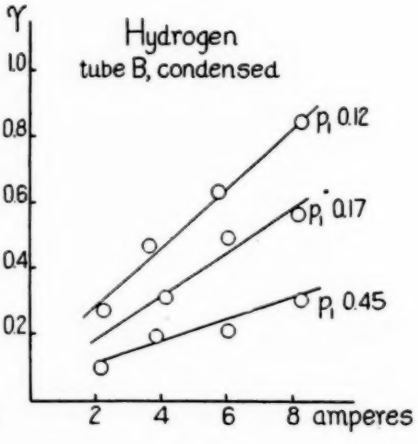

Fig. 5

Fig. 3. Variation with pressure of the percentage dissociation of hydrogen in a discharge tube.
Fig. 4. Variation with power input of the dissociation percentage of hydrogen in a discharge tube.
Fig. 5. Variation with current of the dissociation percentage of hydrogen in a discharge tube.

It is scarcely necessary to point out that the idea (which is manifestly untrue anyway) of conduction alone, and no convection, is not in keeping with the data of curves 1 and 2. For, if we suppose that the energy s, supplied per unit volume, leaves by conduction through the gas, the temperature t at a distance r from the center of the tube is given by $\pi r^2 s = -2\pi r\theta(\partial t/\partial r)$. Upon integrating, this yields $t - t_0 = s(r_0^2 - r^2)/4\theta$, where $t = t_0$ when $r = r_0$,

r_0 being the radius of the tube. The average value of $t-t_0$ across the tube is then, $\bar{t}-\bar{t}_0=sr_0^2/8\theta=q/8\pi\theta$, where $q=s\pi r_0^2$ is the energy supplied per unit length of the tube. This says that $\bar{t}-\bar{t}_0$, or in our former notation $T_2'-T_1$ is independent of the radius of the tube, which is contrary to curves 1 and 2, Fig. 2.

Hydrogen. Hydrogen, obtained from hydrochloric acid and zinc and moistened by passing through distilled water, was introduced into the discharge tubes through a long capillary. The values of γ for hydrogen, calculated from the observed pressures by (4) and (9) using the values of $T_2'-T_1$ for helium from Fig. 2, are given in Figs. 3, 4 and 5. The dissociation percentages are in entire agreement with qualitative spectroscopic evidence. Curve 2, Fig. 3, for tube *A* indicates that there is an optimum pressure around 0.5 mm of mercury for bringing out the atomic lines in greatest purity; this is in accord with Wood's[8] observations on the long tubes. With 600 watts in tube *A* at this pressure sixteen lines of the Balmer series appeared on plates taken with a fifteen minute exposure on the large quartz spectrograph. Curve 3, Fig. 3, for tube *B* shows the increase in the number of atoms as the pressure was lowered, the power being maintained constant. This increase conformed exactly with the appearance of the discharge, which at $p_1=0.7$ was a blue pink and which became progressively redder as the pressure was lowered, until at $p_1=0.3$ the atomic lines were very strong and the molecular lines relatively weak. As seen from the curves for tube *B* in Figs. 4 and 5 higher values of γ were found with condensed than with uncondensed discharges, which agrees with the known suppression of the molecular spectrum in the condensed discharge. The comparison is rather indefinite, because the power of the condensed currents was not known; however, the maximum powers used in the two types of tubes were probably not greatly different, as judged by the heating of the tube and the energy put into the primary of the 25 cycle transformer. With dry hydrogen γ was less than with moist hydrogen. The pressure changes indicating a decrease in γ were very striking to see when the tube was filled with moist hydrogen and operated at high power and low pressure long enough for it to pass from the crimson atomic condition to the white molecular stage. This transition is due, according to Wood and Langmuir, to the burning off of the protective film of water vapor or oxygen from the walls of the tube, which thereupon catalyze the atoms to the molecular state.

In general we may say that if the Balmer lines were strong and if the prominent molecular lines between Hα and Hβ were difficult to see with a visual spectrograph or transmission grating, then γ was certainly greater than 60% and was probably greater than 80%. In a pinkish discharge, in which both spectra were easily visible, γ was 30 or 40%. If the discharge was blue γ was less than 20%. These statements all depend upon the assumption that no complex molecules, such as H_3, were formed in appreciable numbers.

[8] Wood, Proc. Roy. Soc. **A97**, 455 (1920).

For mixtures of atoms and molecules one might be uncertain whether to use the atomic or the molecular constants in (9). This is not a real difficulty, however, for the respective constants give unimportant differences in γ. For example, with a pressure $p_1=0.360$ and 612 watts in tube A, p_2 was 0.400. With $T_2'-T_1=13.4°C$, from curve 1, Fig. 2, for helium at this power and pressure, and with molecular values $C_v=2.43$ and $\rho'/\rho=2$, we find from (9) that $T_2'-T_1=5.84°C$. This in (4) gives $\gamma=0.614$. Similarly, with the atomic values $C_v=3$ and $\rho'/\rho=4$, γ is 0.610.

Oxygen. The oxygen was prepared from water and sodium peroxide and was spectroscopically free of hydrogen and nitrogen. At the high pressures in tube B, however, there was a trace of the green afterglow associated with nitrogen and its oxides; the nitrogen impurity present was believed to be small, for the strong nitrogen bands in the yellow and red were not to be seen. In calculating the dissociation of the oxygen from the observed pres-

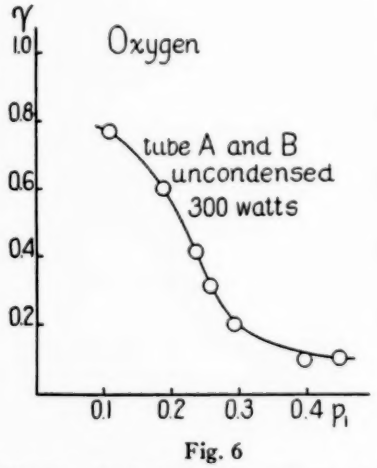

Fig. 6

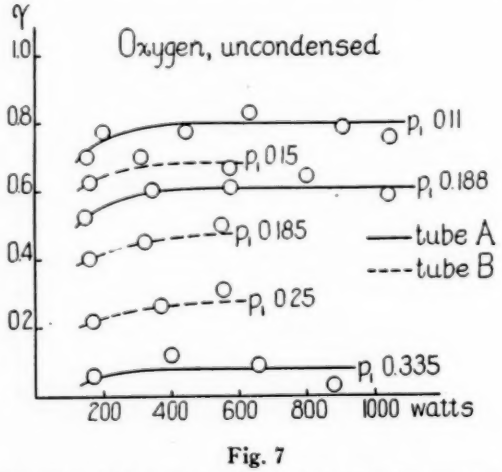

Fig. 7

Fig. 6. Variation with pressure of the dissociation percentage of oxygen in oxygen.
Fig. 7. Variation with power input of the dissociation percentage of oxygen in a discharge tube.

sures it has been assumed that complex molecules, such as ozone, were not found in appreciable quantities. This appears to be a valid assumption for the lower range of pressures at least. The dissociation curves for uncondensed currents are given in Figs. 6 and 7. γ was found to increase with a decrease of pressure, and for pressures below 0.2 mm of mercury to be above 50%; it increased but little with the power. Both tubes gave much the same values for the dissociation. With condensed discharges in tube B, γ varied with the pressure as it did for the uncondensed currents. Indeed, the curve of Fig. 6 represents very well γ as a function of the pressure for eight amperes of condensed current in tube B. In addition, γ varied roughly linearly with the condensed current when the pressure was constant, as in the hydrogen curves of Fig. 5.

Again, just as for hydrogen, the difference in calculating γ for oxygen from the molecular constants and the atomic constants was barely noticeable.

For example with 1050 watts and $p_1=0.188$ in tube *A*, p_2 was 0.214. γ from (9) with the molecular and atomic constants was 0.62 and 0.60, respectively.

Nitrogen. The nitrogen was prepared by heating a solution of ammonium chloride and sodium nitrite, and spectroscopic observations showed that it was free of hydrogen and oxygen. Within the error of measurement and the inexactness of formula (9), the dissociation of nitrogen was found to be close to zero, the values of γ ranging from $+20\%$ to -5% with (9) and a little less with (10). The pressures were from 0.08 to 0.55 mm of mercury and the powers to 1000 watts in tube *A* and 500 watts in tube *B*. Both condensed and uncondensed currents were used. If N_3 molecules were present, the conclusion of no dissociation would have to be modified; but it seems hardly possible that N_3 molecules and nitrogen atoms would occur in all cases in exactly the correct proportions as to conteract each other's effect, the one in decreasing and the other in increasing the pressure. The present experiments indicate that atomic nitrogen is not produced in large quantity in the electric discharge at a fairly low pressure, and therefore that active nitrogen, which signifies its presence by an entrancing yellow-green afterglow, is perhaps the nitrogen molecule. We can not be absolutely certain of this, however, for it may very well be that a few atoms exist and that these are responsible for the nature of the active nitrogen.[9]

Air. Air behaved as a mixture of oxygen and nitrogen, which might be expected. The dissociation values were small, except at the low pressures below 0.25 mm of mercury where values of γ as high as 30% were found. This would mean dissociation values of 50% if γ were reckoned from the partial pressure of the oxygen.

Carbon monoxide and carbon dioxide. These two gases are quickly disposed of. No dissociation was found in them within the error of experiment and the uncertainty of equation (9).

Explanation of the dissociation of the various gases. The dissociation in a gas would be expected to depend primarily upon the dissociation potential of the gas. And, referring only to the effects of electron impacts, in order to acquire the energy requisite to dissociate the molecule, an electron must have a free path which, other things being equal, is the longer the higher the dissociation potential. The dissociation potentials[10] are about 4, 7, 11 and 11 volts for H_2, O_2, N_2 and CO, respectively, and about 24 volts for the dissociation of CO_2 to CO+O. Therefore, in qualitative accord with the observations, hydrogen will be dissociated at the higher pressures, oxygen at lower pressures, and possibly nitrogen, carbon monoxide and carbon dioxide at still lower pressures, below those used in the present experiments. A complete theoretical statement will involve considerations of the energetics of excited molecules and atoms, effects of radiation, etc., as well as the effects of electron impacts.

[9] Cf. Ruark, Foote, Rudnick and Chenault, Jour, Opt. Soc. Amer. **14**, 17 (1927).

[10] Birge and Sponer, Phys. Rev. **28**, 259 (1926).

High pressure observations. As has been said before, the measurements of the discharge pressures from about 2 to 20 mm of mercury were made only for tube B, the potentials available being insufficient to force the discharge at these pressures through the long tube A. At the high pressures the temperatures T_1 of the walls of the tube were sometimes as much as 80°C, and therefore the observed values of T_1 in each case have been used in (5) together with the observed pressures p_1 and p_2 to calculate the discharge temperatures $T_2 - T_1$. With helium excited by uncondensed currents the values of $T_2 - T_1$ are given in the lower set of curves of Fig. 8. These are average values throughout the tube. The temperature of the gas along the center of the tube, where the discharge passed, was of course greater than that in the regions between the discharge and the walls, and was therefore considerably greater than the average temperature. This was supported by the fact that at the

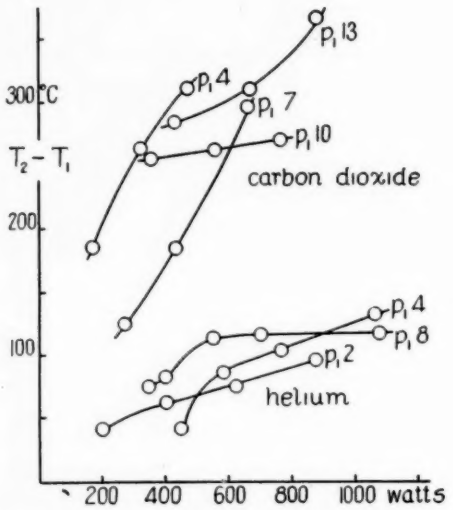

Fig. 8. Variation with power input of the temperature increase of the gas in a discharge tube.

higher powers the aluminum electrodes were heated to redness in a few minutes.

The upper set of curves of Fig. 8 are for carbon dioxide, and were calculated on the assumption that no association or dissociation of the molecules took place. With the same assumption the temperature curves for oxygen, nitrogen and carbon monoxide were much the same as those of carbon dioxide; the curves for hydrogen were like those of helium. The temperatures of the respective gases were about the same with condensed as with uncondensed discharges. The fact that the temperatures of the helium and hydrogen were lower than those of the heavier gases is to be ascribed to their higher specific heats and lower densities.

Very curious striations appeared in tube B when filled with nitrogen at pressures from 4 to 10 mm of mercury and excited by condensed discharges. Photographs of the tube with the striations are given in Fig. 9; the strips

a, *b* and *c* are for pressures 8, 6 and 4 mm of mercury, respectively. The bright pink core of the discharge appeared exactly like a stretched string vibrating at some high harmonic, the nodes and loops are plainly visible in the pictures. Enveloping this was the yellow-green glow of active nitrogen gathered into broad steady striations which under certain conditions of pressure and intensity of discharge were dark at the nodes and bright at the loops of the central core (as in Fig. 9), and under other circumstances bright at the nodes and dark at the loops. In strip *a*, pressure 8 mm, the central core was like a spark, and whipped about the tube breaking into different sets of harmonics. In strip *b*, at a little lower pressure, 6 mm, the central core was a glow discharge, not a spark, and was steadier. In strip *c*, pressure 4 mm,

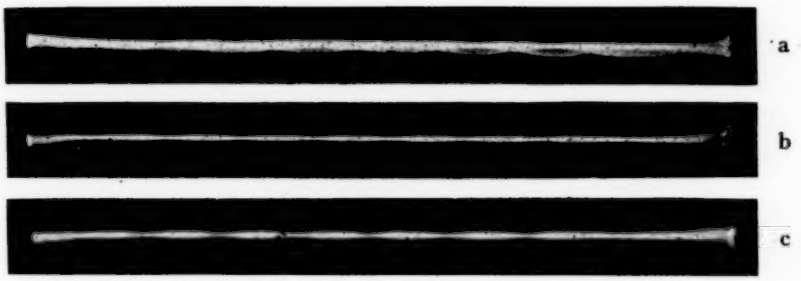

Fig. 9. Striations in nitrogen with condensed discharges, pressures 8, 6, and 4 mm of mercury for the top, middle and bottom strips, respectively.

the central core was wider. In all the strips the striations were about the same distance apart. The appearance of the striations suggested standing sonic waves, as in a Kundt resonance tube, but changing the length of the tube by moving one of the disc electrodes back and forth along the tube by means of an external magnetic control did not affect the striations as pressure waves would be affected. Further investigation is necessary to an understanding of the phenomenon. The striations did not appear with uncondensed currents. Just as in pure nitrogen the striations occurred in the helium which contained a small amount of nitrogen, and in air. In hydrogen, carbon monoxide and carbon dioxide, all of which were free of nitrogen the central bright core again looked like a vibrating string, under the condensed discharge high pressure conditions, but there was no enveloping greenish sheath.

NAVAL RESEARCH LABORATORY,
WASHINGTON, D. C.
March 26, 1927.

ELECTRONIC STATES AND BAND SPECTRUM STRUCTURE IN DIATOMIC MOLECULES. V. BANDS OF THE VIOLET CN ($^2S \rightarrow {}^2S$) TYPE

By Robert S. Mulliken

Abstract

Theoretical intensity formulas applicable to bands of the violet CN ($^2S \rightarrow {}^2S$) type are obtained (cf. Eqs. 5-7 of text) with the help of the summation rules, assuming Hund's case *b* type of interaction of the electron spin. The equations predict two *Q* branches ($Q_{1,2}$ and $Q_{2,1}$), hitherto unrecognized, which should appear as weak satellite series, one accompanying the familiar double *P* branch, the other, the *R* branch. These *Q* branches should decrease in intensity from their first members. The first $Q_{2,1}$ (or $Q_{1,2}$) line should accompany the otherwise single first line of the *R* (or *P*) branch, all other *P* and *R* lines being truly double; this is in agreement with Hulthén's results on the *B* bands of CaH. For low *j* values in the *P* and *R* branches, the doublet component corresponding to the parallel orientation ($+\epsilon$) of the electron spin vector should be appreciably more intense than that corresponding to the anti-parallel orientation ($-\epsilon$). Treating the doublets (and their satellites) as unresolved single lines, the intensities should be exactly as in $^1S \rightarrow {}^1S$ bands (CuH, HCl). The above predictions seem to be confirmed in the CaH, N_2^+, and violet CN bands. Thus the theory appears to afford a satisfactory explanation of the observed lines and intensity relations in $^2S \rightarrow {}^2S$ bands, removing previous difficulties and uncertainties in interpretation.—Other $S \rightarrow S$ transitions are treated briefly.

The nature of the energy differences between the ^2S terms corresponding to $+\epsilon$ and $-\epsilon$ is considered. In all cases where the order of the terms can be determined, with the one exception of the initial states of the *B* bands of CaH, it is found that $F_1 > F_2$. This suggests that the magnetic field which causes $F_1 \neq F_2$ (developed by the molecular rotation in accordance with Kemble's theory) may be in part that of the nuclei as well as of the electrons.

Introduction

EXCEPT for the fact that each line is (usually very closely) double, bands of the violet CN($^2S \rightarrow {}^2S$) type show the same obvious structure (one *P* and one *R* branch) and intensity relations as the single-line bands of the CuH ($^1S \rightarrow {}^1S$) type. Their doublet character was first explained by Kratzer,[1] who assumed the existence of an electronic angular momentum $\epsilon = \frac{1}{2}$ which could orient itself either parallel or antiparallel ($\rho = \pm\frac{1}{2}$) with respect to the axis of rotation. The probable *necessity* of Kratzer's assumption $\rho = \pm\frac{1}{2}$ in bands of the violet CN type, and of the assumption $\rho = 0$ in bands of the CuH type,—and of $\sigma = 0$ in both types,— has been pointed out in a previous paper.[2] The interpretation of both these classes of bands in terms of Hund's theory[3] of molecular electronic states has been discussed by

[1] A. Kratzer, Münch. Ber., p. 107 (1922); Ann. der. Physik, **71**, 72 (1923).

[2] R. S. Mulliken, Phys. Rev. **28**, 481–506 (1926).

[3] F. Hund, Zeits. f. Physik **36**, 657–674 (1926).

Kemble[4] and by the writer.[5] According to the theory, the quantity ϵ in ^2S states represents (in quantum units) the resultant spin s of the electrons. In most cases s may be attributed to a single outer electron. The coupling of the spin corresponds to Hund's case b (or, equally well, to his case d). Since $\sigma_k = 0$,[4,5] we have $m = j_k$, where j_k is the resultant of m and σ_k. In other words the nuclear rotation has the same quantized values as in ^1S states.

Although the intensity relations in $^1S \rightarrow {}^1S$ bands are now well understood in terms of the new mechanics,[6] no satisfactory intensity formulas have yet been given for $^2S \rightarrow {}^2S$ bands. Dieke[7] applied the summation rule to such bands on the *assumption* that they consist of double P and R branches only. In order to avoid alternating or stepwise-advancing intensities (in the individual branches) he was forced to assume a priori probabilities $p = 2j - 1$. This is open to serious theoretical objections, especially since in atomic spectra the relation $p = 2J$ holds for both odd and even multiplicities, and since the corresponding relation $p = 2j$ has been confirmed for both singlet and doublet electronic states of the σ type in molecules (J = Landé's J)[8,9].

Dieke's theory makes the first line in each branch single, by excluding, as did Kratzer, the state $j = 0$; but recent experimental work of Hulthén on the B bands of CaH shows [10] that this line is double like the remaining lines.—According to Dieke's theory, the relative intensities of successive (unresolved double) lines in each branch should be in the ratio $1:3:5:\cdots$, as compared with $2:4:6:\cdots$ in $^1S \rightarrow {}^1S$ transitions.

It now appears that the difficulties mentioned above can be avoided only by giving up the assumption that bands of the violet CN type contain P and R branches only. In fact Dieke himself suggested[7] that in the CN doublets, one doublet component might represent a true P or R line, the other (by assuming $\Delta\rho = \pm 1$) a Q line. As will be shown below, a satisfactory explanation of the structure and intensity relations follows very simply if the bands are treated as an example of Hund's case b.

Theory of Structure and Intensity Relations

General. The theoretical intensity formulas for any transition between two electronic states both of which fall under Hund's case b can be obtained in two steps, as follows: (1) For a given value of $\Delta\sigma_k$, the relative intensities corresponding to the three cases $\Delta j_k = 0, \pm 1$ can be expressed as functions of j_k and σ_k, if the fine structure due to the interaction of j_k and s be neglected. These functions should be identical in form with those (the Hönl and London equations[6]) which are applicable for $\Delta j = 0, \pm 1$ in Hund's case a. It is then

[4] E. C. Kemble, Nat. Res. Council Bulletin on Molecular Spectra, pp. 326–331 and 345–47 (No. 57, Dec., 1926).

[5] R. S. Mulliken, Phys. Rev. **29**, 637 (1927).

[6] Cf. refs. and discussion in ref. 8.

[7] G. H. Dieke, Nature **115**, 875 (1925); Zeits. f. Physik **33**, 161 (1925).

[8] R. S. Mulliken, Phys. Rev. **29**, 391 (1927).

[9] F. A. Jenkins, H. A. Barton and R. S. Mulliken, Nature **119**, 118 (1927); Phys. Rev. **30**, 150 (1927).

[10] E. Hulthén, Phys. Rev. **29**, 97 (1927).

necessary only to substitute j_k and σ_k for j and σ in the appropriate Hönl and London equations. (It may be noted that, unlike case a, σ cannot differ[5] from σ_k in case b). The truth of these statements follows from the fact that the correspondence principle expressions are of the same form and type in the two cases,[5] so that the "sharpening" of these to the corresponding summation rule expressions must evidently proceed in the same manner in both. Further, the summation rule expressions of Hönl and London remain valid in the new mechanics.[11]

(2) The intensities obtained in (1) must now be subdivided corresponding to the fine structure arising from the interaction of j_k and s. This interaction is precisely analogous[3,4,5] to that of k and s in atomic spectra, and, as in the latter, the various possible orientations of s with respect to j_k should yield a set of levels with different j values, constituting a multiple term. The relative intensities of transitions involving different values of Δj and of j' (or j'') should then be given, for any fixed values of Δj_k and of j_k' (or j_k''), by exactly the same expressions as for line spectrum multiplets, if merely j_k be substituted for k in the formulas for the latter. The equations obtained by Kronig and by Sommerfeld and Hönl[12] are applicable here; as has been shown by Dirac,[13] the same expressions can be obtained from the new mechanics.

By combining the results of (1) and (2), complete explicit expressions for the intensities of all band lines should be obtainable for case b, although in practise these may sometimes prove too cumbersome. For case a, the theoretical intensity relations are given by the Hönl and London equations.[6,5] (In both cases, vibration and other disturbing factors are here neglected). The proper procedure for obtaining accurate equations in cases intermediate between a and b is not yet evident.

Application to $^2S \rightarrow {}^2S$ *transitions.*—In the present paper, only $S \rightarrow S$ transitions, in particular $^2S \rightarrow {}^2S$, will be considered. In all these a close approximation to the ideal case b may be expected, except that in some cases the energy of interaction of j_k and s may be so small (especially for low j_k values) that the orientation of s with respect to j_k is not quantized.

In $S \rightarrow S$ transitions in general, $\Delta\sigma_k = \sigma_k' = \sigma_k'' = 0$, and, in terms of j_k and Δj_k, the intensities should be exactly as in $^1S \rightarrow {}^1S$ transitions. Since in S states, $j_k = m = T$, and since the arrangement of the band lines on a frequency scale is determined[2] by T and ΔT, this means that all $S \rightarrow S$ transitions should be identical in obvious structure and intensity relations, if the fine structure is neglected. In all such transitions, there should be only a P-form and an R-form branch ($\Delta j_k = \pm 1$); these should be at least approximately continuous except for a central missing line. The intensities of suc-

[11] D. M. Dennison, Phys. Rev. **28**, 329 (1926); R. de L. Kronig and I. I. Rabi, Phys. Rev. **29**, 262 (1927); F. Reiche, Zeits. f. Physik **39**, 444 (1926); H. Rademacher and F. Reiche, Zeits. f. Physik, **41**, 453 (1927). Cf. ref. 25 of ref. 5.

[12] R. de L. Kronig, Zeits. f. Physik **31**, 885 (1925); A. Sommerfeld and H. Hönl, Sitzungsber. der Preuss. Akad. der Wiss., phys.-math. Klasse, p. 141 (1925).

[13] P. A. M. Dirac, Proc. Roy. Soc. London, *A*..... (192–).

cessive lines in each branch, aside from the Boltzmann factor, should be[6,14] in the ratio 2:4:6: · · · (cf. Fig. 1*a*), as given by the equation[15]

$$i = 2j_k \tag{1}$$

We have now to find how the line corresponding to any pair of values (j_k', j_k'') is split into components. There are two cases to be considered, namely those for which $\Delta j_k = +1$, and those for which $\Delta j_k = -1$. These correspond to $\Delta k = +1$ and $\Delta k = -1$ in line spectra. Sommerfeld and Hönl give equations (Eqs. 5–6 of their paper[12]) which cover both cases at once.

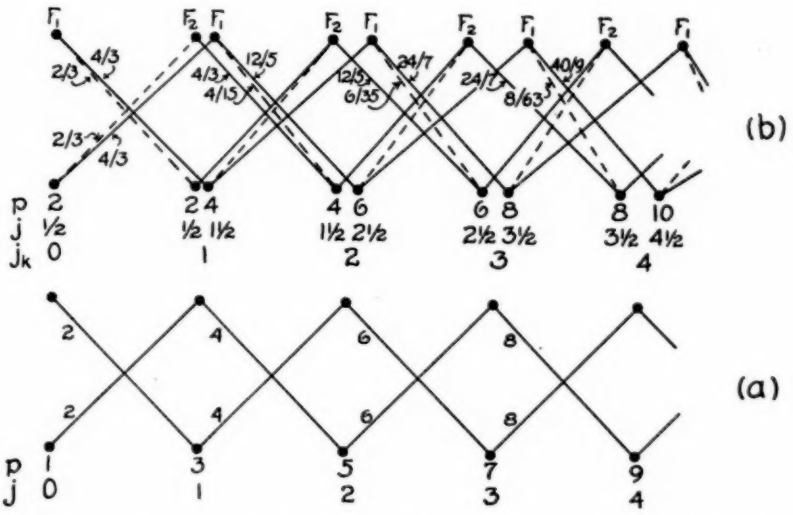

Fig. 1b shows diagrammatically the possible transitions and their relative intensities (neglecting the Boltzmann factor) near the origin of a typical $^2S \rightarrow {}^2S$ band. The a priori probabilities p and the j and j_k values refer both to the initial (upper row of dots) and final (lower row) states. In regard to the actual magnitude of separation, and order, of the levels F_1 and F_2, cf. Fig. 2 description, and text. The intensities, calculated from Eqs. 5–7, are indicated by figures adjacent to the appropriate lines. The intensities which are not given are the same as those for lines which differ only in respect to interchange of initial and final values of j and j_k (e.g., the transition $R_2(1\frac{1}{2})$, with $j' = 2\frac{1}{2}$, $j'' = 1\frac{1}{2}$, $j_k' = 3$, $j_k'' = 2$ has the same intensity as $P_2(2\frac{1}{2})$ with $j' = 1\frac{1}{2}$, $j'' = 2\frac{1}{2}$, $j_k' = 2$, $j_k'' = 3$). The Q branches are shown by dashed lines.

Fig. 1a is typical for a $^1S \rightarrow {}^1S$ band. Fig. 1b can be derived from it by suitable sub-division of the levels and of the transitions and their intensities. E.g., the sum of the intensities for the three transitions corresponding to $j_k' = 2$, $j_k'' = 3$ is the same, namely 6, in Fig. 1b as the intensity of the single transition in Fig. 1a.

After replacing k(j_a of Sommerfeld and Hönl) by j_k and also replacing Sommerfeld's j_s and $r = 2j_s + 1$ by their equivalents in the present notation, namely s and $2s+1$, and after dropping a factor $(2s+1)/4$ which is common

[14] Cf. also R. T. Birge, Bull. Mol. Spectra, pp. 218–19.

[15] This corresponds, with the conventions and j numbering adopted here, to Eq. (2) of ref. 8, except for the omission of a proportionality factor a; j_k in Eq. (1) represents the larger of the quantities j', j''.

to all the equations and therefore is of no significance for the present purpose, these equations are as follows:

For $j \to j-1$, if $j_k \to j_k - 1$; or equally, for $j-1 \to j$, if $j_k - 1 \to j_k$,

$$i^{\pm} = [(j+j_k)(j+j_k+1) - s(s+1)][(j+j_k-1)(j+j_k) - s(s+1)]/jj_k \qquad (2)$$

For $j \to j$, for either $j_k \to j_k - 1$ or $j_k - 1 \to j_k$,

$$i^{0} = (2j+1)[(j+j_k)(j+j_k+1) - s(s+1)][s(s+1) - (j-j_k)(j-j_k+1)]/jj_k(j+1) \qquad (3)$$

For $j-1 \to j$, if $j_k \to j_k - 1$, or for $j \to j-1$ if $j_k - 1 \to j_k$,

$$i^{\mp} = [s(s+1) - (j-j_k)(j-j_k+1)][s(s+1) - (j-j_k-1)(j-j_k)]/jj_k \qquad (4)$$

In these equations, j_k evidently always represents the larger of the two quantities j_k' and j_k''; similarly with j. The j and j_k values correspond to

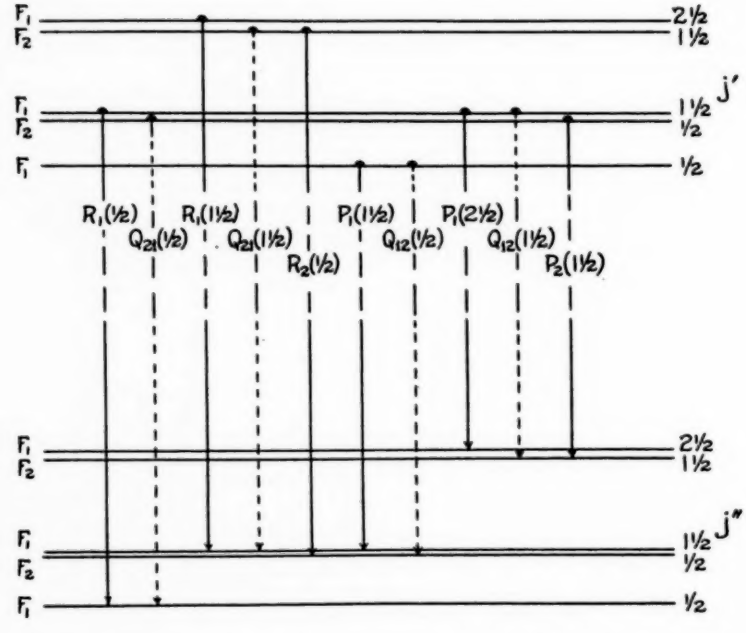

Fig. 2 illustrates the arrangement of the energy levels, and the relative positions on a frequency scale of the band lines, for a $^2S \to {}^2S$ transition. Only a few of the lowest levels are shown here. The relative positions of P_1 and P_2, R_1 and R_2 lines, and their "satellites" (Q lines) can be seen by a study of the diagram. In practise the doublet separation $F_1 - F_2$ is usually greater for the initial than for the final state, but sometimes the reverse is true (cf. text). Except for the hydrides, the separation $F_1 - F_2$ is ordinarily too small to be detected for low values of j. Sometimes (initial state of B bands of CaH) the order $F_2 > F_1$ replaces the usual $F_1 > F_2$. The effect of the various possibilities mentioned on the experimental appearance of the band structure can be seen by a study of the figure.

Sommerfeld's j numbering, and therefore to that of the new mechanics, and so are all ½ unit lower than those used in previous papers of this series. *The new j numbering* has real advantages for the present discussion and so *will be adopted here.*

Now let us consider the typical transition $j_k-1\rightarrow j_k$ (e.g. $1\rightarrow 2$), or $j_k\rightarrow j_k-1$ (e.g. $2\rightarrow 1$). Since $s=\frac{1}{2}$ here, j has two values $j_k\pm\frac{1}{2}$ for each value of j_k (cf. Fig. 1b). Three transitions are possible, according to the selection rule $\Delta j=0,\ \pm 1$, for either of the j_k transitions mentioned. Thus for the j_k transition $1\rightarrow 2$, the j transitions would be $1\frac{1}{2}\rightarrow 2\frac{1}{2}$ (a P_1 line), $\frac{1}{2}\rightarrow 1\frac{1}{2}$ (a P_2 line), and $1\frac{1}{2}\rightarrow 1\frac{1}{2}$ (a $Q_{1,2}$ line); while for the j_k transition $2\rightarrow 1$, the j transitions would be $2\frac{1}{2}\rightarrow 1\frac{1}{2}$ (an R_1 line), $1\frac{1}{2}\rightarrow\frac{1}{2}$ (an R_2 line), and $1\frac{1}{2}\rightarrow 1\frac{1}{2}$ (a $Q_{2,1}$ line); cf. Fig. 2. The subscript notation used here involves an extension to the Q branches of that already adopted,[2] following Kratzer, to distinguish between the $j_k+\epsilon$ (sub-1) and the $j_k-\epsilon$ (sub-2) terms; the first and second subscripts of Q refer to the initial and final states respectively in emission.

The *relative* intensities of the three components associated with each j_k transition are determined by Eqs. (2) and (3),—no transition corresponding to Eq. (4) is possible in the present case,—while the *sum* of their intensities must be, in accordance with Eq. (1), proportional to j_k. These conditions can evidently be met in the following way. Analytical expressions giving the relative intensities of the three fine-structure components are written down in accordance with Eqs. (2) and (3), making in each equation the substitution $s=\frac{1}{2}$, and also substituting $j_k+\frac{1}{2}$ or $j_k-\frac{1}{2}$ for j. After simplifying, and omitting a common factor 8, the three resulting equations are as follows:

$$P_1 \text{ or } R_1(j=j_k+\tfrac{1}{2}) \qquad i_1=(j_k+1)(2j_k-1) \tag{2a}$$

$$P_2 \text{ or } R_2(j=j_k-\tfrac{1}{2}) \qquad i_2=(j_k-1)(2j_k+1) \tag{2b}$$

$$Q_{1,2} \text{ or } Q_{2,1}(j=j_k-\tfrac{1}{2}) \qquad i_3=1 \tag{3a}$$

The sum of the expressions i_3, i_1, and i_2 is $(4j_k^2-1)$. Then if each of the equations (2a), (2b), (3a) is multiplied by $2j_k/(4j_k^2-1)$, the final expressions for the relative intensities of the individual components are obtained. By substitution for j_k in terms of j these are reduced to a very simple form. Both forms are given in the following equations.—It should be remembered that the j and j_k values in these equations refer to the larger of the two quantities j_k' and j_k'', or j' and j''. In calculating actual band intensities, the Boltzmann factor must of course be introduced.[6]

$$P_1 \text{ or } R_1: i_1=2j_k(j_k+1)/(2j_k+1)=(j^2-\tfrac{1}{4})/j \tag{5}$$

$$P_2 \text{ or } R_2: i_2=2j_k(j_k-1)/(2j_k-1)=(j^2-\tfrac{1}{4})/j \tag{6}$$

$$Q_{1,2} \text{ or } Q_{2,1}: i_3=2j_k/(4j_k^2-1)=(2j+1)/4j(j+1) \tag{7}$$

That these equations satisfy the summation rule (sum of intensities of transitions to or from a given state equal to a priori probability $p(=2j+1)$ of that state) can readily be verified from the equations or from Fig. 1b. In this figure the various possible transitions and their relative intensities in accordance with Eqs. (5–7) are shown diagrammatically, for a typical ${}^2S\rightarrow{}^2S$ transition.

The most striking result of the preceding analysis is the prediction of the existence of two weak Q branches in addition to the strong double P and R branches hitherto generally supposed to be alone present. As a result, the difficulties inherent in Dieke's theory are avoided. Another result is that for low values of j_k there should be an appreciable inequality in the intensities of the components of any P or R doublet, the P_1 or R_1 component being the stronger, approximately in the ratio of the j values. For large j_k values, the two components should be asymptotically equal in intensity.

Other $S \rightarrow S$ transitions.—By similar methods, the possible branches and their relative intensities can be predicted in detail for other $S \rightarrow S$ transitions, such as ${}^3S \rightarrow {}^3S$, ${}^3S \rightarrow {}^1S$, ${}^4S \rightarrow {}^4S$, etc. The intense branches should be those for which $\Delta j = \Delta j_k = \pm 1$, additional branches appearing as weak satellite series. The subscript notation adopted above can be readily extended, using e.g. F_1, F_2, and F_3 for the three possible orientations of s in a ${}^3S$ state. In general, double subscripts will be needed for P and R as well as Q branches.

Comparison of Theory with Experiment

General. Except for the first line in each, the predicted intensities of the Q branches are so low that these branches would as a consequence almost certainly pass unnoticed, and in fact usually be undetectable. Furthermore, in the usual case that the (P and R) doublets are unresolved for low j_k values, the $Q_{1,2}$ and $Q_{2,1}$ branches would not be resolved from the P and R branches respectively (cf. Figs. 1b and 2). Even if the doublets are resolved, the Q branches will still fall together with one or the other component (cf. Figs. 1b and 2) of the P or R branches unless appreciable term separations of doublets are present in *both initial and final* electronic states. It is therefore not surprising that these Q branches have not been observed in practise.

The first line of each Q branch is of special interest. In terms of the j_k ($=m$) numbering used by Kratzer[1] and in previous papers of this series, the lowest rotational state was supposed to have $j_k = \frac{1}{2}$, so that one expected from it two rotational sub-states $F_1(1)$ and $F_2(0)$. Kratzer assumed that $F_2(0)$ should be ruled out, so that the first line of each branch should consist of a P_1 or R_1 component only. This question has subsequently been discussed by Birge[16] and Dieke.[7,17] The writer argued[2] against the exclusion of $F_2(0)$ as arbitrary, and concluded that the first line in each branch should have two components. With the change of numbering introduced by the new mechanics, the question appears in a new light. With $j_k = 0$ for the lowest rotational state, only the one rotational sub-state $F_1(\frac{1}{2})$ is possible, and the first P or R line should be single (P_1 or R_1 only),—in agreement with Kratzer. But these lines should *appear* double like the other P and R lines (cf. Figs. 1b and 2) on account of the here relatively intense $Q_{1,2}$ and $Q_{2,1}$ lines which accompany them. Thus a perplexing difficulty is removed, in a way which emphasizes the superiority of the j numbering of the new mechanics.

[16] R. T. Birge, Bull. Mol. Spectra, pp. 185, 203, 218.

[17] G. H. Dieke, Physica **5**, 178 (1925).

CaH *bands*. The best available test of the theory is afforded by the B bands of CaH, two of which (B and B') were measured and analyzed by Hulthén.[10] In these bands the P and R doublets are much wider than for any other $^2S \rightarrow {}^2S$ transition on record, and are resolved down to the first line. In the stronger (B) band, the first line of the R branch appears double like the rest, as predicted; likewise in the first P line a relatively high intensity indicates, according to Hulthén, the presence of two unresolved components. In the weaker (B') band, the first three R_2 and the first four P_2 lines are unrecorded in Hulthén's table, indicating that they are comparatively weak, as predicted by the theory; a the expected P_1 and R_1 lines are recorded (unfortunately Hulthén gives no explicit intensity data). That Hulthén's P_1 and R_1 lines really correspond to $+\epsilon$ and his P_2 and R_2 lines to $-\epsilon$ is shown through combination relations with the A bands of CaH (cf. a following paper of this series); without these combinations it would be impossible to make this identification from the structure alone, although the identification could be made by assuming the correctness of the intensity theory.

Hulthén's "$R_2(0)$," the high frequency component of the first R line in the B band, should evidently be classified according to the theory as $Q_{2,1}(\frac{1}{2})$, the low frequency component "$R_1(1)$" being $R_1(\frac{1}{2})$ in the new j numbering. As can be seen from Figs. 1b and 2, the doublet separation $R_1(\frac{1}{2}) - Q_{2,1}(\frac{1}{2})$ should measure directly the term separation, $F_1'(1) - F_2'(1)$ for $j_k' = 1$; experimentally this amounts to -1.26 wave-number units. Hulthén's "$P_2(1)$ plus $P_1(2)$" (unresolved) should be classified as $Q_{1,2}(\frac{1}{2})$ plus $P_1(1\frac{1}{2})$; their separation, here too small to measure, should represent directly the term separation $F_1''(1) - F_2''(1)$. No lines are recorded by Hulthén which can be identified as additional members of the Q branches. Further experimental work with longer exposures and higher dispersion should disclose some of these lines; a careful study of the intensity relations would also be very desirable.

Making use of the four sets of $\Delta_2 F$ values (for definition of $\Delta_2 F$ cf. ref. 2, p. 490) established by Hulthén from combination relations, and of the separations $F_1' - F_2'$ and $F_1'' - F_2''$ for $j_k = 1$ as obtained above, the term-separations $F_1 - F_2$ can be calculated for any odd value of j_k. Hulthén gives $\Delta_2 F_1''(j+1) - \Delta_2 F_2''(j) \sim 0.09$, from which it follows that $F_1'' - F_2'' \sim +0.0225\, j_k''$. But $\Delta_2 F_1'(j+1) - \Delta_2 F_2'(j)$ has much larger values, of *opposite sign*, e.g. -2.34 for $j = 1\frac{1}{2}$ (i.e., $[F_1'(3\frac{1}{2}) - F_1'(1\frac{1}{2})] - [F_2'(2\frac{1}{2}) - F_2'(\frac{1}{2})] = -2.34$); the numerical value of this difference decreases, at first rapidly, then more and more slowly, with increasing j, the difference approaching a value of about -1.0 for $j \sim 30$. Hence, starting from $F_1'(1) - F_2'(1) = -1.26$ for $j_k' = 1$, we get $F_1'(3) - F_2'(3) = -3.60$, and so on, the differences increasing steadily with j.

The C band of CaH, measured and analyzed by the writer,[18] has been shown by Hulthén to have the same set of final rotational states as the F_2'' states of the B bands. The initial states of the C bands are then presumably

[18] R. S. Mulliken, Phys. Rev. **25**, 509 (1925).

F_2' states of a ^2S type. The complete absence of F_1' states is puzzling, but is perhaps connected with the extreme instability of the molecule[18] in the initial electronic state of the C band.

AlO *bands*. In the AlO bands, as investigated by Pomeroy,[19] the doublets are resolved only for high values of j, so that no evidence is available as to the presence of Q branches or as to the relative intensities of the P and R doublet components for low j values. The intensities of the doublet components are equal for high j values (private communication from Professor R. T. Birge) in agreement with the theory.

The doublet separation is mainly or wholly confined to the *final* electronic state, as is shown by equality of corresponding doublet separations in the (0, 0) and (1, 0) bands.[19] The separation increases nearly linearly with j_k (slightly faster for $j_k > 100$), from about 0.40 wave-number units at $j_k = 28$ to 1.90 units at $j_k \sim 135$. Whether F_1'' or F_2'' is greater cannot be decided from the data, since there is no way of determining how the subscripts 1 and 2 should be assigned to the observed doublet components.

Violet CN *bands*. The violet CN bands are the classical example of a $^2S \rightarrow {}^2S$ transition.[1,2,20] The doublets are not resolved for the smallest values of j, but examination of plates taken by the writer shows indications of slight inequality of the doublet components near where they are first resolved, also some indication of weak satellites; however, this is uncertain.

The doublet width shows conspicuous perturbations which are characteristic for given values of n' and j',[21] so that a considerable doublet separation certainly exists in the initial states.[20] There is at present no means of deciding whether or not a (probably smaller) separation also exists in the final states. The observed doublet separation in each branch increases more or less linearly with j_k at first, reaches a maximum at about $j_k = 75$, and then decreases;[22] if, as in AlO, the term-separation increases somewhat faster than linearly for large j_k values, and if this effect is more pronounced in the final state, so that the final term-separations, although comparatively small at first, approach the initial term-separations for high j_k values, the observed relations would be accounted for. There is no means of deciding, from existing data, the proper assignment of the subscripts 1 and 2, or the order of F_1 and F_2 levels. An analysis of the red CN bands, now in progress in this laboratory, may help to remove the above uncertainties.

As already noted above (p. 140), the intensity relations should be exactly the same in $^2S \rightarrow {}^2S$ as in $^1S \rightarrow {}^1S$ transitions (cf. ref. 8, p. 398–9, 401–2 in regard to the latter) if the fine structure is neglected. From this point of view, the violet CN bands show fairly good agreement with the theory: the intensity at first increases symmetrically in the two branches, approximately linearly with j_k, but is brought to a maximum by the Boltzmann factor, this maximum depending on the temperature, and being higher

[19] W. C. Pomeroy, Phys. Rev. **29**, 59 (1927).
[20] R. T. Birge, Bull. Mol. Spectra, pp. 182–87, 215–21, etc.
[21] T. Heurlinger, Dissertation Lund, 1918.
[22] R. T. Birge, Astrophys. J. **55**, 273 (1922).

(cf. ref. 8 in regard to theory) in the P than in the R branch.[20] This is shown especially by the work of Birge.[22]

Sewig[23] also has made a photometric study of the intensity relations in these bands in various sources. According to him, the intensities of the P and R branches rise at first symmetrically from the missing line, as predicted, but the intensities for the first few lines are more nearly in the ratio 6:8:10 than in the theoretical ratio 2:4:6 (the agreement is evidently better with the present theory, however, than for Dieke's predicted ratios[8] 1:3:5,—cf. introduction). It seems possible that Sewig's measurements have been overcorrected in the case of weak lines; further experimental work would be very desirable. Sewig finds the R branch stronger than the P branch in λ4216, and the two branches about equally intense in λ3883.

N_2^+ *bands.*—In the case of the N_2^+ bands, Fassbender's work[24] shows that a term doublet separation exists in the initial states: there are perturbations in the line doublet separations which are the same for all bands having the same n'. The doublet separations are irregular on account of these perturbations, and larger for $n'=1$ than for $n'=0$.

On plates taken by the writer in the second order of the 21 foot concave grating at Harvard University, the high-frequency components of the doublets are decidedly more intense than the low-frequency components for low values of j_k (the doublets begin to be resolved at about $j_k=10$), while this difference becomes imperceptible as j_k increases (the bands examined were λλ3914 and 4278). In a weak third order exposure of λ3914, the differences for the lower values of j_k are rather marked, probably because of increased photographic contrast. If this evidence is valid (it cannot be regarded as quite certain because of the possibility of slight out-of-focus phenomena, and should be checked by other observers), it shows, assuming the correctness of the intensity theory and granting that the doublet separations are mainly due to the initial states, that $F_1' > F_2'$.

Photometric measurements on the N_2^+ band λ3914 (doublets not resolved) have been made by Sewig.[23] The agreement with theory is similar to that in the violet CN bands. The P branch is, however, definitely more intense than the R branch here, according to Sewig,—in agreement with earlier results of Fassbender. The alternating intensity of successive doublets in the N_2^+ bands (which does not particularly concern us here) is fairly well taken care of by introducing into the intensity equations a factor of about 1.5 for alternate lines.

ZnH, CdH, HgH, MgH, OH *bands.* While $^2S \rightarrow {}^2S$ transitions are not yet on record for the molecules named, their $^2P \rightarrow {}^2S$ or $^2S \rightarrow {}^2P$ bands give valuable information in regard to the doublet separations in ^2S states. In $^2P \rightarrow {}^2S$ transitions, the assignment of the subscripts 1 and 2 for the ^2S states can be made definitely on the basis of the combination relations together with the safe assumption that Δj is confined to the values 0, ± 1. In ZnH,

[23] R. Sewig, Zeits. f. Physik **35**, 511 (1926).
[24] M. Fassbender, Zeits. f. Physik **30**, 73 (1924).

CdH, and HgH, as shown by the work of Hulthén[25] and Kratzer,[1] $F_1(j_k) > F_2(j_k)$; approximately, $F_1(j_k) = Bm^2 + km$, $F_2(j_k) = Bm^2 - km$.[26] The coefficient k is large for HgH, less for CdH, still less for ZnH.[1] In HgH, the initial rate of increase of $F_1 - F_2$ with j_k is not maintained; for $m = 26$, the rate of increase has fallen nearly to zero (cf. Table 9 of ref. 1). The data of Watson and Rudnick[27] on MgH also strongly indicate $F_1 > F_2$, the difference $F_1 - F_2$ being rather small. The relation $F_1 > F_2$ again holds in the initial ^2S state of the OH bands (cf. following paper); in the initial state of CH λ3900 the order of the levels is doubtful.

Nature of Energy Differences Between F_1 and F_2 Terms in ^2S States

Since, as Hund points out,[3] the electron spin probably interacts only magnetically, the energy differences between F_1 and F_2 terms in ^2S states should be attributed to interaction of s with a magnetic field. As Kemble has shown (ref. 3, pp. 345–7), a small electronic orbital angular momentum ϵ_k and a corresponding magnetic field, both of which should be parallel and proportional to m, are to be expected for a rotating molecule, even if the electronic angular momentum and magnetic field are zero for the non-rotating molecule. The effect is analogous to that of the Larmor precession in the theory of diamagnetism. According to this theory, $j_k = m + \epsilon_k$: a small fraction of the molecular angular momentum, proportional to their share of the total moment of inertia, is assigned to the electrons. The theory accounts[3] for the observed initially approximately linear increase with j_k in the energy differences $F_1 - F_2$, and also for the slightly unsymmetrical deviations, for F_1 and F_2 terms, of T from exact half-integral values, as found by Birge[28].

In every case where definite conclusions can be drawn (according to the results summarized in the preceding paragraphs), except that of the initial states of the B bands of CaH, $F_1 > F_2$, i.e., the antiparallel (F_2) orientation of s and m is the more stable. This relation is the reverse of the ordinary relation for a magnet in an external field, but corresponds to that in ordinary atomic multiplets and in most molecular ^2P states. The observed relation in such multiplets is, however, theoretically the correct relation if the interaction is essentially that of the spinning electron in the field due to its own orbital motion.[29] In the present case, the opposite, or normal, magnetic interaction would at first sight seem more probable, since only a small part of ϵ_k would ordinarily belong to the electron to which s belongs. However, the association of the electron spin with the field of its own orbital motion (if any) is so much closer than with the field due to other

[25] E. Hulthén, Zeits. f. Physik **11**, 284 (1922); Dissertation Lund, 1923; Zeits. f. Physik **32**, 32 (1925); etc.

[26] For further details, cf. also R. T. Birge, Bull. Mol. Spectra, pp. 177–86.

[27] W. W. Watson and P. Rudnick, Astrophys. J. **63**, 20 (1926); Phys. Rev. **29**, 413 (1927).

[28] R. T. Birge, Bull. Mol. Spectra, p. 175, 164, etc.

[29] W. Heisenberg and P. Jordan, Zeits. f. Physik **37**, 263 (1926); cf. F. Hund, Linienspektren, J. Springer, Berlin (1927).

electrons that the corresponding magnetic energy might well preponderate over the energy of interaction with all other electrons.

An additional possibility of explanation appears in the magnetic field of the rotating nuclei. Since nuclei and electrons have the same angular velocity[30] and approximately the same charges and mean distances from the center of gravity, they should produce oppositely directed fields of the same order of magnitude. It seems quite possible that the nuclear field might predominate, at least in certain regions of the molecule, and thus account for the order $F_1 > F_2$.[31]

The very marked $F_2' > F_1'$ in the B bands of CaH suggests that the ^2S state here is of an unusual type. Perhaps it constitutes an example of the case[3] $\sigma_k \neq k$; perhaps this molecular ^2S state is derived from one of the low-lying P and D states of the Ca atom.

The writer wishes to express his appreciation of helpful suggestions made by Professor J. H. Van Vleck.

WASHINGTON SQUARE COLLEGE,
NEW YORK UNIVERSITY,
April 9, 1927.

[30] This is, of course, superposed on the orbital angular velocity of the electrons, but, as in the case of the Larmor precession in the theory of diamagnetism, this initial motion does not affect the result.

[31] (Added in proof). Cf. F. Hund, Zeits. f. Physik **42**, 96 (1927), who considers only the nuclear field.

THE BETA BANDS OF NITRIC OXIDE. I. MEASUREMENTS AND QUANTUM ANALYSIS

By Francis A. Jenkins,[1] Henry A. Barton,[1] and Robert S. Mulliken.

Abstract

Band structure and wave-number data for band lines. Using an active nitrogen source, the β bands of NO included in the region of 2300 to 5300A have been photographed in the second order of a 21-ft. Rowland concave grating. Each complete band consists of two sub-bands with a P and an R branch of the ordinary type and also a very weak Q branch. The latter is relatively more intense in the lower frequency sub-band. Here there are four missing lines in the otherwise continuous $P-R$ series, while there are two in the higher frequency sub-band. The lines of the latter are narrow doublets superficially resembling those of the violet CN bands. The six branches for each of eighteen bands have been measured, and wave-numbers are tabulated for 20 to 30 lines in the P and R branches, and for the few visible members of the Q branches. The bands measured include nine of the strong $n'=0$ progression ($n''=4$ to 12), three of $n'=1$($n''=6$, 11, 13), four of $n'=2$($n''=9$, 13, 14, 15), and two of $n'=3$($n''=8$, 16).

Isolation and representation of spectral terms. Combinations involving the P and R branches are found to hold, and show the existence of four different sets of rotational terms, two (one for each sub-band) in the initial electronic state and similarly two in the final state. For low values of j the rotational terms in all four cases are representable by $F(j)=B(j^2-\sigma^2)$. From a consideration of the missing lines, the observed transitions are classified as ${}^2P_1\rightarrow{}^2P_1$, with $\sigma'=\sigma''=\frac{1}{2}$, for the higher frequency system, and ${}^2P_2\rightarrow{}^2P_2$, $\sigma'=\sigma''=3/2$, for the lower frequency system. A table is given of the weighted mean values of Δ_2F in the observed vibrational states of the initial and final electronic levels, and another of the empirical coefficients in analytical expressions for $\Delta_2F(j)$ and $F(j)$. Certain anomalies in the form of the latter in particular the appreciable difference in B for the components of a doublet, are shown to be a necessary consequence of Hund's theory of molecular electronic states as applied quantitatively to doublet states by E. C. Kemble. These effects are found to be larger in the initial state, thus showing, according to the theory, that the doublet separation must be smaller here than in the final state. Equations for the band origins are obtained (Eqs. 8 of the text) which permit a representation of the vibrational energy levels; in these, cubic and biquadratic terms are both definitely required, and when they are included the observed values are reproduced with a mean error of 0.03 cm^{-1}.

Constants of the nitric oxide molecule. The moment of inertia I_0 and the internuclear distance r_0 for the vibrationless molecules are evaluated as $I_0'=(24.80\pm0.02)\times10^{-40}$ gr cm^2, $I_0''=(16.30\pm0.02)\times10^{-40}$, $r_0'=1.418\times10^{-8}$ cm, $r_0''=1.150\times10^{-8}$. B, the coefficient of j^2 in $F(j)$, is represented within experimental error by the linear relation $B=B_0-\alpha n$, where for the ${}^2P_1$ bands $B_0'=1.0704$, $B_0''=1.6754$, $\alpha'=0.01162$, $\alpha''=0.01783$, and for the ${}^2P_2$ bands $B_0'=1.1678$, $B_0''=1.7239$, $\alpha'=0.01892$, $\alpha''=0.01866$. The β bands exhibit a longer series of n'' values than any system yet investigated in respect to the variation of B with n. Equations are given which permit a quantitative representation of the frequencies of all observed lines (Eqs. (2), (8), and (6) in conjunction with Table IV). From the equations for band-origins, the following quantities are obtained for the vibration frequency ω_0 for infinitesimal

[1] National Research Fellow.

amplitudes, $^2P_1$ bands, $\omega_0' = 1029.43$ cm^{-1}, $\omega_0'' = 1892.12$, $x'\omega_0' = 7.460$, $x''\omega_0'' = 14.424$; $^2P_2$ bands $\omega_0' = 1030.88$, $\omega_0'' = 1891.98$, $x'\omega_0' = 7.455$, $x''\omega_0'' = 14.454$. The change of ω_0 (and also of r_0 and I_0) during the emission is exceptionally great. Since the final state of the NO β bands is the normal state of nitric oxide, the above values of I_0'', r_0'', ω_0'', etc., apply to this state. An integration of the vibration frequency curve for the final state to the point of dissociation is carried out to determine the *heat of dissociation*.

Electronic states and relation to other bands. The doublet separation (for the rotationless molecule) in the initial ^2P state is 32.9 cm^{-1}, if that in the final ^2P state is taken as 124.4 in accordance with Frl. Guillery's data on the γ("third positive nitrogen") bands of NO. Only the *difference* between these (91.54 cm^{-1}) can be accurately found from the β bands. (See Fig. 1). The γ bands have the final doublet level in common with the β bands; hence all constants derived for the final state of the β bands apply equally well to that of the γ bands. The ultra-violet O_2^+ bands and certain SiN bands, whose structure is like that of the NOβ bands, are probably also $^2P \rightarrow {}^2P$ transitions.

Introduction

ONE of the most unusual and interesting of band spectra is the β system[2] of nitric oxide, discovered and photographed by E. P. Lewis[3] in 1904. These bands appear with considerable intensity only when excited in active nitrogen. In his original work on the spectrum of the nitrogen afterglow, Lewis stated that traces of oxygen are necessary for the production of this system, and that therefore an oxide of nitrogen is the probable emitter. Later, in connection with the work of Lord Rayleigh[4] on the properties and chemical reactions of active nitrogen, Fowler and Lord Rayleigh[2] remeasured the principal band edges of the β system with sufficient accuracy to permit their arrangement in the usual Deslandres' progressions. These authors were then of the opinion that the bands could be obtained in pure nitrogen. Subsequent work by Lewis,[5] and aso by Lord Rayleigh,[6] has supported the original idea that oxygen must be present.

Let us now consider briefly the evidence which has led to the conclusion that these bands are due to the nitric oxide (NO) molecule. We know[5,6] that the β bands are probably given out by the same molecule as the γ bands[2] (also called third positive nitrogen bands), since the two systems always occur together. In active nitrogen the relative intensity of the β and γ bands is practically constant, although in other sources, such as the uncondensed discharge through air, nitric oxide, or impure nitrogen, the β system is relatively very weak. The γ bands require the presence of traces of oxygen or oxygen compounds for their production,[5,6] as Deslandres[7] first pointed out. These bands are certainly not due to oxygen alone, so that we are limited to a compound of N and O as the emitter of both the β and γ

[2] Following the designation used by A. Fowler and R. Strutt, Proc. Roy. Soc. **85A**, 377 (1911).

[3] E. P. Lewis, Phys. Rev. (I) **18**, 125 (1904), Astrophys, Jour. **20**, 49 (1904).

[4] R. Strutt, Proc. Roy. Soc. **85A**, 227 (1911) and later papers.

[5] E. P. Lewis, Phil Mag. **25**, 826 (1913).

[6] R. Strutt, Proc. Roy. Soc. **93A**, 254 (1917).

[7] H. Deslandres, Compt. rend. **101**, 1256 (1885).

systems. The bands are obtained more efficiently by introducing NO (*not* any *other* oxide of nitrogen) into pure active nitrogen than by introducing oxygen.[6] More recently it has been concluded by Mulliken[8] and by Birge[9] that the vibrational constants in the final state are the same for the β and γ systems. This was only true with the somewhat arbitrary assumption that no β bands are observed with a final vibrational quantum number less than 2.[10] There can now be no doubt as to the correctness of this interpretation, for Sponer and Hopfield[11] have found that the β and γ systems both appear in the ultra-violet absorption spectrum of nitric oxide, as photographed by Leifson.[12] The γ bands had previously been identified on these plates by Sponer,[13] proving that the final electronic state (in emission) of these bands is the normal state of the NO molecule. Combining this with the results of Sponer and Hopfield, we have definite proof that both systems result from transitions to a common final state in nitric oxide, which is its normal state. At present these two band systems constitute the entire known spectrum of nitric oxide.[14]

In connection with work on the electronic states of molecules, one of the writers has given an interpretation of the levels in nitric oxide,[15] based partially on the results to be reported here. The complete evidence for this interpretation will be postponed until the experimental material has been presented, but we may note at this point that the normal state is a doublet P (^2P) state, and that the γ bands result from a transition from a single upper level (^2S) to the double normal level. The doublet interval of the latter is therefore measured by the electronic frequency difference at the (0, 0) band[16] of the (double) γ system, which is 124.4 cm^{-1}; this value is based on Frl. Guillery's recent analysis[17] of the γ bands. Since the β bands also have double heads, with a *different* electronic separation at the system-origin (91.54 cm^{-1}) we conclude that their initial state is also double, with a separation of 32.9 cm^{-1}.[18] Our results show that this is also a ^2P state, and that the observed transitions are $^2P_1 \rightarrow {}^2P_1$ and $^2P_2 \rightarrow {}^2P_2$. These relations are shown in Fig. 1.

[8] R. S. Mulliken, Nature **114**, 349 (1924).

[9] R. T. Birge, Nature **114**, 642 (1924).

[10] As shown in Part II of this paper, this is exactly the condition that we should expect in the light of recent theories of the intensity distribution in band systems.

[11] H. Sponer and J. J. Hopfield, Phys. Rev. **27**, 640 (1926) Abstract.

[12] S. W. Leifson, Astrophys. Jour. **63**, 73 (1926).

[13] H. Sponer, Nature **117**, 81 (1926).

[14] The system of bands in the extreme ultra-violet measured by R. T. Birge and J. J. Hopfield, Phys. Rev. **26**, 283 (1925) Abstract, and attributed to NO by Sponer (Ref. 13) and Birge and Sponer (Ref. 21), has been found by Birge and Hopfield, Phys. Rev. **29**, 356 (1927) Abstract, to be due to N_2.

[15] R. S. Mulliken, Phys. Rev. **28**, 493 (1926), Fig. 1.

[16] The notation used here conforms essentially with that of the recent Report of the National Research Council on "Molecular Spectra in Gases." In one or two cases the symbols are as defined by Mulliken (Ref. 23). As usual, the (n', n'') band denotes that band which has the initial vibrational quantum number n' and final n''.

Since the work of Fowler and Lord Rayleigh, additional β bands in the blue and violet have been found by Lewis[5] and by Lord Rayleigh.[6] Birge[16] has assigned vibrational quantum numbers to the bands, including several additional ones identified on Lewis' spectrograms. New wave-lengths of all the known β bands are given in a recent description of this system by Johnson and Jenkins;[20] vibrational quantum numbers are also given. As stated above, the assigned values for these quantum numbers in the final state of the bands were chosen so as to harmonize with the well-established assignment[13] in the γ system. The intensity distribution among the bands of the system, discussed by Johnson and Jenkins, and also by Birge, is considered in Part II of the present paper. Birge and Sponer[21] give equations and a diagram for the vibrational levels in the various electronic states of nitric oxide, and have calculated from these the heat of dissociation.

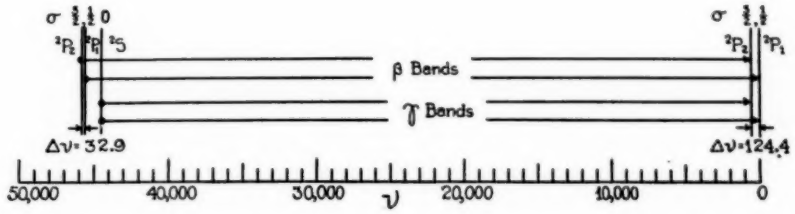

Fig. 1. Electronic states of the nitric oxide molecule. The ^2P doublet separations are magnified five times.

The present article[22] is concerned with a detailed description of the β bands, which have been photographed with sufficient dispersion to resolve them completely. Our analysis has brought out several new features, because the type of electron transition involved is different from that of any other band system hitherto studied. These features are well explained by the present quantum theory of band spectra, and in particular they support the postulates recently advanced by one of the writers[23] concerning the relations between band-spectrum structure and electronic states in molecules.

Experimental Procedure

The usual stream method for obtaining active nitrogen spectra was used in photographing the bands. Nitrogen from a commercial cylinder (stated to

[17] M. Guillery, Zeits. f. Physik, 42, 121 (1927); analysis of NOγ bands. See also reference 38 below. The authors are indebted to Frl. Guillery and Dr. Mecke for the opportunity of examining this paper in proof.

[18] In regard to the alternative possibility that the initial $\Delta\nu$ equals 91.54 + 124.4, see p. 171, below.

[19] R. T. Birge, Report on Molecular Spectra, p. 138.

[20] R. C. Johnson and H. G. Jenkins, Phil. Mag. (7) **2**, 621 (1926).

[21] R. T. Birge and H. Sponer, Phys. Rev. **28**, 277 (1926). See Figs. 3 and 4.

[22] Preliminary reports of this work will be found in Nature **119**, 118 (1927) and Phys. Rev. **29**, 211 (1927) Abstract.

[23] R. S. Mulliken, Phys. Rev. **28**, 481 (1926) (general); *idem*, **28**, 1202 (1926) (σ-type doubling, etc.); Proc. Nat. Acad. Sci. **12**, 151 (1926) (ZnH, CdH, HgH bands).

be 99.5 percent pure) was pumped at a pressure of 13 mm through a tube in which was passed a strong condensed discharge from a transformer, with a spark gap in series; the electrode nearest the after-glow tube was earthed. The nitrogen passed through a short Z-shaped piece of blackened tubing and into a wider perpendicular tube fitted with a quartz window.[24] The after-glow in the latter was lemon yellow under these conditions, showing chiefly the characteristic active nitrogen bands (α bands) in the visible. In order to obtain the NO bands, air was admitted from a stopcock placed before the exciting discharge, causing the yellow color of the after-glow to fade into the faint bluish color characteristic of the NO spectrum.[25] The spectrum then showed only the β and γ bands, with a practical absence of nitrogen and other band or line spectra. Only a slight advantage as regards intensity is obtained if nitric oxide itself is introduced into the nitrogen before its activation, and the spectrum is somewhat *weaker* if either air or NO is admitted into pure active nitrogen in the after-glow tube. To obtain the bands with the best intensity, it is necessary to use a large-capacity pump, and to introduce just enough air to quench completely the α bands. Since the afterglow extended throughout the 20 cm length of the after-glow tube, it was found best to place the latter directly in front of the slit, without the use of a condensing lens.

The 21-foot Rowland concave grating, having a ruled space of 6 inches with 20,000 lines to the inch, was employed. In the second order this gives a dispersion of about 0.97A per mm. The mounting is of the Paschen type, so that the complete spectrum in the first and second orders could be photographed at once. Since the exposures were necessarily long, (the best set of plates was obtained in a 10-hr. exposure), it was essential to maintain constant temperature. This was accomplished by a sensitive thermostatic device mounted in the insulated room containing the grating and plate-holder. The temperature was thus held constant within a few hundredths of a degree. With this precaution it was found possible to resolve doublets in the second order spectrum with a separation of 0.03A.

In determining the wave-lengths, the lines of the international iron arc[26] were used throughout. Two comparison spectra, one exposed before the bands and one after, were always used, in order to detect slight accidental displacements. When these were found, they were always less than 0.02A, and the correct placing of the comparison spectrum in the region concerned was determined from other plates where the two iron spectra showed no displacement relative to each other. It is thus hoped that the wave-lengths are correct to within 0.005A, and the relative accuracy within any band

[24] The arrangement was similar to that shown by Mulliken, Phys. Rev. **26**, 7 (1925) Fig. 1, except that the bulb *B* was omitted.

[25] If still more air is admitted, the blue is suddenly replaced by a dull, yellowish-green glow[6,20] having a continuous spectrum in the visible, beginning at λ4300. This coincides closely with the region of the visible absorption of NO_2, and as suggested by Lord Rayleigh (Proc. Roy. Soc. **86***A*, 57 (1911)), probably represents the emission spectrum of this compound.

[26] W. F. Meggers, C. C. Kiess, and K. Burns, "Redetermination of the Secondary Standards of Wave-Length from the New International Arc," Bull. Bur. Stan. **19**, 263 (1924).

should be greater. In reducing the wave-lengths to vacuum and converting to wave-numbers, Kayser's tables[27] were used. A comparator made by Wolz, having 300 divisions to the mm, and also a Hilger instrument reading directly to 0.001 mm, served for the measurements. Two settings were usually made on each line.

Analysis of Band Structure

Description of bands. The β bands have double heads degraded toward the red, and extend from λ2300 to λ5300, with a maximum intensity at about λ3400. On our most intense exposure, the first band sufficiently strong for measurement was the (0, 4) band at λ2620. Sixteen bands from this to the (2, 14) band at λ4200 were completely measured in the second order, and two more of longer wave-length, λ4479 (2, 15) and λ4572 (3, 16), in the first order.

As will be seen on referring to Plate I, each complete band consists of two sub-bands of similar general appearance and intensity. In accordance with our interpretation of the electronic transitions responsible for these, the first higher frequency band will be called the $^2P_1$ band, and the second, the $^2P_2$ band. Each of these consists of a P and R branch of the usual type, forming a continuous series except for the missing lines near the origin. In addition, a very weak Q branch occurs in each, with an intensity falling off sharply from the first line. The Q branch is much stronger in the $^2P_2$ bands than in the $^2P_1$. The intensity of the P and R branches is approximately symmetrical in both. These intensity relations are in good agreement with the theory, as shown in Part II of this paper, where quantitative measurements and a more complete discussion are given.

The lines of the $^2P_1$ bands are probably all very close doublets, but with an undetectable separation near the origin. The doublets begin to be resolved at about the 15th line in each branch, their separation here being about 0.03A. The components are of equal intensity. The lines soon become too weak for good measurements of the doublet separation, so that only 7 to 10 reliable values could be obtained in any one branch. Within this range a linear increase was found. The quantitative results are given in Eq. (7). The lines of the $^2P_2$ bands, as far as can be observed, are strictly single throughout.

In agreement with theoretical considerations (see below), we find that the number of missing lines is different for the two sub-bands, there being two missing lines in the P-R series near the $^2P_1$ head and four in that near the $^2P_2$ head. Because of the theoretical significance of these missing lines, we have made a particular effort to establish that they are actually absent and not merely of low intensity. Active nitrogen spectra are especially favorable for this purpose, since the intensity maximum in any branch is nearer the band origin than in the case of ordinary high-temperature sources, so that the first lines are relatively strong. Furthermore, a 40-hour exposure

[27] H. Kayser, "Tabelle der Schwingungszahlen," S. Hirzel, Leipzig (1925).

Plate I. This plate shows three of the strongest β bands, together with greatly enlarged details from these and two others.

Enlargements of complete bands. The upper three strips show nearly the entire (0, 10), (0, 9), and (0, 8) bands, enlarged about four times from our plates. The double character of each band is evident from the sudden confusion of the regular sequence of P_1 and R_1 lines by the lines of the second head. The latter, when sorted out from the lines of the first head, form two other series (P_2 and R_2) very similar in appearance to the P_1 and R_1 series. With the exception of lines belonging to a weak Q branch near each head, these four series include all the lines found in a band. The P and R series are marked out for the (0, 10) band, the length of the marks showing qualitatively the rise and fall of intensity in each branch. Each R branch returns upon itself, forming the head. The origins are, however, very close to the heads; they lie about half-way between the points at which the P and R branches begin, in each band. Near the higher frequency ($^2P_1$) head there are two missing lines in the otherwise continuous series formed by the P and R branches, and four near the lower frequency ($^2P_2$) head. The variation in the relative position of the P and R branches in the $^2P_1$ bands with the n'' (and hence with the value of C) is well shown in these three bands. In the (0, 9) band the two series are closely superimposed for the lower values of j.

Details with greater enlargement. The smaller cuts, Nos. 1 to 6, show interesting parts of certain bands, enlarged 10 times.

No. 1, from the head of the (0, 12) band, exhibits to advantage the two missing lines near the origin in the $^2P_1$ sub-band. Here the first lines of the R and P branches ($R_1(1)$ and $P_1(2)$) are marked by a short line below, and the dots indicate the calculated positions of the missing lines. The first lines of the two branches were practically equal in intensity on the original plate. The first two lines of the Q branch, $Q_1(1)$ and $Q_1(2)$, are marked above by lines indicating their relative intensity.

No. 2 shows a portion of the (0, 10) band where the higher members of the $^2P_1$ band become resolved into doublets. The three lines marked are $P_1(17)$, $P_1(18)$ and $P_1(19)$, which were clearly resolved on the plate with doublet separations of about 0.032A.

No. 3 shows the $^2P_2$ head in the (0, 9) band. Four lines of the Q branch are visible, marked above. The first of these, $Q_2(2)$, is stronger than the first line of the P branch, marked by a line below, at the right. The dots and lines drawn below have the same significance as in *No. 1,* but here a double dot means that the position of a missing line is occupied by a known line of another series.

No. 4 is taken from the $^2P_1$ head of the (0, 8) band, which shows the first three lines of the weak Q branch in this head. They are more distinct here than in *No. 1,* the first line $Q_1(1)$ being shown to better advantage. The presence of $R_1(1)$ between the first two stong lines on the left is fairly obvious, while $P_1(2)$ is well separated.

No. 5. This cut and *No.* 6 were taken from a heavy exposure of the (0, 7) band on one of the set of plates which was used to establish definitely the absence of the apparently missing lines. Here we can say with certainty that the lines $R_2(0)$ and $P_2(2)$ do not occur. Owing to frequent superposition of Q lines and lines of the higher frequency band, it was only by considering the evidence from a large number of bands on these plates that we were finally able to conclude with certainty that all four lines near the $^2P_2$ head are missing.

No. 6. This shows the $^2P_1$ head of the (0, 7) head, and affords most convincing evidence of the absence of (at least) two lines near the origin of this band.

The difficulties involved in preserving faint lines during enlargement and reproduction of course render the evidence of Plate I in respect to the missing lines and Q branches less convincing than that obtained by an examination of the original plates. The photometric records described in Part II of this paper are more satisfactory in this respect.

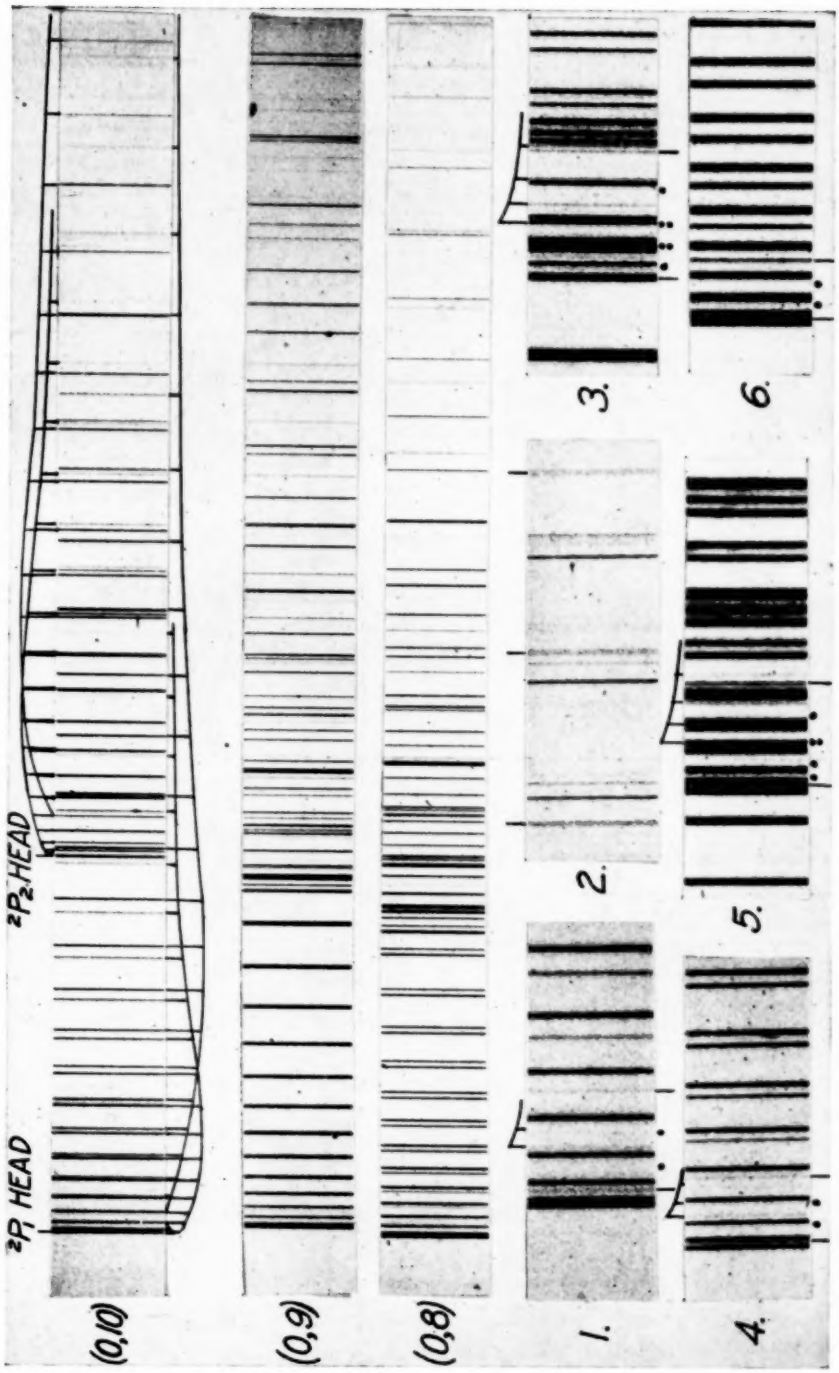
$^2P_2$ HEAD
$^2P_1$ HEAD
(0,10)
(0,9)
(0,8)
1.
2.
3.
4.
5.
6.

TABLE I

Frequencies of band lines in NO β system.

Of the letters following certain wave-numbers, *d* indicates a line which is caused by the coincidence of two lines of the band, *t* of three, and *q* of four. Lines marked in this way therefore show the use of the same wave-number in two or more places. This procedure was in all cases justified by an anomalous intensity of the line, or by a slight dissymmetry. The wave-length given at the top of each double column is that of the *R* line forming the head.

Each frequency given for the $^2P_1$ band represents the mean value obtained by measuring the center of a doublet. The doublet widths are given by Eqs. (7) of the text.

The following bands were measured by one of us on the comparator at the Palmer Physical Laboratory, Princeton University: (0, 7), (0, 8), (0, 12), (1, 6), (2, 9), (2, 13), and (3, 8). Before using the Princeton instrument, checks were made to be sure that its screw gave no systematic errors as compared with the one used at this Laboratory, on which the remaining bands were measured.

Lines above $j=24$ in the stronger bands were measured on a heavy exposure where the resolution was inferior to that of the best plates. Hence the accuracy is of a lower order than for the lines of smaller j, being comparable with that for some of the fainter bands. The relative intensities of the bands and band-lines are given in Part II.

(0, 4)

	λ2620.511		λ2626.628	
j''	$R_1(j)$	$P_1(j)$	$R_2(j)$	$P_2(j)$
1	38,149.14*t*			
2	149.14*t*	38,141.23*d*	38,060.30*t*	
3	149.14*t*	136.58*d*	060.30*t*	38,046.05*d*
4	147.38	130.35	059.44	040.72
5	144.94*d*	123.65	057.24	034.12*d*
6	141.23*d*	115.41	054.39	026.41
7	136.58*d*	106.40	050.10	017.73
8	130.94	096.34	044.99	007.99
9	124.29	085.42	038.85	37,997.37*d*
10	116.47	073.28	031.63	985.58
11	107.84	060.30*t*	023.57	972.97
12	098.14	046.05*d*	014.51*d*	959.36
13	087.51	031.09	004.21	944.56
14	075.59	014.52*d*	37,993.01	928.78
15	062.83	37,997.37*d*	980.57	912.10
16	049.07	979.36	967.49	894.41
17	034.12*d*	959.96	953.03	875.49
18	018.15	940.00	937.97	855.67
19	001.69	918.91	921.30	834.81
20	37,984.11	896.58	903.89	812.98
21		873.61		789.97
22		849.38		766.42
23				
24				
25				

	$Q_1(j)$	$Q_2(j)$
1	38,144.94*d*	
2		38,055.44
3		052.61
4		

(0, 5)

	λ2747.557		λ2754.252	
	$R_1(j)$	$P_1(j)$	$R_2(j)$	$P_2(j)$
	36,385.06*d*			
	385.23	36,377.06	36,296.79*d*	
	385.06*d*	371.99	296.79*d*	36,282.83
	383.63	366.37	295.77	277.17
	381.26*d*	359.67	293.81	270.60
	377.74	351.82	290.92*d*	263.11
	373.34	343.09	287.08	254.68
	367.88	333.32	282.26	245.18
	361.44	322.55	276.44	234.87
	354.11	310.74	269.56*d*	223.50
	345.75	298.02	261.88	211.27
	336.43	284.28	253.17	197.97
	326.11	269.56*d*	243.51*d*	183.70
	314.86	254.03	232.77	168.48
	302.55	237.29	220.95	152.26
	289.29	219.60	208.32*d*	135.01
	275.21	200.98	194.48	116.84*d*
	259.98	181.51	179.80	097.62
	243.79*d*	160.94	163.99	077.46
	226.81	139.41	147.34	056.31
	208.66*d*	116.84*d*	129.67	034.12
	189.58	093.64	110.86	011.02
	169.77	069.21		35,986.80
		038.84		
		017.55		

	$Q_1(j)$	$Q_2(j)$
	36,381.26*d*	
		36,290.92*d*
		288.85
		285.07

(0, 6)

	λ2885.245		λ2892.590	
j''	$R_1(j)$	$P_1(j)$	$R_2(j)$	$P_2(j)$
1	34,648.53			
2	648.96*d*	34,640.56	34,560.98*d*	
3	648.96*d*	636.01	560.98*d*	34,547.47*d*
4	647.60	630.36	560.21	541.90*d*
5	645.36	623.81	558.32	535.48*d*
6	642.11	616.25	555.69	528.04*d*
7	637.97	607.69	552.07	519.75*d*
8	632.76	598.22	547.47*d*	510.55*d*
9	626.69	587.75	541.90*d*	500.41*d*
10	619.64	576.34	535.48*d*	489.40*d*
11	611.66	563.96	528.04*d*	477.56
12	602.76	550.65	519.75*d*	464.75
13	592.86	536.34	510.55*d*	450.95*d*
14	582.04	521.18	500.41*d*	436.23
15	570.35	505.05	489.40*d*	420.54
16	557.64	488.02	477.23	403.89
17	544.02	469.96	464.00	386.31
18	529.53	450.95*d*	449.87	367.77
19	514.13	431.16	434.88	348.34
20	497.68	410.32	418.93	327.74
21	480.38	388.67	401.82*d*	306.47
22	462.18	366.01		
23	442.94	342.40		
24	422.74	317.93		
25	401.82*d*	292.51		
26				
27				
28				
29				
30				

(0, 7)

	λ3034.853		λ3042.973	
	$R_1(j)$	$P_1(j)$	$R_2(j)$	$P_2(j)$
	32,940.30			
	940.96*d*	32,932.39	32,853.07*d*	
	940.96*d*	927.91	853.07*d*	33,839.19
	939.71	922.46	852.49	833.88
	937.60	916.09	850.88	827.71*d*
	934.54	908.64	848.39	820.58
	930.62	900.33	844.94*t*	812.63
	925.73	891.11	840.75*d*	803.81
	919.89	880.94	835.47	794.02
	913.22	869.84	829.43	783.34
	905.56	32,857.82	822.43	32,771.82
	896.96	844.94*t*	814.54	759.42
	887.63	831.08	805.65	746.08
	877.27	816.35	795.98	731.82
	866.00	800.69	785.26	716.68
	853.94	784.20	773.70	700.59
	840.75*d*	766.77	761.13	683.60
	826.93	748.40	747.73	665.74
	811.99	729.24	733.44	646.92
	796.47	709.09	718.15	627.16
	779.76	688.15	701.96	606.55
	762.35	666.48*d*	684.80	585.02
	743.86	643.45	666.61*d*	562.50
	724.49	619.75	647.71	539.06
	704.37	595.16	627.74	514.76
	683.53	569.74	606.96	489.49
	661.31	543.42	585.02	463.28
	638.46	516.27	562.50	436.32
		488.11		408.31
		459.12		379.35

TABLE I (*continued*)

	$Q_1(j)$	$Q_2(j)$	$Q_1(j)$	$Q_2(j)$
1	34,644.10		32,937.01	
2		34,555.23		32,847.25
3		552.87		844.97*t*
4		549.85		842.04
5		545.59		838.10
6		540.72		833.26
7				827.65*d*

(0, 8)

	λ3197.973		λ3206.937		λ3376.428		λ3386.379	
j''	$R_1(j)$	$P_1(j)$	$R_2(j)$	$P_2(j)$	$R_1(j)$	$P_1(j)$	$R_2(j)$	$P_2(j)$
1	31,260.20				29,607.75*d*			
2	260.80*d*	31,252.31	31,173.43*d*		608.62*d*	29,599.77*d*	29,521.21*d*	
3	260.80*d*	247.81	173.43*d*	31,159.54	608.62*d*	595.49*d*	521.62	29,507.76
4	259.70	242.47	172.86	154.35*d*	607.75*d*	590.28*d*	521.21*d*	502.68*d*
5	257.78	236.21	171.41	148.28	605.91	584.22*d*	519.91	496.77
6	254.90	229.05	169.15	141.38	29,603.26*d*	29,577.30*d*	29,517.79	29,490.09
7	251.24	220.93	166.02	133.65	599.77*d*	569.51*d*	514.91	482.56
8	246.60	211.95	161.97	125.06	595.49*d*	560.87	511.19	474.27
9	241.06	202.10	157.12	115.61	590.28*d*	551.28	506.61	465.15
10	234.73	191.35	151.39	105.36	584.22*d*	540.85	501.25	455.20
11	227.49	179.71	144.75	094.16	577.30*d*	529.56	495.03	444.42*d*
12	219.33	167.28*d*	137.23	082.18	569.51*d*	517.46	487.97	432.84
13	210.31	153.79	128.90	069.27	561.01	504.49	480.05	420.42
14	200.44	139.55	119.64	055.54*d*	551.56	490.72	471.30	407.17
15	189.75	124.42	109.53	040.86	541.36	476.11	461.70	393.03
16	178.15	108.47	098.47	025.38	530.28	460.67	451.24	378.12
17	165.55*d*	091.67	086.63	009.02	518.40	444.42*d*	439.96	362.35
18	152.34	073.85*d*	073.85*d*	30,991.75	505.75	427.28	427.71	345.71
19	138.07	055.38*d*	060.17	973.61	492.23	409.42	414.80	328.27
20	123.12	035.84	045.55	954.56	477.92	390.65	400.92	309.96
21	107.21	015.55	030.04	934.62	462.79	370.97	386.23	290.79
22	090.51	30,994.43	013.75	913.88	446.71	350.74	370.67	270.81
23	072.92	972.44*d*	30,996.48	892.20	429.92	329.51	354.22	249.97
24	054.60	949.63*d*	978.33	869.67	412.11	307.54	336.97	228.36
25	035.16	925.90*d*	959.33	846.25	393.75	284.70	318.85	205.76
26	015.23	901.36	939.34	821.93	374.63	261.02	299.91	182.39
27	30,994.08	875.98	918.60	796.73	354.98	236.61	280.11	158.20*d*
28	972.44*d*	849.71	896.91	770.63	333.63	211.31	259.42	133.15
29	949.63*d*	822.50	874.40	743.70	311.81	185.38	237.87	107.24
30	925.90*d*	794.69	850.84	715.87	289.27	158.20*d*	215.45	080.48
31		765.89		687.24		130.62		052.89
32		736.20		657.58		102.18		024.54

	$Q_1(j)$	$Q_2(j)$	$Q_1(j)$	$Q_2(j)$
1	31,256.88		29,604.57	
2	255.40	31,167.34*d*	603.25*d*	29,515.60
3	253.23	165.46*d*	601.09	513.57
4	250.45	162.45		510.77
5		158.72		507.07
6		154.31*d*		502.70*d*
7		148.66		497.47
8		142.14		491.58
9		135.22		484.66
10		127.24		477.04
11		118.16		468.69

(0, 10)

	λ3572.392		λ3583.484		(0, 11) λ3788.483		λ3800.914	
j''	$R_1(j)$	$P_1(j)$	$R_2(j)$	$P_2(j)$	$R_1(j)$	$P_1(j)$	$R_2(j)$	$P_2(j)$
1	27,983.71*d*				26,387.29			
2	984.49*d*	27,976.13	27,897.51*d*		388.32*d*	26,379.61	26,302.02*q*	
3	984.49*d*	971.60	897.87	27,884.15*d*	388.32*d*	375.48	302.02*q*	26,288.27
4	983.71*d*	966.47	897.51*d*	879.11*d*	387.71	370.51	302.02*q*	283.47
5	982.09	960.53	896.45	873.29*d*	386.24	364.71	301.04	277.84
6	979.64	953.72	894.56	866.69*d*	383.98*d*	358.09	299.34	271.63*d*
7	976.36	946.12	891.84*d*	859.51	380.94	350.72	296.89*d*	264.58
8	972.23	937.66	888.45	851.47	377.15	342.57	293.76	256.81
9	967.35	928.41	884.15*d*	842.71	372.53	333.56	289.86*d*	248.32
10	961.65	918.32	879.11*d*	833.12	367.14	323.81	285.12	239.00
11	955.09	907.40	873.29*d*	822.72	361.02	313.28	279.68	229.06
12	947.79	895.72	866.69*d*	811.56	354.10	302.02*q*	273.44	218.34*d*
13	939.68	883.21	859.23	799.58	346.40	289.86*d*	266.43	206.85
14	930.79	869.89	850.98	786.84	337.93	277.09	258.69	194.56
15	921.11	855.79	841.89	773.28	328.80	263.53	250.16	181.55
16	910.59	840.91	832.03	758.92	318.80	249.18	240.85	167.79
17	899.24	825.22	821.32	743.77	308.15	234.06	230.81	153.23
18	887.18*d*	808.76	809.83	727.81	296.89*d*	218.34*d*	219.93	137.89
19	874.31	791.45	797.57	710.99	284.54*d*	201.64	208.30	121.80*d*
20	860.68	773.41	784.38	693.41	271.59*d*	184.27	195.80	104.96*d*
21	846.22	754.70	770.41	675.01	257.81	166.19	182.72	087.30*d*
22	831.08	734.96	755.64	655.80	243.48	147.35	168.73	068.90
23	815.00	714.59	740.02	635.79	228.26	127.73	153.93	049.71
24	798.23	693.39	723.76	614.96	212.24	107.44	138.46	029.78
25	780.64	671.47	706.47	593.32	195.22	086.38	121.98*d*	009.07
26	762.26	648.73	688.39	570.89	178.03	064.53	104.97*d*	25,987.56
27	743.64	625.21	669.57	547.61	159.99	041.97	087.30*d*	965.35
28	723.48	600.89	649.88	523.60	140.80	018.66	068.56	942.35
29	702.41	575.78	629.40	498.74	121.85	25,994.64	049.12	
30	681.15	549.92	608.03	473.06		969.81	028.99	
31		523.46		446.60		944.33		
32		495.97		419.38				

TABLE I (*continued*)

	$Q_1(j)$	$Q_2(j)$	$Q_1(j)$	$Q_2(j)$
1	27,980.36		26,383.98*d*	
2	979.15	27,891.85*d*	382.72	26,295.90
3	977.64	889.79		294.04
4		887.20*d*		291.55
5		884.22*d*		288.02
6		880.79		284.54*d*
7		876.29		280.03

	(0, 12)				(1, 6)			
	λ4027.812		λ4041.784		λ2802.593		λ2809.399	
j''	$R_1(j)$	$P_1(j)$	$R_2(j)$	$P_2(j)$	$R_1(j)$	$P_1(j)$	$R_2(j)$	$P_2(j)$
1	24,819.22				35,670.69*t*			
2	820.39*d*	24,811.59			670.69*t*		35,584.34*d*	
3	820.39*d*	807.48	24,734.59*d*	24,720.71*d*	670.69*t*		584.34*d*	35,570.36
4	819.92	802.67	734.59*d*	715.98	669.22	35,652.30	583.14	564.72
5	818.58	797.01	733.81*d*	710.68	666.89*d*	645.50	581.11	558.38
6	816.50	790.62	732.31	704.53	663.57	637.90	578.31*d*	550.88
7	813.69	783.45	730.11	697.74	659.08	629.24	574.40	542.47
8	810.11	775.55	727.22	690.30	653.82	619.59	569.65	533.13
9	805.85	766.82	723.60	682.12	647.50	608.99	563.82	522.91
10	800.82	757.44	719.27	673.23	640.23	597.34	556.88*d*	511.60
11	794.98	747.34	714.21	663.63	631.92	584.79	549.41	499.56
12	788.62	736.48	708.40	653.33	622.70	571.24	540.99*d*	486.26
13	781.31	724.84	701.89	642.28	612.58	556.88*d*	531.11	472.36
14	773.35	712.50	694.62	630.50	601.40	540.99*d*	520.31	457.03
15	764.67	699.45	686.63	618.03	589.17	524.74	508.64	440.94
16	755.31	685.63	677.89	604.80	576.11*d*	507.34	496.28	423.96
17	745.15	671.10	668.44	590.80	562.22	488.98	482.71	406.01
18	733.81*d*	655.88	658.22	576.18	547.21	469.59	468.06	386.97
19		639.99	647.30	560.75		449.34	452.44	367.07
20		623.24*d*	635.56	544.59		427.94		346.11
21			623.24*d*	527.75				
22			610.00	510.12				
23				491.89				

	$Q_1(j)$	$Q_2(j)$	$Q_1(j)$	$Q_2(j)$
1	24,816.03		35,666.89*d*	
2		24,728.26		35,578.31*d*
3		726.52		576.11*d*
4		724.10		573.05
5		720.95*d*		
6		717.22		

	(1, 11)				(1, 13)			
	λ3647.236		λ3658.544		λ4113.628		λ4127.887	
j''	$R_1(j)$	$P_1(j)$	$R_2(j)$	$P_2(j)$	$R_1(j)$	$P_1(j)$	$R_2(j)$	$P_2(j)$
1	27,409.56*d*				24,301.49			
2	410.24*d*	27,401.75	27,325.12*d*		302.20*d*	24,293.82	24,218.11	
3	410.24*d*	397.60	325.52	27,311.76*d*	302.62	289.93	218.67*d*	24,205.03
4	409.56*d*	392.57	325.12*d*	306.76*d*	302.20*d*	285.14	218.67*d*	200.34
5	407.98	386.67	324.09	301.07*d*	300.92	279.59	217.91	194.99
6	405.53	379.94	322.11	294.70	29 .87	273.31	216.38	188.97
7	402.33	372.42	319.38*d*	287.51	2' .	266.24	214.22	182.25
8	398.37	364.07	315.99	279.54	292.6	258.47	211.34	174.87
9	393.48	354.95	311.76*d*	270.85	288.46	249.92	207.77	166.79
10	387.83	345.03	306.76*d*	261.31	283.50	240. 6	203.48	158.01
11	381.42	334.30	301.07*d*	251.09	277.85	230.69	198.47	148.54
12	374.23	322.71	294.51	239.99	271.45	219.96	192.75	138.34
13	366.24	310.45	287.12	228.13	264.37	208.48	186.31	127.46
14	357.52	297.29	278.99	215.55	256.64	196.38	179.14	115.81
15	347.95	283.48	269.97	202.08*d*	248.05	183.53	171.25	103.51
16	337.56	268.67	260.23	187.95	238.80	169.89	162.63	090.45
17	326.42	253.19	249.57	172.93	228.89	155.57	153.33	076.68
18	314.76*d*	237.04	238.15	157.18	217.98	140.65	143.24	062.21
19	301.73	220.02	226.11	140.60	206.83	124.95	132.41	046.96
20	288.13	202.15*d*	213.09	123.21*d*	194.33	108.65*d*	121.01	031.07
21	274.07	183.50	199.35	104.99	182.01	091.43	108.65	014.37
22	259.07	164.21	184.66	086.08		073.57	095.65*d*	23,997.04
23	243.22	144.17	169.36	066.32		055.05		978.95
24		123.21*d*		045.66				960.11
25		101.61		024.32				

	$Q_1(j)$	$Q_2(j)$	$Q_1(j)$	$Q_2(j)$
1	27,406.11		Not visible	
2		27,319.43*d*		24,212.42
3		317.41		210.78
4		314.63*d*		
5		310.95		

TABLE I (*continued*)

(2, 9)

j''	λ3159.825 $R_1(j)$	$P_1(j)$	λ3168.301 $R_2(j)$	$P_2(j)$
1	31,636.98*d*			
2	638.19*d*		31,553.56*d*	
3	638.19*d*	31,625.42	553.56*d*	31,540.53*d*
4	636.98*d*	619.99	552.96	534.92
5	634.92	613.80	551.39	528.80
6	631.98	606.61	548.82	521.92
7	628.20	598.54	545.51*d*	513.98
8	623.38	589.52	541.23	505.30
9	617.70	579.65	536.14	495.70
10	611.20	568.79	530.15	485.30*d*
11	603.86	557.07	523.13	473.89
12	595.49	544.52	515.47	461.76
13	586.19	531.02	506.80	448.63
14	576.10	516.65	497.26*d*	434.66
15	565.23	501.38	486.68	419.76
16	553.40	485.30*d*	475.35	404.07
17	540.53*d*	468.15	463.01	387.43
18	527.06	450.20	449.97	369.84*d*
19	512.56	431.56	435.77	351.37
20	497.26*d*	411.76	420.79	332.11
21	480.96	391.37	404.78	311.79
22		369.84*d*		290.73
23		347.68		

	$Q_1(j)$	$Q_2(j)$
1	Not visible	
2		31,547.88
3		545.58*d*
4		542.78

(2, 13)

j''	λ3949.850 $R_1(j)$	$P_1(j)$	λ3962.834 $R_2(j)$	$P_2(j)$
1				
2	25,310.27*d*	25,301.71	25,227.34*t*	
3	310.27*d*	297.67	227.34*t*	25,214.00
4	309.68	292.83	227.34*t*	209.25
5	308.31	287.17	226.37*d*	203.83
6	306.10*d*	280.80	224.74	197.63
7	303.23	273.62	222.32	190.79
8	299.50	265.70	219.18	183.20
9	295.10	257.02	215.32	175.01*d*
10	289.98	247.59	210.71	165.87
11	284.01	237.29	205.41	156.11
12	277.33	226.37*d*	199.29	145.63
13	269.91	214.66	192.51	134.39
14	261.73	202.22	184.94	122.41
15	252.83	189.01	176.64	109.67
16	243.16	175.01*d*	167.49	096.24
17	232.85	160.43	157.62	082.05
18	221.77*d*	145.03	147.08	067.06
19		128.88	135.77	051.33
20		111.99	123.65	034.92
21			110.94	017.74
22				
23				

	$Q_1(j)$	$Q_2(j)$
1	25,306.10*d*	
2		25,221.81*d*
3		219.74
4		217.17

(2, 14)

j''	λ4200.677 $R_1(j)$	$P_1(j)$	λ4215.243 $R_2(j)$	$P_2(j)$
1	23,797.86			
2	798.71*d*	23,790.31	23,716.27*d*	
3	799.01	786.44	716.77*d*	23,703.32
4	798.71*d*	781.74	716.77*d*	698.66
5	797.41	776.28	715.96	693.39*d*
6	795.44	770.08	714.49	687.53
7	792.75	763.14	712.37	680.84*d*
8	789.36	755.47	709.51	673.57
9	785.26	747.09	705.85	665.59
10	780.41	738.01	701.76	656.91
11	774.85	728.15	696.81	647.54
12	768.58	717.63	691.17	637.44
13	761.57	706.42	684.82	626.69
14	753.97	694.41	677.77	615.25
15	745.54	681.77	670.02	603.06
16	736.48	668.33	661.52	590.20
17	726.71	654.33	652.21	576.62
18	716.27*d*	639.56	642.37	562.33
19	704.99	624.08	631.74	547.28
20	693.39*d*	608.10	620.32	531.57
21	680.84*d*	591.12		515.17
22		573.59		498.06
23				
24				
25				

	$Q_1(j)$	$Q_2(j)$
1	Not visible	
2		23,710.63
3		708.96
4		

(2, 15)

j''	λ4479.783 $R_1(j)$	$P_1(j)$	λ4496.197 $R_2(j)$	$P_2(j)$
1	22,316.27*q*			
2	316.27*q*	22,307.79*d*	22,234.24*d*	
3	316.27*q*	303.95*d*	234.80*d*	22,221.44*d*
4	316.27*q*	299.38*d*	234.80*d*	216.87*d*
5	315.13	294.21*d*	234.24*d*	211.68*d*
6	313.40	288.28*d*	232.95	205.89*t*
7	310.92	281.34	231.08	199.45*d*
8	307.79*d*	273.93	228.53*d*	192.51
9	303.95*d*	265.84	225.33	184.86
10	299.38*d*	257.09	221.44*d*	176.67*d*
11	294.21*d*	247.61	216.87*d*	167.63
12	288.28*d*	237.51	211.68*d*	158.00
13	281.89	226.73*d*	205.89*t*	147.77*d*
14	274.74	215.28	199.45*d*	136.74
15	266.88	203.12	192.16	125.14
16	258.37	190.33	184.25	112.85
17	249.23	176.67*d*	175.57	099.86*d*
18	239.39	162.71	166.37	086.30
19	228.70	147.77*d*	156.38	071.99
20	217.68	132.54	145.78	057.05
21	205.89*t*	116.41	134.59	041.41
22		099.86*d*	122.46	025.16
23		082.44	109.85	008.25
24				21,990.43
25				972.11

	$Q_1(j)$	$Q_2(j)$
1	22,312.12	
2		22,228.53*d*
3		226.73*d*
4		224.77

TABLE I (*continued*)

	(3, 8)				(3, 16)			
	λ2915.949		λ2923.099		λ4574.018		λ4590.776	
j''	$R_1(j)$	$P_1(j)$	$R_2(j)$	$P_2(j)$	$R_1(j)$	$P_1(j)$	$R_2(j)$	$P_2(j)$
1	34,284.14*t*				21,856.51*q*			
2	284.14*t*		34,200.31*t*		856.51*q*	21,848.26*d*	21,776.18*d*	
3	284.14*t*	34,271.55	200.31*t*		856.51*q*	844.51*d*	776.73*d*	21,763.68*d*
4	282.69	266.08	199.75		856.51*q*	839.82	776.73*d*	759.15*d*
5	280.34	259.57	197.65	34,175.35	855.38	834.57	776.18*d*	754.04*d*
6	277.11	252.06	194.80*d*	168.07	853.73	828.65	774.96	748.31*t*
7	272.88	243.58	190.90	159.85	851.32	822.06	773.11	741.92*d*
8	267.64	234.17	186.17	150.64	848.26*d*	814.76	770.58*d*	734.99*d*
9	261.44	223.77	180.50	140.62	844.51*d*	806.85	767.47	727.47
10	254.36	212.46	173.86	129.71	840.14	798.26	763.68*d*	719.44*d*
11	246.38	200.28*t*	166.32	117.58	835.14	788.97	759.15*d*	710.49
12	237.41	186.96	157.75*d*	104.65	829.44	779.02	754.04*d*	701.05
13	227.39	172.74	148.18*d*	090.82	823.08	768.39	748.31*t*	690.98*d*
14	216.53	157.71*d*	137.81	076.03	816.08	757.20	741.92*d*	680.16
15	204.66	141.48	126.31	060.26	808.36	745.27	734.99*d*	668.70
16	191.77	124.47	113.98*d*	043.51	800.10	732.72	727.16	656.66
17	178.07	106.44	100.80	025.66*d*	791.10	719.44*d*	718.76	643.88*d*
18	163.45	087.69	086.41	007.30	781.46	705.68	709.83	630.53
19	148.06*d*	067.88	071.86	33,987.67	771.01	690.98*d*	700.01	616.53
20	131.19	046.99	055.01	967.12	760.33	676.11	689.58	601.89
21	113.96*d*	025.56*d*	037.67	945.70	748.31*t*	660.17	678.39	586.55
22		002.73	019.49	923.16	736.33	643.88*d*	666.64	570.54
23		33,979.04				626.75	654.35	554.02
24						608.73		536.50
25								518.49
	$Q_1(j)$		$Q_2(j)$		$Q_1(j)$		$Q_2(j)$	
1	Not visible				21,852.25			
2			34,194.83*d*				21,770.58*d*	
3			192.43				769.26	
4			189.65				766.80	

was made under favorable conditions, by which the brighter bands were considerably over-exposed, but no trace of the lines in question was found.

Measurements. Table I gives the wave-number data for all of the bands measured. The six branches, R_1, Q_1, P_1, R_2, Q_2, P_2, of the complete band are given in each case. The first three branches mentioned constitute the $^2P_1$ band, and the other three the $^2P_2$ band. The wave-length of the line forming the head is given for these two sub-bands in each case. The precision is greater for the stronger bands ($n'=0$ progression, $n''=6$ to 11) than for the others. For the former, as the combination relations show, the relative errors of measurement within a band appear to be about 0.02 cm^{-1}. For the sake of uniformity, however, wave-numbers are given to two places even for the weaker bands. The measurements given here include all the stronger bands of the system.[28] Several fainter bands could also have been measured, but would probably have contributed little to the value of the data here included.

Application of the combination principle. According to the quantum theory of band spectra,[16] the rotational energy levels[29] of a molecule may in general be assumed to be given[30] for low speeds of rotation by the familiar Kramers and Pauli expression

$$F(j)=Bm^2=B\left[(j^2-\sigma^2)^{1/2}-\rho\right]^2 \qquad (1)$$

The lines of the P, Q, and R branches are conveniently designated by their

[28] For a diagram of all bands which occur, and their relative intensities, see Part II, p. 185.

[29] The actual energies are obtained on multiplying $F(j)$ by hc.

[30] Cf. R. S. Mulliken, Phys. Rev. **28**, 490–3 (1926).

j in the final state. That is (neglecting fine-scale rotational doubling, which will be considered in a later section).

$$\begin{aligned} R(j) &= \nu^0 + F'(j+1) - F''(j) \\ Q(j) &= \nu^0 + F'(j) - F''(j) \\ P(j) &= \nu^0 + F'(j-1) - F''(j) \end{aligned} \tag{2}$$

The spacing of the rotational levels in the initial or final states can be investigated by certain combination relations. Thus

$$R(j) - P(j) = F'(j+1) - F'(j-1) = \Delta_2 F'(j) \tag{3a}$$

gives a series of quantities, each representing the sum of two adjacent intervals between the levels in the initial state, while

$$R(j-1) - P(j+1) = F''(j+1) - F''(j-1) = \Delta_2 F''(j) \tag{3b}$$

gives a similar series for the final state. Further information may often be obtained from combinations involving the Q branch, but in the present case the latter is too weak to be of use for this purpose. Since all bands having the same value of n' must have identically the same set of initial rotational levels, it should be possible to obtain from all such bands a set of initial-state combination differences $\Delta_2 F'(j)$ which are identical for all. An analogous statement holds with regard to n'' and $\Delta_2 F''(j)$.

Choosing two bands with the same value of n', for instance the (0, 10) and (0, 11) $^2P_1$ bands, it was found after a few trials that one (and only one) set of $R-P$ differences can be obtained which is identical within experimental error for both bands. These differences should represent $\Delta_2 F_1'$ values, and from Eqs. (2) and (3a) the members of each $P-R$ pair should have a common value of j''. For the correct absolute assignment of j values, we depend on the fact that the $\Delta_2 F'$ quantities should in this case (see below under *Term formulation*) be approximately equal to $4B'j$. The designation of every line in these two bands by an appropriate j' and j'' is now possible.

Considering next the final state, differences were taken in the (1, 11) band between lines suspected of being $R_1(j-1)$ and $P_1(j+1)$, and compared with the corresponding $\Delta_2 F_1''$ values from the (0, 11) band. The numbering of the lines in the (1, 11) band to give the desired equalities was easily found, and the proper assignment of j values was established by the relations $\Delta_2 F_1''(j) = 4B''j$, and Eq. (3b). The same procedure could be carried throughout the band system, but was not needed for the assignment of j values, since the regular variation in the relative positions of the P and R lines in any progression (or sequence) of bands was obvious. For the $^2P_2$ bands, an analogous procedure to the above yielded the values of $\Delta_2 F_2'$ and $\Delta_2 F_2''$ and established the correct j numbering.

The combination differences in the (0, 10), (0, 11), and (1, 11) bands are given in Table II. The combination relations were tested for all the

eighteen bands here measured, and agreements similar to the above were found. The identities found in the Δ_2F quantities for both initial and final states render it certain that the $F(j)$ levels concerned differ by two units in j.

As far as could be determined, the required combinations with the Q branch are also fulfilled. In general this would permit one to obtain sets of Δ_1F values, but in the present case the Q lines are obviously too few and weak. In regard to possible Q branch doubling, "crossing over," etc., cf. p. 169, below.

TABLE II

Example of combination differences.

For the values marked by asterisks one (or both) of the lines entering into the combination was superimposed on, or incompletely resolved from, another line of sufficient intensity to render the measurement of the former less reliable.

The $\Delta_2F_1''(j)$ values were obtained from the $^2P_1$ bands by taking the wave-number differences between the lines $R_1(j-1)-P_1(j+1)$, while $\Delta_2F_2''(j)$ represents the corresponding differences $R_2(j-1)-P_2(j+1)$ in the $^2P_2$ bands. For the initial state, $\Delta_2F_1'(j)$ and $\Delta_2F_2'(j)$ give the differences $R_1(j)-P_1(j)$ and $R_2(j)-P_2(j)$, respectively.

	(1, 11)		(0, 11)				(0, 10)	
j''	$\Delta_2F_1''(j)$	$\Delta_2F_2''(j)$	$\Delta_2F_1''(j)$	$\Delta_2F_2''(j)$	$\Delta_2F_1'(j)$	$\Delta_2F_2'(i)$	$\Delta_2F_1'(j)$	$\Delta_2F_2'(j)$
2	11.96*		11.81*		8.71*		8.36*	
3	17.67*	18.36*	17.81*	18.55*	12.84*	13.75*	12.89*	13.72*
4	23.57*	24.45*	23.61*	24.18*	17.20*	18.55*	17.24*	18.40*
5	29.62*	30.42*	29.62*	30.39*	21.53	23.20	21.56	23.16*
6	35.56	36.58	35.52	36.46	25.89*	27.71*	25.92	27.87*
7	41.46	42.57	41.41*	42.53	30.22	32.31*	30.24	32.33*
8	47.38	48.53	47.38	48.57*	34.58	36.95	34.57*	36.98*
9	53.34	54.68	53.34	54.76	38.97	41.54*	38.94	41.44*
10	59.18	60.67*	59.25	60.80*	43.33	46.12	43.33*	45.99*
11	65.12	66.77*	65.12*	66.78*	47.74	50.62	47.69	50.57*
12	70.97	72.94*	71.16*	72.83	52.08*	55.10*	52.07	55.13*
13	76.94	78.96*	77.01	78.88	56.54*	59.58	56.47	59.65*
14	82.76	85.04*	82.87	84.88	60.84	64.13	60.90	64.14
15	88.85	91.04	88.75	90.90	65.27	68.61	65.32*	68.61
16	94.76	97.04	94.74	96.93	69.62	73.06	69.68*	73.11
17	100.52	103.05	100.46*	102.96	74.09	77.58	74.02	77.55
18	106.40	108.97	106.51	109.01*	78.55*	82.04	78.42*	82.02
19	112.68*	114.99*	112.65*	115.00*	82.90	86.50*	82.86	86.58
20	118.23	121.07	118.22	121.02*	87.32*	90.84*	87.27*	90.97*
21	123.92	127.01	124.24*	126.90	91.62*	95.43*	91.52	95.40
22	129.90	133.03	130.08*	133.01	96.13	99.83	96.12	99.84
23	135.86*	139.00	136.04	138.95	100.53	104.22	100.41	104.23
24	141.61	145.04	141.88	144.86	104.80	108.68	104.84*	108.80*

Term formulation. It is at once evident that the combinations give four different sets of Δ_2F values, two in the initial state and two in the final, thus confirming the supposition that the bands are due to a transition between two doublet electronic states. As has been said, we are here concerned with a final state which is probably $^2P_{1,2}$ from analogy with aluminium, the corresponding atom. In ^2P states, (as is shown especially by the HgH type bands)[23] we expect $\rho\sim 0$, $\sigma=\frac{1}{2}$ ($^2P_1$) and $1\frac{1}{2}$ ($^2P_2$). From a study of systematic relations in band spectra,[23] we also expect j to have integral values for NO, since it has an odd number of electrons. Both of these suppositions are in harmony with the empirical form of the Δ_2F's, which may

be approximately represented (cf. Tables 2 and 3) in every case by $4BT$ where T is an *integer*. The term formulation

$$F(j)=B(j^2-\sigma^2)+D(j^2-\sigma^2)^2+\cdots \tag{4}$$

requires (cf. Eqs. (3)) that the Δ_2F's be given by $4Bj$, and therefore agrees with our observations if $T=j$. Other possibilities, e.g. j half-integral, $\sigma=0$, $\rho=\frac{1}{2}$, are not immediately excluded, since this cannot be decided from the empirical form of the Δ_2F's alone.[30] The latter must be supplemented by evidence from the number of missing lines, or from intensity relations.

TABLE III

Mean values of $\Delta_2F(j)$ for various vibrational states.

In obtaining the sets of average Δ_2F values in Table III, the data from each band were weighted according to the intensity of the bands, the apparent consistency of the measurements, etc. The weights actually used where data on the same set were given by more than one band were as follows:

$n'=0$: (0, 4)0, (0, 5)1, (0, 6)2, (0, 7) to (0, 11) each 4, (0, 12)2
$n'=1$: (1, 6)1, (1, 11)2, (1, 13)2
$n'=2$: (2, 9)2, (2, 13)2, (2, 14)2, (2, 15)1
$n'=3$: (3, 8)1, (3, 16)1
$n'=6$: (0, 6)2, (1, 6)1
$n'=8$: (0, 8)4, (3, 8)1
$n'=9$: (0, 9)4, (2, 9)1
$n''=11$: (0, 11)1, (1, 11)1
$n''=13$: (1, 13)1, (2, 13)1

Every individual value obtained by using a superimposed line was, however, given only half the above weight.

All differences derived from the (0, 4) band are considerably less accurate than the rest, because this band is relatively very weak. It was thought desirable to obtain data from this band, however, to permit the comparison of the Δ_2F values for the final state with those of the γ bands. The results of this comparison show accurate numerical agreement.[17]

Owing to the fact that the lines of the $^2P_1$ bands are doublets, the tabulated Δ_2F_1's, for both initial and final levels (as is shown by a consideration of work[17] on the γ bands) represent mean values between two levels each of which is a close double (cf. text, p. 169).

j	n'	0	1		2		3		n''	4	5	
	Δ_2F_1'	Δ_2F_2'	Δ_2F_1'	Δ_2F_2'	Δ_2F_1'	Δ_2F_2'	Δ_2F_1'	Δ_2F_2'	Δ_2F_1''	Δ_2F_2''	Δ_2F_1''	Δ_2F_2''
2	8.57		8.44		8.48		8.25		12.56		13.07	
3	12.98	13.81	12.66	13.76	12.60	13.29	12.29	13.05	18.79	19.58	18.86	19.62
4	17.26	18.52	16.99	18.37	16.91	18.06	16.64	17.58	25.49	26.18	25.39	26.19
5	21.56	23.15	21.33	22.89	21.11	22.57	20.79	22.23	31.97	33.03	31.81	32.66
6	25.89	27.76	25.59	27.41	25.33	27.00	25.07	26.73	38.54	39.51	38.17	39.13
7	30.26	32.35	29.90	31.93	29.62	31.54	29.28	31.26	44.89	46.40	44.42	45.74
8	34.60	36.94	34.25	36.47	33.85	35.96	33.48	35.57	51.16	52.73	50.79	52.21
9	38.96	41.48	38.53	40.94	38.10	40.36	37.67	39.96	57.63	59.41	57.14	58.76
10	43.36	46.06	42.83	45.44	42.39	44.84	41.89	44.17	63.99	65.88	63.42	65.17
11	47.73	50.59	47.14	49.92	46.73	49.27	46.15	48.73	70.42	72.27	69.83	71.59
12	52.08	55.10	51.50	54.49	50.94	53.70	50.43	53.05	76.75	79.01	76.19	78.18
13	56.51	59.61	55.82	58.89	55.19	58.14	54.67	57.33	83.62	85.74	82.40	84.69
14	60.87	64.14	60.26	63.37	59.50	62.56	58.86	61.76	90.14	92.11	88.82	91.25
15	65.29	68.64	64.48	67.77	63.81	66.96	63.13	66.18	96.23	98.60	95.26	97.76
16	69.66	73.12	68.89	72.26	68.12	71.39	67.34	70.50	102.87	105.08	101.57	104.11
17	74.03	77.59	73.27	76.66	72.42	75.59	71.65	74.98	109.07	111.82	107.78	110.70
18	78.46	82.05	77.59	81.02	76.76	80.06	75.77	79.23	115.21	118.22	114.27	117.02
19	82.83	86.54	81.79	85.46	80.95	84.43	80.10	83.48	121.57	124.99	120.57	123.49
20	87.31	90.98	85.98	89.91	85.36	88.72	84.21	87.69	128.08	131.33	126.95	129.87
21	91.64	95.42	90.57	94.33	89.59	93.11	88.31	91.84	134.73	137.47	133.17	136.32
22	96.05	99.83		98.59		97.30	92.45	96.10			139.45	142.87
23	100.46	104.23		103.04		101.60		100.33			145.56	
24	104.78	108.67									152.22	
25	109.13	113.07										
26	113.62	117.47										
27	118.08	121.89										
28	122.33	126.24										
29	126.93	130.66										
30	131.18	134.97										

TABLE III (*continued*)

j	n''	6	7		8		9		10		11	
		Δ_2F_1''	Δ_2F_2''	Δ_2F_1''	Δ_2F_2''	Δ_2F_1''	Δ_2F_2''	Δ_2F_1''	Δ_2F_2''	Δ_2F_1''	Δ_2F_2''	Δ_2F_1''	Δ_2F_2''
2		12.52		12.39		12.43		12.12		12.11		11.88	
3		18.53	19.26	18.50	19.19	18.28	19.08	18.31	18.57	18.02	18.40	17.74	18.46
4		25.16	25.66	24.87	25.36	24.59	25.13	24.40	24.84	23.96	24.58	23.59	24.31
5		31.34	32.22	31.07	31.91	30.65	31.50	30.43	31.10	29.99	30.82	29.62	30.40
6		37.66	38.61	37.27	38.25	36.83	37.77	36.39	37.36	35.97	36.94	35.54	36.52
7		43.92	45.15	43.43	44.58	42.95	44.12	42.41	43.52	41.98	43.09	41.44	42.55
8		50.18	51.57	49.68	50.92	49.13	50.41	48.51	49.77	47.95	49.13	47.38	48.54
9		56.44	58.06	55.89	57.41	55.24	56.59	54.62	55.98	53.91	55.33	53.34	54.72
10		62.73	64.30	62.07	63.65	61.33	62.96	60.69	62.21	59.95	61.43	59.22	60.74
11		68.99	70.69	68.28	70.01	67.43	69.19	66.73	68.41	65.93	67.55	65.12	66.78
12		75.26	77.07	74.48	76.35	73.69	75.50	72.82	74.59	71.88	73.71	71.03	72.87
13		81.61	83.52	80.61	82.72	79.77	81.70	78.81	80.80	77.90	79.85	76.98	78.91
14		87.82	90.09	86.94	88.97	85.89	88.02	84.87	87.02	83.89	85.95	82.82	84.93
15		94.03	96.43	93.07	95.39	91.99	94.26	90.87	93.18	89.88	92.06	88.80	90.97
16		100.32	102.86	99.23	101.66	98.11	100.53	96.99	99.33	95.89	98.12	94.75	96.98
17		106.63	109.41	105.54	107.96	104.23	106.72	103.06	105.53	101.83	104.22	100.50	103.00
18		112.86	115.65	111.51	114.21	110.18	113.04	108.98	111.68	107.79	110.33	106.46	108.98
19		119.21	122.07	117.81	120.60	116.42	119.30	115.14	117.78	113.79	116.44	112.66	115.00
20		125.46	128.41	123.85	126.95	122.50	125.49	121.11	124.01	119.68	122.56	118.22	121.05
21		131.67		129.99	133.13	128.61	131.67	127.21	130.10	125.72	128.58	124.03	126.96
22		137.98		136.31	139.46	134.80	137.84	133.28	136.26	131.63	134.62	129.96	133.02
23		144.25		142.60	145.74	140.88	144.08	139.17	142.31	137.69	140.68	135.98	138.98
24		150.43		148.70	151.85	147.02	150.23	145.22	148.46	143.53	146.70	141.74	144.95
25				154.75	158.22	153.24	156.40	151.09	154.58	149.50	152.87	147.71	150.90
26				160.95	164.46	159.18	162.60	157.14	160.65	155.43	158.86	153.25	156.63
27				167.26	170.64	165.52	168.71	163.32	166.76	161.37	164.79	159.37	162.61
28				173.20	176.71	171.58	174.90	169.60	172.87	167.86	170.84	165.35	
29				179.36	183.15	177.75	181.04	175.43	178.94	173.56	176.82	170.99	
30						183.74	187.16	181.19	184.98	178.95	182.79	177.52	
31						189.70	193.26	187.09	190.91	185.18	188.65		

j	j	n''	12	13		14		15		16	
			Δ_2F_1''	Δ_2F_2''	Δ_2F_1''	Δ_2F_2''	Δ_2F_1''	Δ_2F_2''	Δ_2F_1''	Δ_2F_2''	Δ_2F_1''	Δ_2F_2''
2			11.74		11.56		11.42		12.32		12.00	
3			17.72		17.25	17.87	16.97	17.61	16.89	17.37	16.69	17.03
4			23.38	23.91	23.07	23.60	22.73	23.38	22.06	23.12	21.94	22.69
5			29.30	30.06	28.88	29.70	28.63	29.24	27.99	28.91	27.86	28.42
6			35.13	36.07	34.69	35.62	34.27	35.12	33.79	34.79	33.32	34.26
7			40.95	42.01	40.40	41.52	39.97	40.92	39.47	40.44	38.97	39.97
8			46.87	47.99	46.22	47.39	45.66	46.78	45.08	46.22	44.47	45.64
9			52.67	53.99	51.96	53.32	51.35	52.60	50.70	51.86	50.00	51.14
10			58.51	59.97	57.80	59.23	57.11	58.31	56.34	57.70	55.54	56.98
11			64.34	65.94	63.56	65.11	62.78	64.32	61.87	63.44	61.12	62.63
12			70.14	71.93	69.36	71.01	68.43	70.12	67.48	69.10	66.75	68.17
13			76.12	77.90	75.09	76.91	74.17	75.92	73.00	74.94	72.24	73.88
14			81.86	83.86	80.87	82.82	79.80	81.76	78.77	80.75	77.81	79.61
15			87.72	89.82	86.74	88.69	85.64	87.57	84.41	86.60	83.36	85.26
16			93.57	95.83	92.44	94.58	91.21	93.40	90.21	92.30	88.92	91.11
17			99.43	101.71	98.14	100.43	96.92	99.19	95.66	97.95	94.42	96.63
18			105.16	107.69	103.96	106.33	102.63	104.93	101.46	103.58	100.12	102.23
19			110.57	113.63	109.57	112.17	108.17	110.80	106.85	109.32	105.35	107.94
20				119.55	115.40	118.03	113.87	116.57	112.29	114.97	110.84	113.46
21				125.44	120.76	123.97	119.80	122.26	117.82	120.62	116.45	119.04
22				131.35	126.96	129.70			123.45	126.34	121.56	124.37
23						135.54				132.03	127.60	130.14
24										137.74		135.86

A consideration of the missing lines supports the formulation of Eq. (4), with the σ'' values $\frac{1}{2}$ and $1\frac{1}{2}$, and also gives the σ' values. Since j'' is limited

to values equal to or greater than σ, the line j $(1\rightarrow 0)$ should be missing for all bands having the final state $^2P_1$ $(\sigma''=\frac{1}{2})$. Similarly in the bands with the final state $^2P_2$, at least three lines should be absent, corresponding to the transitions $1\rightarrow 0$, $0\rightarrow 1$ and $2\rightarrow 1$. Actually we have two lines missing in the first instance and four in the second. This establishes the values of σ', since the additional missing line ($0\rightarrow 1$ in the first case and $1\rightarrow 2$ in the second) is evidently due to the exclusion $j'=0$ in the first case and $j'=1$ in the second. Hence σ must also be $\frac{1}{2}$ and $1\frac{1}{2}$ for the components of the upper doublet, and we conclude that this is also a $^2P_{1,2}$ state. The observed transitions then are:

Higher frequency bands: $^2P_1\rightarrow{}^2P_1$; $\sigma'=\frac{1}{2}$; $\rho'=\rho''=0$

Lower frequency bands: $^2P_2\rightarrow{}^2P_2$; $\sigma'=\sigma''=1\frac{1}{2}$; $\rho'=\rho''=0$

Therefore the rotational terms of both initial and final states are given by Eq. (4). In support of this picture we have further very strong evidence from the intensity relations (see Part II), since weak Q branches having intensities in agreement with those observed are required by the theory for transitions where $\sigma'=\sigma''$.

Evaluation of rotational terms. Since the application of the combination principle has shown that bands with a common n' (or n'') give identical values of Δ_2F' (or Δ_2F''), we are justified in averaging the appropriate individual values from such bands in order to obtain a more accurate representation of the particular set of rotational terms involved. Table III gives the complete set of combination differences for the four initial and thirteen final vibrational states ($n'=0$ to 3; $n''=4$ to 16). The weighted mean has been taken wherever more than one set of data was available. The quantities given in each column of this table have been fitted empirically by equations of the form

$$\Delta_2F(j)=a+bj+cj^2+dj^3 \qquad (5)$$

For this purpose a method of least squares was used which is particularly suitable for band-spectrum analysis.[31] The accuracy of the data did not appear to justify the inclusion of terms higher than the cubic. The numerical coefficients in Eq. (5) obtained in this way are summarized in Table IV, columns 2 to 5.

To obtain the corresponding equations for $F(j)$, a knowledge of the theoretical form of the energy expression is necessary. If we assume merely that the rotational terms may be represented by a power series of the form

$$F(j)=\text{const.}+Aj+Bj^2+Cj^3+Dj^4+\cdots \qquad (6)$$

we can compute these new coefficients from those of Eq. (5), leaving the value of the constant term undetermined. Thus we have

$$D=d/8,\quad C=c/6,\quad B=b/4-d/4,\quad A=a/2-c/6.$$

[31] R. T. Birge and J. D. Shea, "A Method for the Rapid Calculation of the Least Squares Solution of a Polynomial of any Degree," Phys. Rev. **24**, 206 (1924) Abstract; Univ. Calif. Publ. Math. **2**, 67 (1927). We are indebted to Prof. Birge for the use of the tables before publication.

The values of these coefficients are given in the remaining columns of Table IV. With the exception of B, they show no consistent variations with n, and hence have been averaged over the various values of n for each electronic state.

Since we may assume B to be given by $B_0-\alpha n$,[32] the least squares solution of the weighted values for such a linear relation is given in each case

TABLE IV

Empirical coefficients in rotational energy function.

	a	b	$c\cdot10^3$	$d\cdot10^5$	Wt.	A	B	$C\cdot10^3$	$D\cdot10^5$
$^2P_1n'=0$	0.0280	4.2802	6.233	−10.85	4	0.0130	1.0701	1.039	−1.356
1	−0.0789	4.2423	6.846	−16.88	2	−0.0408	1.0607	1.140	−2.110
2	0.0684	4.1788	6.468	−11.48	2	0.0331	1.0447	1.077	−1.435
3	−0.0823	4.1492	6.817	−16.98	1	−0.0423	1.0374	1.136	−2.122
				Av.		−0.0006 ±0.0132	(1.0704 −0.01162n') ±0.0007	1.081 ±0.017	−1.626 ±0.149
$n''=6$	0.0445	6.2595	1.191	−3.520	1	0.0220	1.5649	0.199	−0.440
7	0.0052	6.2159	−0.862	0.154	2	0.0029	1.5539	−0.144	0.019
8	−0.0683	6.1526	−1.608	3.053	3	−0.0340	1.5382	−0.268	0.382
10	0.0886	5.9716	2.000	−7.229	5	0.0438	1.4930	0.333	−0.904
11	0.0839	5.8976	2.500	−9.547	4	0.0415	1.4744	0.417	−1.193
12	−0.0108	5.8558	0.110	−3.854	4	−0.0053	1.4639	0.018	−0.482
13	−0.0637	5.7876	−0.114	−2.309	4	−0.0318	1.4469	−0.019	−0.289
				Av.		0.0071 ±0.0081	(1.6754 −0.01783n'') ±0.0011	0.106 ±0.064	−0.506 ±0.137
$^2P_2n'=0$	−0.0405	4.6733	−6.871	3.632	8	−0.0190	1.1683	−1.145	0.454
1	0.0534	4.5909	−5.049	0.404	4	0.0276	1.1477	−0.841	0.051
2	0.0612	4.5182	−3.744	−2.236	4	0.0311	1.1296	−0.624	−0.279
3	0.1489	4.4550	−5.373	9.814	1	0.0754	1.1137	−0.896	1.227
				Av.		0.0093 ±0.0150	(1.1678 −0.01892n') ±0.0006	−0.936 ±0.076	0.232 ±0.224
$n''=6$	0.0869	6.4255	0.110	−2.336	1	0.0436	1.6063	0.018	−0.292
7	0.0024	6.3864	−1.778	−1.736	3	0.0015	1.5966	−0.296	−0.217
8	0.0512	6.2843	1.315	−10.05	6	0.0253	1.5711	0.219	−1.260
9	−0.0693	6.2349	0.046	−8.824	8	−0.0348	1.5589	0.008	−1.103
11	−0.0776	6.1075	−2.375	−1.329	3	−0.0385	1.5269	−0.396	−0.166
12	0.1913	5.9664	2.160	−10.46	3	0.0954	1.4916	0.360	−1.307
13	0.0444	5.9250	−0.124	−5.617	5	0.0223	1.4812	−0.021	−0.702
				Av.		0.0070 ±0.0121	(1.7239 −0.01866n'') ±0.0015	0.010 ±0.069	−0.871 ±0.135

in place of the average. The occurrence of an exceptionally large range of n'' values in the β bands shows well the effect of increasing vibration on the spacing of the rotational terms. The value of B_0'' obtained from the γ bands by Frl. Guillery[17] (1.663 for $^2P_1$ and 1.694 for $^2P_2$) are slightly lower than those of Table IV, due probably to the method of evaluation, which

[32] A. Kratzer, Zeits. f. Physik **3**, 289 (1920).

neglects higher power terms and would be expected to give lower values than the more accurate procedure used here.

Rotational doubling. As stated in an earlier section (cf. p. 155), the lines of the $^2P_1$ band are double. In the analysis just given, this doubling has been left out of account. An investigation of the doublet separations in the (0, 10) and (0, 11) bands shows that their value, $\Delta\nu$, is practically the same for corresponding lines of the two bands, and can be represented within experimental error by

$$\Delta\nu_R = 0.0154j \qquad \Delta\nu_P = 0.0138j \tag{7}$$

The analysis of the γ bands[17] shows that the rotational doubling in the F_1'' levels may be represented (with reference to the *mean* F_1'' values) by $\pm 0.005\ j''$. If we take Eqs. (7) to hold within the range of measurements ($j = 16$ to 22), the rotational doubling in the initial (F_1') states becomes $\pm 0.0123\ j'$. In the data for the γ bands, there are also indications of a small combination defect, hence of a small rotational doubling, in the $^2S \rightarrow {}^2P_2$ bands, which is practically constant with increasing j. If this is real, there must also be a doubling of equal magnitude in the initial $^2P_2$ levels of the β bands, since the lines of the $^2P_2$ bands are strictly single on our plates. Presumably at least a *latent* doubling is present in *all* (F_1 and F_2) levels and in all the P, Q, and R branches, as would be expected from the theory. Probably the branches in each sub-band are given by a scheme (Eq. (2) of p. 1206 of ref. 23) involving "crossing over" in the Q branches.

Band-origins and equations for vibrational terms. For the calculation of band-origins, and conversely for the empirical representation of the lines, we employ Eqs. (2), evaluating the $F(j)$ terms by Eq. (6) with the mean values of the coefficients given in Table IV. If the rotational terms are represented by Eq. (4),[33] the term $F(0)$ equals $-B\sigma^2 + D\sigma^4$. We therefore give this value to the constant term of Eq. (6).[34] In this way the position of the origin of each band was computed, using the first three accurately measured lines of the R branch and the first four of the P branch. The mean of the seven values of ν^0 thus obtained, which never differed among themselves by more than a few hundredths cm^{-1}, is recorded in Table V as ν^0 (*obs.*), for each band. Under ν^0 (*calc.*) are entered the values given by the following equations for band origins

$$\begin{aligned} {}^2P_1 \qquad \nu^0 &= 45{,}486.12 + 1029.429n' - 7.460n'^2 + 0.1017n'^3 - 1892.119n'' \\ &\quad + 14.4243n''^2 - 0.04021n''^3 + 0.001351n''^4 \\ {}^2P_2 \qquad \nu^0 &= 45{,}394.58 + 1030.883n' - 7.455n'^2 + 0.0917n'^3 \\ &\quad - 1891.976n'' + 14.4543n''^2 - 0.04229n''^3 + 0.001423n''^4 \end{aligned} \tag{8}$$

[33] E. C. Kemble, Report on Molecular Spectra Ch. VII, part 2A, p. 310. (Derivation of Kramers and Pauli formula).

[34] In the formulation of the new quantum mechanics, Eq. (4) becomes

$$F(j) = B[j^*(j^*+1) - \sigma^2] + D[j^*(j^*+1) - \sigma^2]^2 + \cdots$$

If j^* is taken $\frac{1}{2}$ unit lower than the integral j used here, $F(0)$ should be taken as $-B(\sigma^2 + \frac{1}{4}) + D(\sigma^4 + \frac{1}{2}\sigma^2 + 1/8)$. Hence the essential result of this change would be a small shift in the ν^0 values obtained below of approximately $\frac{1}{4}C(C = B' - B'')$. The new mechanics also requires that the vibrational quantum numbers, n, used here be replaced throughout by $n + \frac{1}{2}$.

Combining these expressions with the empirical coefficients for Eq. (6) given in Table IV, and defining the band lines by Eqs. (2), we obtain a precise representation of all the frequencies found in this extensive band system. No evidence was found for perturbations in either rotational or vibrational terms.

TABLE V

Frequencies of band origins.

Band	ν^0 (*obs*)	ν^0 (*calc*)	$o-c$	Band	ν^0 (*obs*)	ν^0 (*calc*)	$o-c$
(0, 4)	38,146.21	38,146.21	±0.00	(0, 10)	27,980.71	27,980.67	+0.04
	38,055.59	38,055.59	±0.00		27,892.16	27,892.19	−0.03
(0, 5)	36,382.00	36,382.08	−0.08	(0, 11)	26,384.44	26,384.42	+0.02
	36,291.68	36,291.66	+0.02		26,296.40	26,296.36	+0.04
(0, 6)	34,645.74	34,645.75	−0.01	(1, 11)	27,406.57	27,406.49	+0.08
	34,555.77	34,555.78	−0.01		27,319.95	27,319.92	+0.03
(1, 6)	35,667.69	35,667.82	−0.13	(0, 12)	24,816.31	24,816.23	+0.08
	35,579.24	35,579.30	−0.06		24,728.69	24,728.72	−0.03
(0, 7)	32,937.54	32,937.53	+0.01	(1, 13)	24,298.63	24,298.62	+0.01
	32,847.91	32,847.91	±0.00		24,212.95	24,212.95	±0.00
(0, 8)	31,257.27	31,257.28	−0.01	(2, 13)	25,306.41	25,306.38	+0.03
	31,168.04	31,168.02	+0.02		25,222.10	25,222.11	−0.01
(3, 8)	34,281.14	34,281.17	−0.03	(2, 14)	23,795.06	23,795.04	+0.02
	34,196.07	34,196.07	±0.00		23,711.28	23,711.26	+0.02
(0, 9)	29,604.99	29,604.97	+0.02	(2, 15)	22,312.40	22,312.48	−0.08
	29,516.10	29,516.10	±0.00		22,229.13	22,229.16	−0.03
(2, 9)	31,634.78	31,634.80	−0.02	(3, 16)	21,852.65	21,852.60	+0.05
	31,548.80	31,548.78	+0.02		21,771.36	21,771.36	±0.00

DISCUSSION OF RESULTS

Form of rotational energy function. The term-form $B(j^2-\sigma^2)+D(j^2-\sigma^2)^2 + \cdots$, involving only even powers[16] of $m=(j^2-\sigma^2)^{1/2}$ does not successfully represent the empirical form of the rotational terms found in the β bands. Thus C, the coefficient of the cubic term is relatively large in the initial electronic state, and is positive for the $^2P_1$ and negative for the $^2P_2$ level. Also the quantity B, which should be substantially equal to $h/8\pi^2I$, and would be expected to be practically the same for $^2P_1$ and $^2P_2$, is decidedly greater for $^2P_2$. Both of these effects tend to bring the lines $P_1(j)$ and $P_2(j-1)$, together for high j values, likewise the lines $R_1(j)$ and $R_2(j-1)$; and similarly with the F and Δ_2F values (cf. Table 3). Such a drawing together of the branches is found to a more pronounced degree in other bands involving multiplet electronic states (OH, MgH, CaH(A), CH, N_2 (second positive) and Swan bands).

The above phenomena are qualitatively accounted for by Hund's theory of molecular electronic states.[35] In the initial state of the β bands

[35] F. Hund, Zeits. f. Physik **36**, 657 (1926).

of NO we evidently have an example of a ^2P doublet electronic state which approaches Hund's case *a* for low values of j, but case *b* for high j values, corresponding to a gradual change of the orientation of the electron spin vector from positions parallel and anti-parallel to σ_k for low j, to an orientation parallel and anti-parallel to j_k (resultant of σ_k and m) for large values of j (cf. Hund's paper and discussion by Kemble[36] and by Mulliken.[37])

From the B and C values of Table IV, it is evident that the transition from case *a* toward case *b* proceeds much less rapidly in the *final* than in the initial ^2P state. This justifies the conclusion that the doublet separation (which is a measure of the energy of orientation) is considerably less in the initial than in the final ^2P state. This lends support to our original assumption that the separation of 91.54 wave-number units between the origins ($n'=n''=0$) of the $^2P_1$ and $^2P_2$ systems, as given in Eqs. (8), represents the *difference*, rather than the sum, of the initial and final electronic doublet separations. Since from the γ bands the final $\Delta\nu$ is 124.4 units,[38] the initial $\Delta\nu$ is thus evaluated as 32.9 units. It then also follows, from the relative position of the two sub-bands and the preceding analysis, that the ^2P doublets are *normal* (not inverted) in both cases. (cf. Fig. 1).

The effect on the rotational term formulae of the transition from case *a* to case *b* has been carried through quantitatively by Professor E. C. Kemble for the case of doublet states. At his suggestion, the resulting equations were tested by one of the writers with the data reported here, and found to give satisfactory agreement.[39] A more complete consideration of these quantitative results will be given in a later paper.

The assumption that for low values of j the terms are given by $F(j) = \text{Const.} + Bj^2$ permits an approximation from the equations, making possible the evaluation of the true moment of inertia, I, from the empirical B. Thus Kemble has found:

$$B=\frac{h}{8\pi^2 I}(1\mp z)^2\pm z^2\Delta\nu$$

where

$$z=\frac{h}{8\pi^2 I\Delta\nu-2h\pm 2h} \tag{9}$$

and $\Delta\nu$ = term difference for zero rotation. The upper sign goes with the lower level of the pair. First taking $h/8\pi^2 I$ as given approximately by the mean value of B for $^2P_1$ and $^2P_2$, Eq. (9) gives the true values as follows (B_0 = value of B for $n=0$, obtained by extrapolation in Table IV).

[36] E. C. Kemble, Report on Molecular Spectra, p. 326.

[37] R. S. Mulliken, Phys. Rev. **29**, 637 (1927.)

[38] This was obtained from the results of Miss Guillery (Ref. 17) on the separation of the null lines by extrapolation to $n''=0$ and addition of $9/4B_2''-1/4B_1''$.

[39] Cf. preliminary report, E. C. Kemble and F. A. Jenkins, Phys. Rev. **29**, 607 (1927) Abstract.

	B_0 values from Table IV.		Values of $h/8\pi^2 I_0$ by Eq. (9)	
	B_0'	B_0''	$h/8\pi^2 I_0'$	$h/8\pi^2 I_0''$
$^2P_1$	1.070	1.675	1.122	1.701
$^2P_2$	1.168	1.724	1.112	1.700

Thus the apparently anomalous difference in the moment of inertia for the doublet components is quantitatively accounted for.

As already noted, the final state doublet separation ($\Delta\nu = 124.4$) is much less affected by the rotation than is that of the initial state ($\Delta\nu = 32.9$). Kemble's equations show that the rate of transition from case *a* to case *b* is determined by the ratio $\Delta\nu/B$, so it is evident that the wider doublet should show the smaller rate. In a limiting case where the rotation has no effect on the electronic separation, the coefficient of j^4 (and of m^4) should satisfy a theoretical relation derived by Kratzer,[40] namely

$$D_0 = -4B_0^3/\omega_0^2.$$

This relation is approximately fulfilled for the final state, where the observed values for the mean D from Table IV are $(-5.0 \pm 1.4) \times 10^{-6}$ and $(-8.7 \pm 1.4) \times 10^{-6}$ for $^2P_1$ and $^2P_2$ respectively. The theory predicts -5.49×10^{-6}. In the initial state the two observed values are widely different.

Constants of the nitric oxide molecule. The true values of $h/8\pi^2 I_0$ obtained above now permit the calculation of the moment of inertia, I_0, for the vibrationless molecule in its initial and final electronic states. The values of I_0 are given in Table VI, together with computed values of r_0, the internuclear distance.

TABLE VI

Molecular constants of nitric oxide.

	Initial electronic state		Final electronic state	
	$^2P_1$	$^2P_2$	$^2P_1$	$^2P_2$
ω_0	1029.43 cm^{-1}	1030.88	1892.12	1891.98
$x\omega_0$	7.460+ cm^{-1}	7.455+	14.424+	14.454+
Q_D			6.810 volts	6.775
I_0	$(24.80 \pm 0.02) \times 10^{-40}$ gr cm^2		$(16.30 \pm 0.02) \times 10^{-40}$	
r_0	1.418×10^{-8} cm		1.150×10^{-8}	

The table also gives ω_0, the frequency of vibration for infinitesimal amplitudes, and $x\omega_0$, which measures the rate of change of the vibration frequency with n. It is noteworthy that the admission of cubic and biquadratic terms in n'' in deriving Eqs. (8) brings the experimental values of ω_0'' for $^2P_1$ and $^2P_2$ much closer together (perhaps equal within experimental error) than those obtained if a parabolic law is assumed. This suggests that the larger difference which we find for the two values of ω_0' may result from our inability to evaluate sufficient higher power terms in this case, owing to the limited number of experimental values. In this connection it is of interest

[40] A. Kratzer, Ann. d. Physik **71**, 72 (1923).

that in the final state (probably ^2P) of the SnCl bands as analysed by Jevons,[41] ω_0 is greater for the upper (probably $^2P_2$) state by 2.1 parts in 350; in these bands the doublet separation is very large ($\Delta\nu\sim 2360$) so that the ^2P state should closely approximate Hund's case *a*.

For the final state of the NO β bands the heat of dissociation into atoms, Q_D, obtained by analytical extrapolation of the $\omega_n : n$ curve[42] and integration to $\omega_n = 0$, is also given in Table VI. The result is considerably lower than that obtained by Birge and Sponer,[21] which was 7.93 volts. The discrepancy arises from the fact that we have here carried the experimental curve to somewhat higher values of n'' and taken into account the quadratic and cubic terms, while Birge and Sponer assumed a linear relation. Direct measurements of the heat of dissociation of NO into N_2 and O_2, combined with the heats of dissociation of O_2 and N_2 obtained from band spectrum data,[21] give Q_D as 8.3 volts, so that it is doubtful whether the band spectrum method in this case is capable of yielding more than a rough approximation. The rule of Birge[43] and Mekce,[44] which states that a decrease in the moment of inertia is invariably accompanied by an increase in the vibration frequency ω_0, holds true in the β bands. It is interesting to note that the semi-quantitative relations found by Mecke[44] are supported in this extreme case where the changes in ω_0 and in the moment of inertia between the initial and final states are exceptionally large. Applying them in the form given by Birge,[16] if we denote by a subscript m the mean value over the initial and final states, we find

$$\omega_m/(\omega_0' - \omega_0'') = -1.70, \qquad I_m/(I_0' - I_0'') = -2.43.$$

A further relation found by Mecke also holds approximately in this case: $I_m \times \omega_m$ nearly equals $I_0'' \times \omega_0''$, and the resulting quantities, 29,970 and 30,830 respectively, lie very near those found[16] for several other molecules having molecular weights of the same order of magnitude.

Since the energy levels of the normal state of NO are given (at least by extrapolation) by the data presented here, it should be possible to calculate from them accurate values of the specific heat of gaseous nitric oxide, and its variation with temperature. Preliminary results[45] show that the existence of a doublet normal state results in an appreciable contribution to the specific heat at low temperatures which are within the range subject to experimental test. Unfortunately no measurements have yet been made at these temperatures.

The magnetic susceptibility of the gas is another property whose theoretical evaluation has been made possible by a knowledge of the molecular electronic states.[46]

[41] W. Jevons, Proc. Roy. Soc. **110A**, 365 (1926).

[42] This is obtained directly from Eqs. (8) by differentiation with respect to n of the appropriate expression for E_n.

[43] R. T. Birge, Phys. Rev. **25**, 240 (1925) Abstract.

[44] R. Mecke, Zeits. f. Physik **32**, 823 (1925).

[45] E. E. Witmer, Paper before the Washington meeting of the American Physical Society, Apr. 1927 (Preliminary report of more accurate calculations).

[46] J. H. Van Vleck, Phys. Rev. **29**, 613 (1927) Abstract; Nature **119**, 670 (1927).

Relation of NO β *bands to theory of band-structure and electronic states.* The NO β bands constitute the first band system for which the existence of integral effective rotational quantum numbers (T) in both initial and final states has been established. The existence of integral j values ($T=j$), and of σ-type terms with $\sigma=\frac{1}{2}$ and $1\frac{1}{2}$ give strong support to previous generalizations of one of the writers,[23] according to which the j values are integral for all odd molecules, and the j_e (here $=\sigma$) values are the same as Sommerfeld's j values for the corresponding atomic electronic states.

The NOβ bands are in all respects in agreement with Hund's theory.[35] The existence of a $^2P\rightarrow{}^2P$ transition, which would have been very surprising in the case of an atom, is in harmony with the theory. The occurrence of the transitions $^2P_1\rightarrow{}^2P_1$ and $^2P_2\rightarrow{}^2P_2$, without $^2P_1\rightarrow{}^2P_2$ and $^2P_2\rightarrow{}^2P_1$, gives striking confirmation of Hund's selection rule $\Delta\sigma_s=0$. The detailed intensity relations agree excellently with the theory, as will be shown in Part II of this paper. The presence, in the $^2P_1$ bands at least, of a fine-scale doubling (σ-type doubling) with equal *a priori* probabilities (as indicated by the relative intensities of the components of the double lines, cf. p. 155) of the doublet components, is in agreement with Hund's theory.

Classification of O_2^+ *and* SiN *bands.* The ultraviolet O_2^+ bands,[47] and also certain SiN bands,[48] have the same obvious structure,—just two well-separated heads of approximately equal intensity, in each band,—as the NOβ bands, and may be tentatively calssified as $^2P\rightarrow{}^2P$ transitions ($^2D\rightarrow{}^2D$ might also be a possibility). If these bands were $^2S\rightarrow{}^2S$, there would be no doubling of the heads; if they involved a change in σ_k (e.g. $^2S\rightarrow{}^2P$ or $^2P\rightarrow{}^2D$), strong Q branches should be present, giving quadruple heads as in the NOγ or CO^+ comet-tail bands.

In conclusion we wish to thank Professor E. C. Kemble for valuable suggestions and for the interest he has taken in this work.

JEFFERSON PHYSICAL LABORATORY,
HARVARD UNIVERSITY,
WASHINGTON SQUARE COLLEGE,
NEW YORK UNIVERSITY,
April, 1927.

[47] R. C. Johnson, Proc. Roy. Soc. **105***A*, 683 (1924); V. M. Ellsworth and J. J. Hopfield, Phys. Rev. **29**, 79 (1927); etc.

[48] R. S. Mulliken, Phys. Rev. **26**, 334 (1925).

THE BETA BANDS OF NITRIC OXIDE. II. INTENSITY RELATIONS AND THEIR INTERPRETATION

By Henry A. Barton,[1] Francis A. Jenkins,[1] and Robert S. Mulliken

Abstract

Relative intensities of band lines.—The equations of Hönl and London predicting the relative intensities of band spectrum lines have been tested with the NO β bands ($^2P \rightarrow {}^2P$ transition), a system emitted by an odd molecule, in the same way that they were recently tested by one of the writers with certain spectra of even molecules. Plates of the β bands used n connection with Part I were measured with a densitometer. The data are compared with theory, first, as to order of intensity of lines, and, second, as to quantitative intensities calculated from densities under reasonable assumptions. (Calibration curves of the relationship between light intensity and photographic density for the plates were unfortunately not available.) Best agreement is obtained if it is assumed that the effective *temeperature of the active nitrogen* source was about 47°C. The observed relative line intnsities are then in essential agreement with those predicted by the Hönl and London equation s. Possible slight departures from exact agreement are discussed. The two sub-bands ($^2P_1 \rightarrow {}^2P_1$ and $^2P_2 \rightarrow {}^2P_2$) in each band are found to be approximately equal in intensity, in agreement with Hund's theory.

Missing lines and Q branches.—The densitometer curves confirm the conclusions of Part I as to the actual absence of lines expected to be missing if the electronic transitions are $^2P_1 \rightarrow {}^2P_1$ and $^2P_2 \rightarrow {}^2P_2$. The shape of the quantitative intensity curves as a function of j is given correctly by the equations of Hönl and London, for low values of j, only if the values $\sigma_1' = \sigma_1'' = \frac{1}{2}$ for $^2P_1$ and $\sigma_2' = \sigma_2'' = 1\frac{1}{2}$ for $^2P_2$ are used in the equations. The values of σ are thereby directly determined to within about a quarter unit.

Band intensities.—Curves for the potential energy of the NO molecule as a function of nuclear separation have been calculated from the data of Part I. These have been used by Condon's method to predict the relative intensities of the bands of the β system. These are compared with the relative intensities observed recently by R. C. Johnson and H. G. Jenkins. The principal features of the intensity distribution, which is that typical of a molecule whose moment of inertia changes considerably during emission, are as predicted, but certain discrepancies are noted.

Section A: Line Intensities

Introduction

In A recent paper,[2] one of the writers has tested the accuracy of the theory expressed in the equations first given by Hönl and London[3] predicting the relative intensities of P, Q, and R branch lines in certain molecular spectra. It was shown that in the case of various even molecules, the rather crude data available are in agreement with the theory. The cases dealt with were all examples of singlet band systems involving ro-

[1] National Research Fellow.

[2] R. S. Mulliken, Phys. Rev. **29**, 391 (1927).

[3] H. Hönl and F. London, Zeits. f. Physik. **33**, 803 (1925).

tational terms of the form $B(j^2-\sigma^2)$ with values of 0, 1, and 2 for σ corresponding to ^1S, ^1P, and ^1D states respectively.

The theory should apply equally well to doublet systems in odd molecules, provided that both initial and final states involve only rotational terms of the form $B(j^2-\sigma^2)$, and provided also that the electronic doublet separations are of considerable size, corresponding to Hund's case *a*.[4] It is important to test the theory by means of spectra from such molecules. The first section of the present paper describes densitometer measurements made, with this purpose chiefly in view, of the NO β bands. These bands are described and analyzed in Part I (to which the reader is referred for more complete information) where it is shown that they correspond to $^2P_1 \rightarrow {}^2P_1$ and $^2P_2 \rightarrow {}^2P_2$ transitions fulfilling the condition stated above, with $\sigma_1 = \frac{1}{2}$ for $^2P_1$ and $\sigma_2 = 1\frac{1}{2}$ for $^2P_2$.

A further purpose has been to supplement Part I in confirming the existence of the weak Q branches and the predicted absence of several P, Q, and R lines of low j values. The intensity data also confirm the assignment of σ and j values made in Part I.

Apparatus and Experimental Methods

As stated in Part I the second order of a Rowland 21 foot concave grating was used to photograph the bands. The wide dispersion, high resolving power, and purity of the spectrum obtained are circumstances very favorable to a study of band line intensities with a densitometer. The scale of the spectrum is large enough to permit the use of a wide slit in the densitometer, thereby increasing its sensitivity. The absence of extraneous lines and bands in the active nitrogen source reduces the number of cases where partial or total superpositions prevent the measurement of intensity. Another advantage is the presence of a large number of bands having the same initial vibrational state $n'=0$ and therefore presumably the same distribution of line intensities. For when two lines of different branches happen to be superposed in one band they are likely to be clearly separated in some of the others. A few bands of the $n'=1$, 2, 3 and 4 progressions are visible and some of these overlap the principal progression, but this happens seldom and the overlaping band is usually relatively very weak. The γ bands, which are also excited by active nitrogen, overlap only the high frequency end of the β spectrum.

In view of these advantages it was felt that the existence of the plates taken for the analysis presented an opportunity not to be neglected. Unfortunately the idea of intensity work was not in mind when the plates were made. For this reason none of the photographic precautions and calibrations usual in intensity work were provided for. This obstacle proved to be less serious than might have been expected, as will be shown.

For the measurement of photographic density use was made of a densitometer of special design built and installed in Palmer Physical Laboratory

[4] F. Hund, Zeits. f. Phys. **36**, 657 (1926). Cf. discussion by E. C. Kemble, "Molecular Spectra in Gases," pp. 326–31, and by R. S. Mulliken, Phys. Rev., **29**, 637 (1927.)

at Princeton University. A collimated beam of light passed up through a slit. The plate being measured was clamped, emulsion side down, as close to this slit as possible, and then moved across the latter by an accurate screw. The light after passing through the plate was focussed on a thermopile, the current from which was measured by a sensitive galvanometer. Deflections were read with a telescope and scale at intervals of 0.0125 mm along the plate. The width of the slit defining the light beam was 0.025 mm. Under these conditions the instrument proved to be fully as sensitive as the eye for the detection of weak lines, and more discriminating than the eye

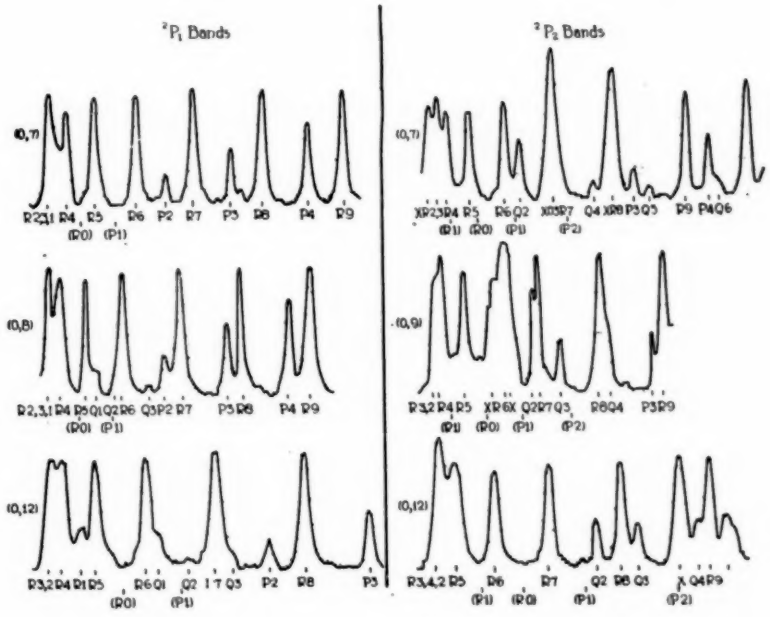

Fig. 1. Densitometer curves. Missing lines are indicated by parentheses. Q lines in the (0, 7) $^2P_1$ band are too faint to be visible with the exception of $Q(1)$ which is too close to $R(5)$ to be resolved by the densitometer. The lines marked with a cross in the $^2P_2$ curves belong to the overlapping $^2P_1$ bands (in some cases a $^2P_1$ line is superposed on a $^2P_2$ line). Designations in this figure give the *final* quantum number j'' for convenience in comparison with Plate I of Part I. In the rest of Part II the designation will indicate j. Examples: $R(6)$ becomes $R(6\frac{1}{2})$ when j is used, $P(4)$ becomes $P(3\frac{1}{2})$, and $Q(3)$ remains $Q(3)$.

in comparing lines of nearly equal intensity. (The comparatively large slit width of 0.025 mm was used in order to measure the weak Q branch lines satisfactorily. Otherwise a slit width of 0.01 mm could have been used, increasing the resolving power of the instrument.)

Fig. 1 shows the results of densitometer runs over portions of several plates. The abscissas are distances along the plate while the ordinates are galvanometer deflections, proportional to transmitted light. The latter are plotted downward, so peaks upward in the curves represent spectrum lines.

Missing Lines and Q Branches

Missing lines. From the point of view of missing lines and Q branch lines Fig. 1 supplements Plate I in Part I of this paper. It shows densitometer measurements of the heads of several $^2P_1$ and $^2P_2$ bands in which these features are most clearly brought out. The calculated positions of missing lines are shown in the figure. In instances where the presence of a line of another branch does not prevent decision, there is, in general, no evidence of lines whose absence is predicted, thus confirming the evidence (cf. Part I, Table I) of visual examination. One or two irregularities of the densitometer curves which might be taken as contrary to this are probably accidental. The beginnings of the P branches are clearly shown in several cases and in the (0, 12) band the first R branch line $R_1(1)$ may be distinguished among the close lines at the band head.

Q branches. The curves of Fig. 1 show undeniably the presence of the weak Q branches. Here, as in Plate I, it is obvious that the Q_2 branch is stronger relative to the P and R branches than is Q_1. In bands other than those shown in Fig. 1 the Q lines are also present with intensities of the order expected.

Intensities

Calculation of intensity from photographic density. Considering now the lines which are actually present, the problem of converting densitometer readings into line intensities arises. The readings are a measure of I, the amount of light passing through the plate and falling on the thermopile. Thus

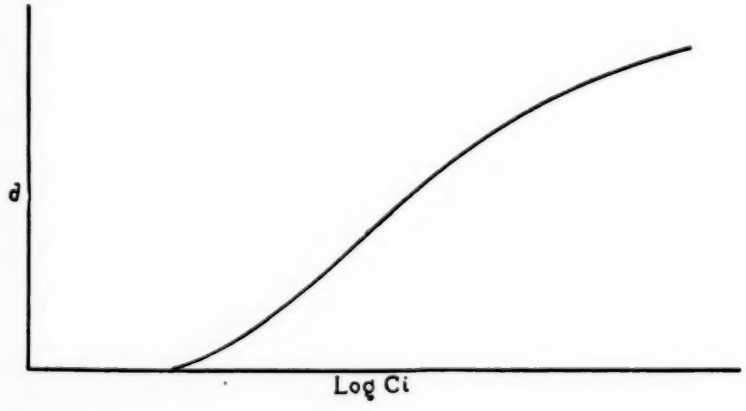

Fig. 2. Type of curve which shows relationship between light intensity i and photographic density d.

the ratio $I_0/I = e^d$ can be determined, where I_0 is the amount of light which passes through an unexposed portion of the plate and d is the density.

The familiar relationship[5] between density and intensity of radiation during exposure i is shown in Fig. 2. Over the relatively straight portion

[5] Hurter and Driffield, J. Soc. Chem. Ind., May (1890).

of the curve, $d=\gamma \log Ci$ where C is a constant for all lines obtained in a single exposure on a single plate. In this equation both γ and C vary with wave-length, but this variation may be neglected over the small wave-length range covered by any one of the NO β bands. Assuming any optical fog to be practically uniform, the relation:

$$d-d_0=\gamma \log Ci-\gamma \log Ci_0,$$

where i_0 is the intensity of light producing the fog, reduces to $d=\gamma \log C'i$. Combining the two expressions involving d, the equation $i=C'I_0^{-\gamma}/I^{-\gamma}$ results. If a whole band is measured at one time with constant I_0, the simple expression $i=C''/I^{-\gamma}$ can be used to determine the relative intensities of the lines, C'' being any convenient arbitrary constant. This, however, is not true in the case of weak lines whose intensities fall on the toe of the curve in Fig. 2. where γ is no longer constant.

Since the plates here used were not developed by standardized methods, the value of γ is not known exactly. An examination of data concerning the value of γ for strongly developed plates such as were employed (Eastman Speedway) has indicated that this value cannot be far different from unity.[6] In computing intensities γ was assumed to be one and C'' was taken as 1000. For the values of I, the actual scale readings of the thermopile galvanometer were used. For each line the lowest value of I (corresponding to maximum density) reached during the transit of the line over the densitometer slit was taken as the measure of the photographic blackening of the whole line. It would be more correct to take the area of the I curve across the line, but the error here introduced is small compared with other experimental uncertainties. In this manner, the "observed" points in Fig. 3 were obtained. An attempt has been made to draw smooth curves through these points. Although some quantitative uncertainty is attached to the method of calculating i from I, it is important to note that the form of the curves changes comparatively little with the value assumed for γ. It should also be emphasized that the order of sequence of the lines according to intensity is necessarily correct since none of the lines was overexposed.

Theory of line intensities. Both $^2P_1$ and $^2P_2$ bands correspond to the case $\sigma'=\sigma''$. In this case the line intensities in the R, P and Q branches are given theoretically by the formulas:

$$\begin{aligned} i_R=i_P&=2\frac{(\bar{j}^2-\sigma^2)}{\bar{j}}e^{-E'/kT} \\ i_Q&=4\frac{\bar{j}\sigma^2}{\bar{j}^2-\frac{1}{4}}e^{-E'/kT} \end{aligned} \qquad (2)$$

where $\bar{j}$ denotes the arithmetic mean of the initial and final j values. E' in the Boltzmann factor is the rotational energy of the molecule in the initial (j') state. The values of E' are accurately known from the analysis of rotational levels in Part I.

[6] R. Davis and F. M. Walters, Jr., Bull. Bur. Stand. **18**, 1 (1922–23).

Only T, the absolute effective temperature of the emitting molecules, is now needed to calculate the theoretical intensity for each line. By means of the following equation, a preliminary estimate of this temperature can be made using any R or P branch, from the value of j'_{max}, the value of j' for which the intensity curve reaches its maximum. Thus:

$$T = B'j'_{max}(2j'_{max} \pm 1)/k \tag{3}$$

In Eq. (3) the + sign holds for R and the − sign for P branches. The expression is obtained from Eq. (2) by neglecting σ^2 in the probability factor, expressing the exponent in the equivalent form $B'(j'^2-\sigma'^2)/kT + \cdots$, and setting the first derivative di/dT equal to zero. From twelve different R or P branches measured with the densitometer as far out as the maximum, a rather scattering set of T values was calculated. These indicate that the true value was between 290° and 330°K.

Significance of T. Previous less certain estimates by Birge[7] from CN bands and by Mulliken[8] from SiN bands have placed the effective temperature of the active nitrogen source at about 100° and 80°C respectively. The afterglow tube used by the writers was only slightly warm to the touch and it is probable, therefore, that the estimated effective temperature is about the same as was the actual temperature of the gas. This is in agreement with Birge's general conclusion that the two closely correspond in various sources and over a wide range of temperatures. Why this should be true for emission bands not thermally excited will probably remain uncertain until more is known about the mechanism of excitation.

Comparison of theory with experiment: General. Of the bands measured with the densitometer, the (0, 12) band is the most satisfactory for detailed examination because most of its lines are free from superposition and the intensities appear to fall, for the most part, on the straight (γ constant) part of the curve in Fig. 2. This band will, therefore, be used as an example for the discussion to follow although the conclusions drawn are supported by a similar examination of two other bands.

The curve best fitting the data for the (0, 12) $^2P_2$ band corresponds to a temperature of 320°K. Both the "theoretical" curves in Fig. 3 were calculated using this temperature, the scale of ordinates being chosen, for convenience in comparison, so as to make the maxima about equal to those of the "observed" curves. Examination of the figure shows at once that in general the shape of the theoretical and observed intensity curves is the same. Thus the R and P branches are of almost equal strength, the P branch however being slightly stronger and coming to a maximum at a slightly higher value of j, due to the effect of the Boltzmann factor. The Q branch starts with a low intensity and rapidly falls off. According to the theory (cf. Eqs. (2)) the intensity of the Q branch should be proportional

[7] R. T. Birge, Astrophys. J. **55**, 273 (1922); "Molecular Spectra in Gases," Bull. Nat Res. Council v. 11. (1926), pp. 219–222.

[8] R. S. Mulliken, Phys. Rev. **26**, 319 (1925).

to σ^2, hence Q_2 $(\sigma = 1\frac{1}{2})$ should be much more intense than $Q_1(\sigma = \frac{1}{2})$. The curves of Fig. 1 obviously support this prediction.

The significance of these agreements can best be realized by reference to Figs. 1, 2 and 3 of a previous paper by one of the authors, which show how differently the curves run if $\Delta\sigma \neq 0$; thus, in the cases $\Delta\sigma = \pm 1$, the Q branch is about as strong as the P and R branches combined, and the latter are not as nearly equal as is the case here.

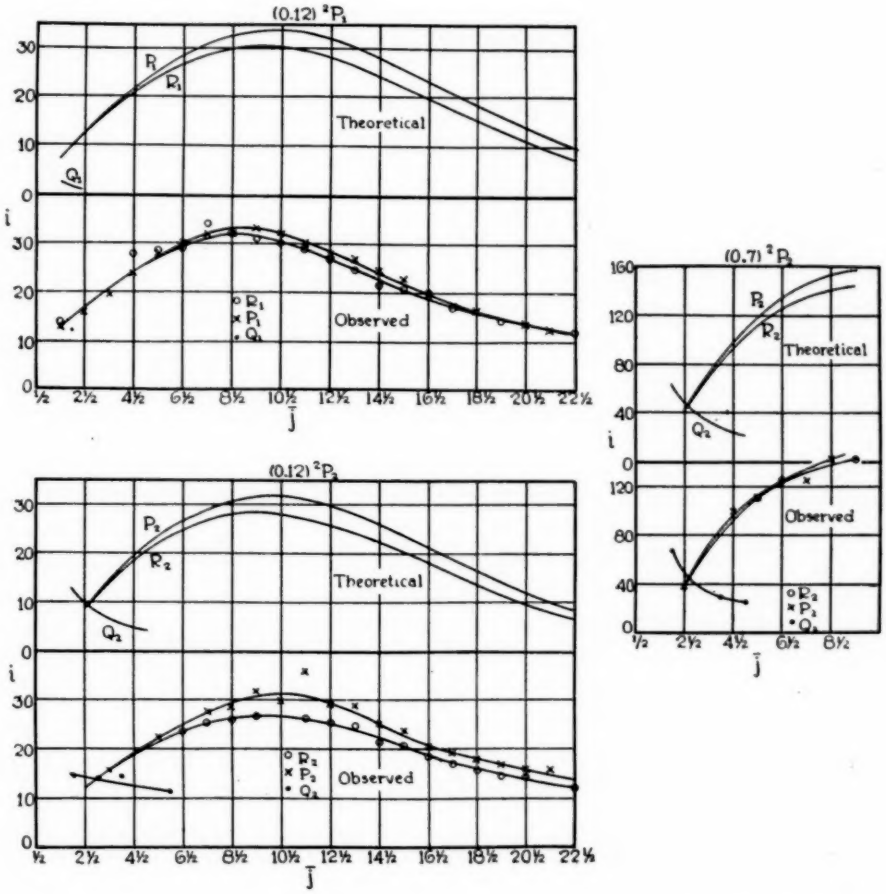

Fig. 3. Curves showing intensities of band lines as a function of j. The $(0, 12)^2P_1$ and $^2P_2$ curves are plotted on the same scale. Omitted points correspond to lines unmeasurable because of superposition of other lines.

Considering Fig. 3 more closely, it is interesting to note that the curves for the R_1 and P_1 branches are closer to one another than would be expected: closer also than the R_2 and P_2 branches, which follow the theoretical course well. Possible further refinements in the theory of intensities will account for this.[9]

[9] The effect of molecular vibration has not been considered in Eq. (2), (cf. Ref. 2).

The maxima of the intensity curves in the R_1 and P_1 branches are displaced to the left, indicating that the chosen temperature (320°K) for the theoretical curves fits the $^2P_2$ bands but is too high for the $^2P_1$ bands. It is not, however, necessary to suppose that the effective temperature was actually different. The effect is probably due to the fact noted in Part I that, although the lines of the $^2P_2$ bands appear strictly single, those of the $^2P_1$ bands are close doublets. These are at first too close to resolve, but with increasing j, the separation increases until, well past the heaviest lines in the band, the components are distinct. The "observed" points in Fig. 3, as has been said, are based on the maximum density at the center of the line, rather than the integrated density across the line. The figure so obtained obviously becomes less accurate as the line widens preparatory to separation. This has the effect of multiplying the observed line intensities by a factor decreasing with j increasing, which obviously shifts the maximum toward lower values of j, as is observed.

Comparison of intensities of components of the electronic doublet. According to Hund's theory of molecular electronic states,[4] two states having the same value of j but differing in respect to the orientation of s with respect to σ_k, as do $^2P_1$ and $^2P_2$ states in Hund's case a (which is here approximately reallized; cf Part I), should have equal a priori probability. Hence aside from the possible effect of the difference in the Boltzmann factor for corresponding j values of $^2P_1$ and $^2P_2$ states, equal intensities would be predicted for the $^2P_1$ and $^2P_2$ sub-bands if each is taken as a whole. As shown in Fig. 1 of Part I, the $^2P_2$ initial level is 32.9 cm^{-1} higher than $^2P_1$ in the limit for $j=0$. (The difference decreases for higher values of j'). For thermal equilibrium at 320 K, there should be only about $e^{-32.9hc/kT}=0.87$ times as many emitters in the $^2P_2$ as in the $^2P_1$ initial levels (the ratio should be nearer unity for higher values of j'), and the intensities of the two sub-bands should differ correspondingly.

The data for the two (0, 12) sub-bands in Fig. 3, having been obtained simultaneously from a single plate, permit a comparison between the total intensities. The predicted approximate equality is verified, but the R_1 branch seems to be a little stronger than the R_2, and would probably prove even stronger if proper allowance were made for the effect of rotational doubling, which tends to make the observed R_1 points too low (cf. discussion elsewhere.) (The relative weakness of the low j R_2 and P_2 lines is made up,—and in a sense caused by,—the greater relative strength of the Q_2 lines; this effect has been allowed for in the conclusion just stated.) Evidence from the P branches is uncertain but the superior intensity of the R_1 branch just noted may very likely be attributed to the differential effect of the Boltzmann factor as discussed in the preceding paragraph. It is shown elsewhere in this paper that the rotational and probably the vibrational energies show approximately a Boltzmann distribution so that the above result is not surprising.

Comparison of theory with experiment: order analysis. The predictions of the theory in regard to the relative intensities of the lines in a band can

be subjected to a rigorous test in one respect without any uncertainty as to the relationship between plate density and line intensity: the lines can be arranged in order of increasing observed intensity and this order can be compared with that predicted. This procedure was followed in the case of the (0, 12) $^2P_2$ band using the data of Fig. 3. A single list was made of all the 37 measurable R, P and Q lines in order of their intensities and this is compared in Table I with a similar theoretical list. (To avoid errors due to inaccuracy in the densitometer measurements and to other minor causes, the observed values were taken from the smooth curves of Fig. 3.)

TABLE I

Lines in order of increasing intensity for the (0, 12)$^2P_2$ band (numbering in terms of j, with the usual parentheses omitted).

Obs.	Calc.	Obs.	Calc.	Obs.	Calc.
$Q6$	$Q6$	$R17\frac{1}{2}$	$R17\frac{1}{2}$	$R12\frac{1}{2}$	$R12\frac{1}{2}$
$R22\frac{1}{2}$	$Q4$	$P18\frac{1}{2}$	$P18\frac{1}{2}$	$R7\frac{1}{2}$	$R7\frac{1}{2}$
$Q4$	$Q3$	$R16\frac{1}{2}$	$R16\frac{1}{2}$	$R11\frac{1}{2}$	$R11\frac{1}{2}$
$R20\frac{1}{2}$	$R22\frac{1}{2}$	$P17\frac{1}{2}$	$P17\frac{1}{2}$	$R8\frac{1}{2}$	$R8\frac{1}{2}$
$Q3$	$R20\frac{1}{2}$	$R15\frac{1}{2}$	$R15\frac{1}{2}$	$R10\frac{1}{2}$	$R10\frac{1}{2}$
$Q2$	$P21\frac{1}{2}$	$P16\frac{1}{2}$	$P16\frac{1}{2}$	$R9\frac{1}{2}$	$R9\frac{1}{2}$
$R19\frac{1}{2}$	$Q2$	$P5\frac{1}{2}$	$R14\frac{1}{2}$	$P13\frac{1}{2}$	$P13\frac{1}{2}$
$P21\frac{1}{2}$	$R19\frac{1}{2}$	$R14\frac{1}{2}$	$P5\frac{1}{2}$	$P7\frac{1}{2}$	$P7\frac{1}{2}$
$P3\frac{1}{2}$	$P20\frac{1}{2}$	$P15\frac{1}{2}$	$P15\frac{1}{2}$	$P12\frac{1}{2}$	$P12\frac{1}{2}$
$P20\frac{1}{2}$	$P3\frac{1}{2}$	$R6\frac{1}{2}$	$R6\frac{1}{2}$	$P8\frac{1}{2}$	$P8\frac{1}{2}$
$R18\frac{1}{2}$	$R18\frac{1}{2}$	$R13\frac{1}{2}$	$R13\frac{1}{2}$	$P9\frac{1}{2}$	$P9\frac{1}{2}$
$P19\frac{1}{2}$	$P19\frac{1}{2}$	$P14\frac{1}{2}$	$P14\frac{1}{2}$	$P11\frac{1}{2}$	$P11\frac{1}{2}$
				$P10\frac{1}{2}$	$P10\frac{1}{2}$

(NOTE: The transpositions $R_2(14\frac{1}{2})-P_2(5\frac{1}{2})$, $P_2(20\frac{1}{2})-P_2(3\frac{1}{2})$, and $R_2(19\frac{1}{2})-P_2(21\frac{1}{2})$ are cases of lines of nearly equal theoretical intensity. The observed intensity of $Q_2(2)$ is too low while $Q_2(3)$ and $Q_2(4)$ as observed are too strong. The Q_2 values are taken from the smooth curve in Fig. 3 which is determined from only four experimental points, two of which ($Q_2 3$ and $Q_2 4$) are certainly high owing to incomplete resolution. (See Fig. 1.) This uncertainty together with the great sensitivity of the method of comparison renders the discrepancies insignificant. In order to make a further comparison, the weak lines of the (0, 7)$^2P_2$ band were arranged in a table similar to Table I. In this case the lines $Q_2(4)$ and $Q_2(5)$ come, as they should, below all the other observed lines in intensity; $Q_2(3)$ is unmeasurable due to superposition, while $Q_2(2)$ is too strong—the opposite from the case of $O_2(2)$ in (0, 12).

Since in band spectra many lines occur within a very short range of intensity values, a slight error in the determination of the intensity of any one line is very likely to throw it out of place. The good correspondence in most of Table I is, for this reason, remarkable. The support given the theory by the "order" analysis may be considered complete within the limits of experimental accuracy, and in particular the analysis upholds the assigned values of σ and j. Further support will be presented later.

Quantitative intensities. It has been shown that the lines of the (0, 12) $^2P_2$ band fall in approximately the correct order when arranged according to intensity. It may now further be pointed out that, as a matter of fact, the relative intensities also agree *quantitatively* with the theoretical, except for the weakest lines. The "theoretical" and "observed" curves of Fig. 3 were drawn with ordinate scales so chosen as to give their maxima about the same ordinates. The agreement then extends through all the lines of intensity greater than about 18. Below that the "observed" intensities are too great, the effect being the more pronounced the weaker the line. Thus

the intensity curve flattens out for R and P lines of high j, and the Q lines are shown relatively much stronger than would be predicted.

It is quite certain that the difficulty here is not with the intensity theory but with the method of converting photographic densities to intensities. Difficulty would be expected with weak lines because they fall on the toe of the density-intensity curve in Fig. 2. This means that the appropriate value of γ is no longer that given by the slope of the straight line portion, but something less and varying from point to point. The weaker the line the more pronounced becomes the error of using the original γ. The direction of the error is such that weak lines appear relatively too strong.

If the above discrepancies for weak lines are entirely due to erroneous translation of density to intensity, they should disappear if we make use

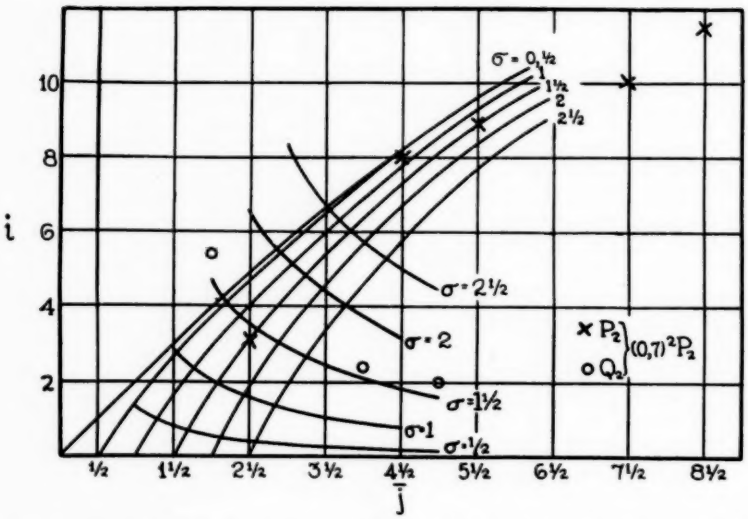

Fig. 4. Comparison of observed intensities with the theoretical intensities calculated assuming several different values of σ. The Q curve for $\sigma=0$ coincides with the zero intensity axis. To avoid confusion no attempt has been made to draw curves through the experimental points. The smoothest curve through the P line intensities would obviously pass below the $P(4\frac{1}{2})$ and above the $P(7\frac{1}{2})$ points and thus closely follow the theoretical curve for $\sigma=1\frac{1}{2}$.

of more intense exposures on which the same lines occur with sufficient intensity so that the method of translation is adequate. To test this a blacker band (0, 7) was examined, and the data for it are also presented in Fig. 3. It will be observed at once that all the lines, even those of the Q_2 branch, have relative intensities in very good accord with those expected. The blackest lines of the (0, 7) band cut off practically all of the light of the densitometer and so were unmeasurable.

The combination of the results for the (0, 7) and (0, 12) bands as here presented constitutes strong *quantitative* support for the intensity theory expressed in equation 2. For the shape of the curves supports the general form and relative magnitude of the probability factors for the three branches, while the relative intensities of the Q lines and of the R and P lines of low

j support both the σ values and the way in which σ enters into the probability factor. Fig. 4 illustrates the extent to which this is the case. The curves represent the theoretical intensities of the P and Q branches for several different values of σ as shown. The experimental points are taken from the observed data in Fig. 3 for the (0, 7) P_2 and Q_2 branches. The intensities have been multiplied by a constant factor chosen to give the P_2 curve about the slope of the theoretical family of P_2 curves. First, it is apparent that the observed P_2 branch intersects the axis of zero intensity at $1\frac{1}{2}$ in the same way as does the theoretical curve for $\sigma = 1\frac{1}{2}$. Second, the general course of the observed Q_2 curve is the same as that of the Q_2 curve for $\sigma = 1\frac{1}{2}$ in the theoretical set. Third, the j coordinate of the intersection of the observed P_2 and Q_2 curves corresponds to that expected for $\sigma = 1\frac{1}{2}$. These considerations appear sufficiently accurate to exclude any value of σ as much as a quarter unit larger or smaller.

No sufficiently intense plates showing the Q_1 branch of the $^2P_1$ bands were available for application of the above procedure. However, Fig. 1 shows that $Q_1(1)$ exists and is of lower intensity than $P_1(1\frac{1}{2})$. From Fig. 4 it will be seen that this relation should be true only in the case $\sigma = \frac{1}{2}$, and so further supports this assignment.

Section B: Band Intensities

Up to this point there has been made no comparison of intensity between *bands*, the discussion being limited to the relative intensities of the lines within a band. The problem of the dependence of intensity upon the initial

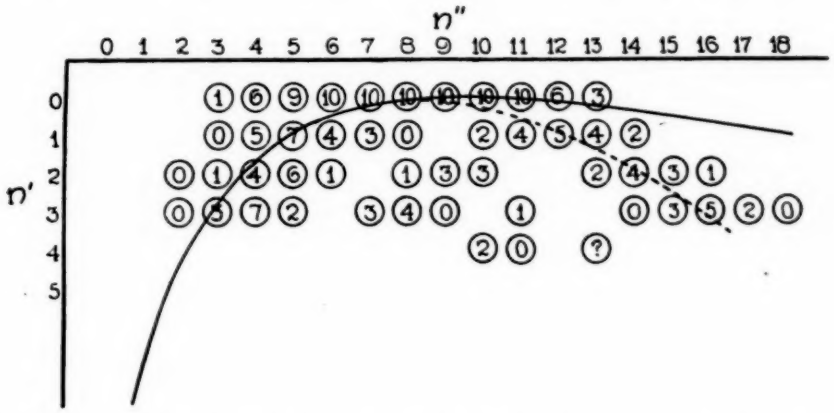

Fig. 5. Distribution of intensity among bands of the NO β system. The solid curve is the "corrected curve" of Condon's theory.[15]

and final *vibrational* quantum numbers is more unsatisfactory from the standpoint of both experiment and theory. Sufficiently definite conclusions can be drawn, however, to justify a full discussion of the matter, especially since considerable new material is available.

Data available. No measurements have been made with the plates used for the data of Part I since (a), the NOβ system extends through too great

a range of the spectrum to permit neglecting the dependence of plate sensitivity on wave length, (b) no precautions were taken to insure uniform development of the plates. It is more satisfactory to base a discussion of relative band intensities on the very complete data of Johnson and Jenkins,[10] obtained with a spectrograph of smaller dispersion. The results of these investigators are presented in Fig. 5; the data for this are taken directly from their paper. The bands (2, 8), (2, 9), (2, 10), (3, 11), (4, 10), (4, 11), and (4, 13), which all appear, although without quantum number assignments, in the wave-length tables of Johnson and Jenkins, have been included.

Interpretation of intensity distribution. The main features of Fig. 5 have been discussed by Johnson and Jenkins[10] and by Birge.[11] It is pointed out by the latter that the energy distribution is, in the main, of a type characteristic of band systems during the emission of which the molecule undergoes a large change in its moment of inertia. Especially noteworthy in this connection is the absence of bands for which both n' and n'' are low. Similar examples are furnished by the absorption spectrum of iodine[12] and by the first negative bands of oxygen (O_2^+).[13]

It is fairly certain, as pointed out by Birge,[14] that the relatively great intensity of the $n'=0$ progression in the β bands is due in part to a low temperature Boltzman distribution of the molecules among the initials vibrational states, corresponding to the actual low temperature of active nitrogen (cf. Section A). But this effect alone obviously does not account for the intensity distribution of Fig. 5. The closest approach to an accurate explanation is furnished by the theory of Condon[15] which is based on a mechanism of quantum transitions in molecules suggested by Franck.[16] Assuming with Condon that electronic transitions take place without change in the instantaneous separation of the nuclei, and most often occur while the latter are near the position either of minimum or of maximum separation in their vibration, it is possible to determine, from the potential energy curves for the two electronic states, the two most likely values of n'' for each value of n'. The results of Part I of the present paper make possible the calculation of the potential energy $V(r)$ as a function of r, the internuclear distance. The values of the following characteristic constants taken from Part I are needed for the calculation.

	ω_0	α	x	B_0	$r_0\times10^8$(cm)
Initial state:	1030.15	0.0152	0.00724	1.117	1.42
Final state:	1892.05	0.0182	0.00764	1.699	1.15

[10] R. C. Johnson and H. G. Jenkins, Phil. Mag. **2**, 621 (1926).

[11] R. T. Birge, Phys. Rev. **25**, 240 (1925); "Molecular Spectra in Gases," pp. 138–139.

[12] R. Mecke, Ann. d. Physik. **71**, 104 (1923); F. W. Loomis, "Molecular Spectra in Gases." Chap. VI.

[13] R. C. Johnson, Proc. Roy. Soc. **105A**, 683 (1924); V. M. Ellsworth and J. J. Hopfield, Phys. Rev. **29**, 79 (1927).

[14] R. T. Birge, "Molecular Spectra in Gases," p. 141 and footnote 87 on p. 139.

[15] E. Condon, Phys. Rev. **28**, 1182 (1926).

[16] J. Franck, Trans. Far. Soc. (1925).

(Note. These data are an average of the data for the $^2P_1$ and $^2P_2$ bands. The results apply equally well to either set since there is very little if any, difference between the two in intensity distribution.)

Formulas are given by Condon for obtaining $V(r)$ from the above constants. The resulting curves for the states involved in the NO β system are shown by the solid lines in Fig. 6. Following Condon's procedure, the curve is drawn in Fig. 5 (solid) along which the strongest bands, theoretically, should lie.

In the region of small values of n'', it is evident that there is approximate agreement, since the most intense of the bands observed lie very closely along the theoretical locus. (The failure to observe bands on the lower

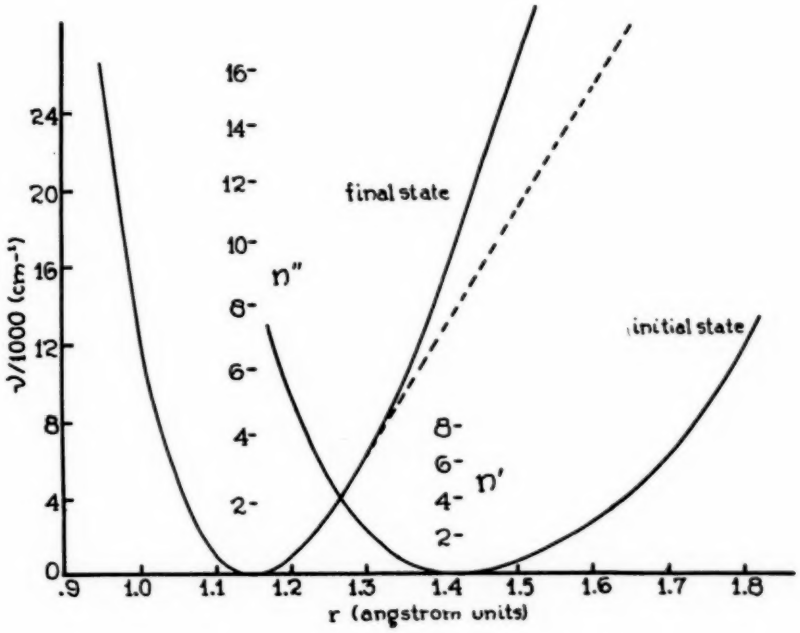

Fig. 6. Potential energy curves for the electronic states of the NO molecule involved in the β bands.

branch of the curve is due partly to the fact that the system here extends into the Schumann region.) For bands having n'' greater than about ten, however, the theoretical curve deviates widely from a curve drawn through the most intense observed bands. The writers believe this is due to inaccuracy, rather than to any fundamental defect, in the Condon theory. $V(r)$ is expressed as a power series in $(r-r_0)$. Coefficients are evaluated only as far as the fourth power. Thus, as r increases, the $V(r)$ curve becomes less and less accurate through neglect of the higher powers. It is known that the curve must actually flatten out as V approaches a value equivalent to the heat of dissociation. Possibly therefore, the true course of the curve is more like that shown by the broken line branch. This would give much better

agreement with the intensity data, as can be seen from the broken curve in Fig. 5, which corresponds to that in Fig. 6.

The absence of bands having n' greater than four may be due to the Boltzmann distribution, although the change after $n'=3$ is sufficiently abrupt to suggest that there may be some other cause not yet taken into account. In absorption, bands up to $n'=5$ have been observed.[17]

Features not explained by the theory. The most striking departure from theory was pointed out by Birge,[11] namely that certain bands appear with unexpectedly high intensities in the scheme of Fig. 5. This is true of the bands (3, 7), (3, 8), (3, 9), (2, 8), (2, 9), (2, 10), (3, 11), (4, 10), (4, 11), and (4, 13). The significant fact is that these bands not only lie well removed from the theoretical curve but that they are separated from it by bands of lower intensity. It appears that a single progression, such as that for which $n'=3$, may have three or four separate maxima of intensity, whereas the Condon theory can predict no more than two. Loomis [18] has very recently worked out the scheme corresponding to Fig. 5 for the "magnetic rotation spectrum" of the diatomic sodium molecule as observed by R. W. Wood. He finds that here too certain relatively intense bands appear distinctly separated by gaps from the course of the empirical curve passing through the region of maximum intensity. It is to be hoped that the new quantum mechanics will give a more accurate account of the vibrational distribution of intensity than is now available.

The writers are greatly indebted to Professor K. T. Compton and others of the Department of Physics at Princeton University for permission to use the densitometer; also for the interest shown and the help afforded by them during the measurements. They are also indebted to Professor E. C. Kemble for advice and suggestions.

JEFFERSON PHYSICAL LABORATORY,
HARVARD UNIVERSITY.
WASHINGTON SQUARE COLLEGE,
NEW YORK UNIVERSITY.
April 16, 1927.

[17] H. Sponer and J. J. Hopfield, Phys. Rev. **27**, 640 (1926) from plates of Leifson, Astrophys. J. **63**, 73 (1926).

[18] F. W. Loomis, Phys. Rev. **29**, 607 (1927).

A THEORY OF THE GRAVITATIONAL FIELD IN THE LIGHT OF MAXWELL'S THEORY

By C. K. Venkata Row

Abstract

In this paper, a complete physical theory of the gravitational field is formulated, which, without recourse to the hypothesis of equivalence or of non-Euclidean geometry, has yet all the advantages of Einstein's theory for describing inertial and gravitational phenomena. The theory starts from the fact that gravitational forces obey the inverse square law in common with electric and magnetic forces; from this it is inferred that Newton's law of gravitation must be developed into a theory of field-action on much the same lines as Coulomb's law has followed; as a first step towards this, the two principles, namely, Hamilton's principle and the special principle of relativity, on which Maxwell's theory is founded, are shown to be sufficient to determine uniquely Lorentz's law of electromagnetic force. Analogous considerations on the same two principles are also found to determine uniquely the law of motion in a gravitational field represented by an invariant potential. The law is found to be a comprehensive law of motion under both inertia and gravitation—the two effects being recognised as only different aspects of the same phenomenon; all the principles of mechanics including the theorems of energy and momentum are actually deduced from the laws of gravitation and the equality of inertial and gravitational mass is proved. Newton's inertial frame is also shown to mark a fundamental physical medium in which matter is embedded—a conclusion confirmed by the experimental detection of this frame by Foucault's pendulum and by the gyro-compass.

Applications of the theory.—The theory also shows that this medium is modified near large masses such as the sun and this modification is found to be responsible for the observed values of the spectral shift and of the deflection of light. The fine-structure of spectral lines and the so-called variation of electronic mass with velocity also follow from the theory. The question of Mercury's perihelion is also discussed and it is considered that the problem of perturbations must be treated as a whole in the light of the present law, and a re-examination on the observational side also must be entered into, before the Mercury problem can be dealt with with certainty.

1. Scope and Method of Investigation

THE object of this paper is to formulate a complete physical theory of the gravitational field, which without introducing the hypothesis of equivalence or of non-Euclidean geometry and other complications of the general theory, shall yet have all the advantages of that theory in explaining inertial and gravitational phenomena, particularly the equality of inertial and gravitational masses.

The theory starts from the fundamental fact that the gravitational forces obey the inverse-square law in common with electric and magnetic forces—a fact which cannot be regarded as an accidental coincidence and which therefore strongly suggests that Newton's law of gravitation must be developed into a theory of field-action on much the same lines as Coulomb's law has followed in its development into the electromagnetic theory; and it

is well known that such a development, in the case of Maxwell's theory, is based on two principles: Hamilton's principle and the special principle of relativity—all the laws being obtained from a single invariant function by the well known process of the variation of its parameters namely, of the field-quantities and of the coordinates of the singularities.[1] Hence it is clear that our gravitational theory also must be developed on the same two principles.

Before we seek the aid of Hamilton's principle, we must first of all recognise how the action of the field is represented by that principle, particularly noticing an important aspect of it which is necessary for developing our theory. For this purpose, consider the action of two electrons, separated by a finite distance, on each other. In studying this, the old idea of action-at-a-distance has to be replaced by that of an intervening medium to transmit the action. When this is done, the action of one electron on the other is resolvable into two parts: (a) the action of one electron in exciting the field around, (b) the action of the field so excited on the other electron. The specification of the part (a) constitutes the field-laws and that of part (b) constitutes the law of motion of the singularities. Hamilton's principle possesess the important property, namely, that *when the part (a) i.e. the field-laws are given, that principle is sufficient to determine uniquely the part (b) i.e. the law of motion of the singularities.* Let us illustrate this point from Maxwell's theory. Suppose the field-law to be given by the fundamental equation of Maxwell, viz.,

$$\frac{\partial F^{\mu\nu}}{\partial x_\nu} - \sigma_0 \frac{dx_\mu}{ds} = 0, \qquad \left(F_{\mu\nu} \equiv \frac{\partial k_\mu}{\partial x_\nu} - \frac{\partial k_\nu}{\partial x_\mu} \right) \tag{1}$$

then it has been shown[2] that, in order to obtain this equation by the variation of the potentials k_μ alone, the Hamiltonian invariant function must be of the form

$$\frac{1}{4} F^{\mu\nu} F_{\mu\nu} + k_\mu \sigma_0 \frac{dx_\mu}{ds} \tag{2}$$

the first and second terms on the left of Eq. (1) necessitating respectively the first and second terms of (2). A little consideration shows that, to obtain the term $\sigma_0 dx_\mu/ds$ by the variation of k_μ alone, it is necessary to introduce in the action-function the contracted product of k_μ and $\sigma_0 dx_\mu/ds$, namely, $k_\mu \sigma_0 dx_\mu/ds$; this is how the second term in (2) is formed. Thus we find that Hamilton's invariant function is completely determined as soon as the field-laws are given, so that it only remains for us to see to what results it will lead on a variation of the parameters other than the potentials, namely, of

[1] J. Larmor. Aether and Matter, Chap. vi (Camb. Univ. Press 1900); G. H. Livens. Phil. Mag. **32**, 195 (1916); K. Schwarzchild. Gott. Nachr. (math. phys. Kl.) 1903, p. 125; H. A. Lorentz. La theorie electromagnetique, §§ 55–61; Helmholtz. Ann. Phys. Chem. **47**, 1 (1892); A. Sommerfeld. Ann. d. Phys. **46**, 139 (1892).

[2] H. Weyl. Space-Time-Matter (fourth edition), translated by Brose, pp. 210, 211, (Methuen).

the coordinates of the singularities. This process of variation,[3] as is well known, leads to Lorentz's law of electromagnetic force, so that the above-mentioned part (b) is uniquely determined.

Hence the question arises: can we not determine the law of motion of a material particle in the gravitational field in an analogous manner? To answer this, we must first of all settle what the laws of the field are; and in this connection, we are struck by the fact that Eq. (1) when expressed in terms of the potentials k_μ alone, is exactly of the form of Poisson's equation in the Newtonian theory; hence we see that the electromagnetic and gravitational fields are described by a four-potential k_μ and a single potential ϕ respectively, *both* satisfying differential equations of Poisson's type. These facts strongly suggest that we should adopt for our field-law the following equation:

$$\frac{1}{c^2}\frac{\partial^2\phi}{\partial l^2}-\nabla^2\phi=4\pi\gamma\rho_0 \tag{3}$$

where ϕ is an invariant potential, γ the gravitation-constant, and ρ_0 the proper-density of matter. With this field-law, Hamilton's principle must, as in the electromagnetic case, make it possible to determine uniquely the law of motion of a material particle in the gravitational field. We proceed to consider this question in the next section.

2. Mathematical Theory of the Invariant Potential

Since we have assumed Eq. (3) to be the field-law, we have first to discover the Hamiltonian action-function which, on a variation of ϕ alone, will lead γ to Eq. (3); and a little consideration shows that, to obtain the term $4\pi\gamma\rho_0$ in Eq. (3) by the variation of ϕ alone, the action-function must contain a term of the form $4\pi\gamma\rho_0\phi$; similarly the term on the left of (3) could only be obtained from one of the form $\frac{1}{2}\phi^\alpha\phi_\alpha$ where ϕ_α denotes $\partial\phi/\partial x_\alpha$, for,

$$\begin{aligned}\delta\int\frac{1}{2}\phi^\alpha\phi_\alpha d\omega=\int\phi^\alpha\delta\left(\frac{\partial\phi}{\partial x_\alpha}\right)d\omega=\int\phi^\alpha\frac{\partial}{\partial x_\alpha}(\delta\phi)d\omega\\ =\int-\frac{\partial}{\partial x_\alpha}(\phi^\alpha)\delta\phi d\omega\end{aligned} \tag{4}$$

rejecting the part which is a complete differential, since it yields a surface-integral which vanishes over the boundary; the expression under the integral in (4) is exactly the term on the left of (3). Hence the complete action-function for our case becomes

$$\tfrac{1}{2}\phi^\alpha\phi_\alpha+4\pi\gamma\rho_0\phi \tag{5}$$

Now that this is determined, we must expect it, as in the electromagnetic case, to yield the law of motion for matter in a gravitational field, on a

[3] H. Weyl. Loc. cit., pp. 215, 216.

variation of the coordinates alone. To see this, let us write the principle of variation, which in view of (5) becomes for this case,

$$\delta \int \rho_0 \phi d\omega = 0$$

where $d\omega = dx\, dy\, dz\, dt$; and this again may easily be seen to become

$$\delta \iint \phi dm\, ds = 0 \tag{6}$$

where dm represents an infinitesimal element of matter: but since

$$g_{\mu\nu} \frac{dx_\mu}{ds} \cdot \frac{dx_\nu}{ds} = 1$$

the variational integral in (6) may be written as

$$\delta \int dm \int \phi A_\nu dx_\nu$$

where $A_\nu \equiv g_{\mu\nu} dx_\mu / ds$,

$$= \int dm \int \{\delta(\phi A_\nu) dx_\nu + \phi A_\nu \delta(dx_\nu)\}$$

$$= \int dm \int \{\delta(\phi A_\nu) dx_\nu - \delta x_\nu d(\phi A_\nu)\}$$

interchanging differentiation and variation and then integrating partially and rejecting the integrated part since δx_ν vanishes at the boundary,

$$= \int dm \int \left\{ \frac{\partial}{\partial x_\mu}(\phi A_\nu) - \frac{\partial}{\partial x_\nu}(\phi A_\mu) \right\} A^\nu \delta x_\mu ds$$

making slight alterations involving the introduction and change of dummy-suffixes. Hence we obtain from (6)

$$\{(\phi A_\nu)_\mu - (\phi A_\mu)_\nu\} A^\nu = 0$$

or
$$(\phi_\mu A_\nu - \phi_\nu A_\mu) A^\nu + \phi(A_{\nu\mu} - A_{\mu\nu}) A^\nu = 0$$

or
$$\phi_\mu - \phi_\nu A^\nu A_\mu - \phi A^\nu A_{\mu\nu} = 0$$

since $A_\nu A^\nu = 1$ and $A^\nu A_{\nu\mu} = 0$; or writing this equation fully:

$$-g^{\mu\alpha} \frac{\partial \phi}{\partial x_\alpha} + \frac{d\phi}{ds} \cdot \frac{dx_\mu}{ds} + \phi \frac{d^2 x_\mu}{ds^2} = 0 \tag{7}$$

This can also be expressed in the form:

$$\partial S^{\mu\nu} / \partial x_\nu = 0 \tag{8}$$

where

$$S^{\mu\nu} \equiv -\frac{1}{4\pi\gamma}(\phi^{\mu}\phi^{\nu} - \tfrac{1}{2}g^{\mu\nu}\phi^{\alpha}\phi_{\alpha}) + \phi\rho_0 \frac{dx_\mu}{ds} \cdot \frac{dx_\nu}{ds} \tag{9}$$

To verify (8) we write

$$\frac{\partial S^{\mu\nu}}{\partial x_\nu} = -\frac{1}{4\pi\gamma}(\phi^{\mu}\phi^{\nu} - \tfrac{1}{2}g^{\mu\nu}\phi^{\alpha}\phi_{\alpha})_{,\nu} + \left(\phi\rho_0 \frac{dx_\mu}{ds} \cdot \frac{dx_\nu}{ds}\right)_{,\nu}$$

$$= -\frac{1}{4\pi\gamma}(\phi^{,\nu}_{,\nu}\phi^{\mu} + \phi^{\nu}\phi_{,\nu}{}^{\mu} - g^{\mu\nu}\phi^{\alpha}\phi_{\alpha,\nu}) + \left(\phi\rho_0 \frac{dx_\mu}{ds} \cdot \frac{dx_\nu}{ds}\right)_{,\nu}$$

$$= -\frac{1}{4\pi\gamma}\{\phi^{,\nu}_{,\nu}\phi^{\mu} + \phi^{\nu}(\phi_{,\nu}{}^{\mu} - \phi_{,\nu}{}^{\mu})\} + \phi_{,\nu}\rho_0 \frac{dx_\mu}{ds} \cdot \frac{dx_\nu}{ds} + \phi\left(\rho_0 \frac{dx_\mu}{ds} \cdot \frac{dx_\nu}{ds}\right)_{,\nu}$$

interchanging the dummy-suffixes α and ν,

$$= -\rho_0\phi^{\mu} + \phi_{,\nu}\rho_0 \frac{dx_\mu}{ds} \cdot \frac{dx_\nu}{ds} + \phi\left(\frac{dx_\mu}{ds}\right)_{,\nu} \rho_0 \frac{dx_\nu}{ds} + \phi \frac{dx_\mu}{ds} \cdot \left(\rho_0 \frac{dx_\nu}{ds}\right)_{,\nu}$$

since $\phi_{,\nu}{}^{,\nu} = 4\pi\gamma\rho_0$ by Eq. (3) and $\phi_{,\nu}{}^{,\mu}$ is identically equal to $\phi_{,\nu}{}^{,\mu}$,

$$= -\rho_0\phi^{\mu} + \rho_0 \frac{d\phi}{ds} \cdot \frac{dx_\mu}{ds} + \rho_0\phi \frac{d^2x_\mu}{ds^2}$$

since $(\rho_0 dx_\nu/ds)_{,\nu} = 0$ by the law of conservation of matter, which is the required result.

3. Identification of the Theory of the Last Section with the Theory of Newton

To interpret Eq. (7), we have first to determine the value of ϕ from (3); but since this equation is a differential one and as such expresses only how the values of ϕ are connected from point to point, it is necessary to supplement them by boundary conditions. Newton's theory, as is well known, corresponds to the condition of ϕ vanishing at the boundary; but in a strictly deductive theory like the present, we must not commit ourselves to such an assumption too soon but must instead adopt the more general condition of a constant value for ϕ at infinity and determine this constant from our actual experience. Let us anticipate this constant to be $-c^2$ subject to future verification and we may therefore write ϕ for our case as

$$\phi = \phi_1 - c^2 \tag{10}$$

where ϕ_1 is the solution of (3) corresponding to the condition of the potential vanishing at the boundary so that ϕ_1 represents approximately the Newtonian potential.

Substituting the value of ϕ from (10) in (7) and then dropping the suffix in ϕ_1 with the understanding that henceforward ϕ shall carry the meaning hitherto attached to ϕ_1, we get

$$-g^{\mu\alpha}\frac{\partial\phi}{\partial x_\alpha}+\frac{d\phi}{ds}\cdot\frac{dx_\mu}{ds}+(\phi-c^2)\frac{d^2x_\mu}{ds^2}=0. \tag{11}$$

which, for velocities small compared with that of light, may easily be seen to simplify, in the first instance, as follows:

$$\frac{d^2x_\mu}{dt^2}=\frac{\partial\phi}{\partial x_\mu}+\frac{1}{c^2}\frac{\partial\phi}{dt}\cdot\frac{dx_\mu}{dt}+\frac{\phi}{c^2}\frac{d^2x_\mu}{dt^2}\,; \qquad (\mu=1,2,3)$$

and

$$c^2\frac{d}{ds}\left(\frac{cdt}{ds}\right)=-\frac{1}{c}\frac{\partial\phi}{\partial t}+\frac{1}{c}\frac{d\phi}{dt}+\phi\frac{d}{ds}\left(\frac{cdt}{ds}\right)$$

or

$$c^2\cdot\frac{1}{c}\frac{d}{dt}\left\{\left(1-\frac{v^2}{c^2}\right)^{-1/2}\right\}=-\frac{1}{c}\frac{\partial\phi}{\partial t}+\frac{1}{c}\frac{d\phi}{dt}+\phi\cdot\frac{1}{c}\frac{d}{dt}\left\{\left(1-\frac{v^2}{c^2}\right)^{-1/2}\right\}$$

or

$$c\frac{d}{dt}\left(1+\frac{1}{2}\frac{v^2}{c^2}\right)=-\frac{1}{c}\frac{\partial\phi}{\partial t}+\frac{1}{c}\frac{d\phi}{dt}+\frac{\phi}{c}\frac{d}{dt}\left(1+\frac{1}{2}\frac{v^2}{c^2}\right), \qquad (\mu=4)$$

where $v^2=(dx_1/dt)^2+(dx_2/dt)^2+(dx_3/dt)^2$. These equations again simplify to

$$d^2x_\mu/dt^2=\partial\phi/\partial x_\mu \qquad (\mu=1,2,3)$$

and

$$\frac{d}{dt}\left(\frac{1}{2}v^2\right)=-\frac{\partial\phi}{\partial t}+\frac{d\phi}{dt}=u_1\frac{\partial\phi}{\partial x}+v_1\frac{\partial\phi}{\partial y}+w_1\frac{\partial\phi}{\partial z} \qquad (\mu=4)$$

where u_1, v_1, w_1 are the cartesian components of the velocity, v.

These are exactly the equations of motion and of activity in the Newtonian theory; hence we recognise Eq. (7) as the fundamental law governing the motion of material particles under both inertia and gravitation; further Eq. (8) shows that the laws of conservation of energy and momentum are satisfied for the gravitational field, so that $S^{\mu\nu}$ of (9) is the corresponding stress-energy tensor.

Furthermore, the gravitational potential (10) is made up of two parts: a constant part $-c^2$ and a variable one, namely, the Newtonian potential ϕ; the substitution of the former in equations (7) and (8) leads respectively to Newton's laws of motion and to the law of conservation of material energy and momentum, and the substitution of the latter to the Newtonian law of gravitation. Hence we recognise that inertial phenomena such as the centrifugal forces are real gravitational effects and are due to the accidental circumstance of the potential being constant over a finite region, the variation of the potential being alone responsible for the main features of Newtonian gravitation.

This derivation of the laws of inertia and gravitation from a common root explains also the equality of inertial and gravitational masses. Originally we introduced ρ_0 in Eq. (3) as a measure of the attractive power of matter, but now it reappears in the stress-energy tensor (9) which measures the inertial properties; hence we see that the inertial and gravitational mass are only different aspects of the same quantity; similarly the non-appearance of the mass of the particle in its equations of motion (7)—a circumstance which corresponds to the dividing out of inertial and gravitational mass in Newton's equations of motion, explains the fact that all bodies fall with equal acceleration in a gravitational field.

Since the phenomenon of inertia has pointed to the existence of a constant potential c^2 throughout the universe, it becomes clear that the enormous amount of energy mc^2 which the special theory of relativity has considered to be locked up in the atom is nothing else than the gravitational potential energy mc^2 of the mass m in the field of potential c^2.

Thus we see that for the description of inertial and gravitational phenomena, the potential ϕ has all the advantages of the geometrical tensor $g_{\mu\nu}$; we further notice the significant fact that these potentials are each calculated from the corresponding differential laws by introducing the boundary conditions of a constant potential $-c^2$ and the Galilean constant values of $g_{\mu\nu}$ respectively, these boundary values being made responsible in each case for the inertial phenomena; although these constant values at the boundary are *admitted* by the differential laws, they are in no way *explained* by the laws themselves—a circumstance which clearly shows in each case that inertial and gravitational phenomena are distinguishable. But the choice of $g_{\mu\nu}$ for the gravitational potential demands a complete fusion of the two effects; and it was to justify this choice that the principles of general relativity and of equivalence were originally introduced, but we now find, from what $g_{\mu\nu}$ actually achieves, that the objects of these principles are defeated in the end. If really such a complete fusion as these principles claim exists, what should happen is this: we must be able to construct a differential law which, *without containing any arbitrary constant and introducing only the boundary condition of de Sitter's array of sixteen zeros*, would explain inertial and gravitational phenomena; such a boundary condition is demanded by both the principles: the general principle requires it because it is the only boundary condition which remains unaltered by any transformation of axes; the principle of equivalence requires it because it could only then assert that inertia and gravitation are indistinguishable by pointing out that the *whole* of the inertial field can be calculated just as well as the Newtonian gravitational fields are from the distribution of matter around, *through the gravitation constant*; but these conditions are clearly unfulfilled in Einstein's theory and inertia is introduced through the boundary conditions.

To get over this difficulty, Einstein introduces an *ad hoc* cosmological constant; but it may easily be shown[4] that, if the identical constant is introduced in the present law (3) also, the constant value $-c^2$ which we had to introduce

[4] Cf. A. Einstein. Berlin. Sitzungsberichte (1917), p. 143, § 1.

at the boundary is obtained from the law itself, just as the Galilean conditions at the boundary in Einstein's theory are avoided under the same circumstances; but this solution in our case has the advantage over that of Einstein, in that it leads, as a little consideration will show, to the problem of inertia and the cosmological difficulties of Newton's theory being solved at one stroke in a manner consistent with an *infinite* universe without the complications of the closed unbounded universes of Einstein and of de Sitter, which have no relation to reality.

These considerations clearly show that the "flat" and "curved" spaces of Einstein are only geometrical analogues of the constant part $-c^2$ and of the variable part ϕ_1 in the physical potential (10) and that the fusion of inertial and gravitation contemplated by $g_{\mu\nu}$ has no real physical foundation. This conclusion is further confirmed by the experimental detection of the inertial frame by the Foucault's pendulum and by the gyro-compass.

On the other hand, we recognise from the present theory that the inertial frame of Newton is not a mere system of mathematical axes introduced by the observer but marks a fundamental physical medium which carries the constant potential $-c^2$ which is only slightly disturbed by the matter embedded in the medium.

The present theory, like Einstein's, also goes further than Newton's in that it points out, as we shall presently see, that this medium is modified round the sun—a fact which we will show to be responsible for the observed values of the spectral shift and of the deflection of light.

4. Gravitational Shift of the Spectral Lines Towards the Red; the Fine Structure of the Lines of H and He^+; Kaufmann's Experiment

Consider two small regions A and B far away from matter and in the neighborhood of it respectively, where the corresponding potentials are c^2 and $(c^2-\phi)$; suppose further that each of these potentials is constant over its region. Then, for these regions, the law of motion (7) reduces to

$$c^2\frac{d^2x_\mu}{ds^2}=0\ ; \qquad (c^2-\phi)\frac{d^2x_\mu}{ds^2}=0 \tag{12}$$

respectively; similarly the corresponding energy-tensors become, in view of (9),

$$c^2\rho_0\frac{dx_\mu}{ds}\cdot\frac{dx_\nu}{ds}\ ; \qquad (c^2-\phi)\rho_0\frac{dx_\mu}{ds}\cdot\frac{dx_\nu}{ds} \tag{13}$$

These expressions make it clear that inertial phenomena have exactly the same features at all places with the only difference of the *scale* on which they manifest themselves being different at the different points; or, in other words, if m_0 and m_1 are *ceteris paribus*, the effective inertial masses of a particle at A and B respectively, then

$$m_1/m_0=(c^2-\phi)/c^2=1-\phi/c^2 \tag{14}$$

Bearing this fact in mind and remembering that it is the inertial properties alone of the electron that enter throughout in the Bohr calculation of the Rydberg constant, we see from the Bohr expression $2\pi^2e^4m/h^3$ that

$$R_1/R_0=m_1/m_0=1-\phi/c^2 \quad \text{by (14)}$$

where R_0 and R_1 are the values of the Rydberg constant at A and B respectively; hence the corresponding frequencies are given by

$$\nu_1=\nu_0(1-\phi/c^2)$$

which gives the displacement of the spectral lines observed by W. S. Adams.[5]

Further, since the Eqs. (12) are of the same form as those given by the special theory of relativity, it is clear that they lead also to the so-called variation of electronic mass with velocity and to the fine structure of the lines of hydrogen and ionized helium.

5. Gravitational Deflection of Light

According to Maxwell's theory, the electromagnetic momentum, the magnetic and electric energies per unit volume of the field are given respectively by

$$EH\sin\theta/c, \qquad H^2/2 \text{ and } E^2/2 \tag{15}$$

where θ is the angle between E and H, the direction of the momentum being perpendicular to both E and H. The transference of this energy and momentum has been represented by J. J. Thomson[6] in a remarkably clear manner, by means of Faraday tubes in motion. He has shown that a Faraday tube moving at right angles to itself with a velocity v generates in a direction perpendicular both to itself and to its direction of motion a magnetic field of value H given by

$$H=E\cdot v/c \tag{16}$$

For this particular case of motion of the tubes, the electromagnetic momentum and magnetic energy per unit volume may be easily seen from (15) and (16) to be

$$E^2v/c^2 \text{ and } E^2v^2/2c^2$$

But since the magnetic field is caused only by the motion of the tubes, its energy must be regarded as the kinetic energy of the tubes; with this understanding, the above expressions show that the mass of the tubes per unit volume is E^2/c^2. These identifications are further supported by the expression for the time-integral of the Lagrangian function for the electromagnetic field, namely,

$$\int dt\iiint \tfrac{1}{2}(E^2-H^2)\,dx\,dy\,dz \tag{17}$$

[5] W. S. Adams. Nat. Acad. of Sci. Proc. 11, 382–387 (1925); reprinted in Observatory, 48, 337 (1925).

[6] J. J. Thomson. Recent Researches in Electricity and Magnetism (Clarendon Press, Oxford 1893), Chap. I; Electricity and Matter (Yale. Univ. Press, 1911), Chaps. I and II.

which is of the familiar form in dynamics, the electric and magnetic energies being regarded as the potential and kinetic energy of the Faraday tubes; we may therefore write (17), in view of (16), also as

$$\int dt \iiint \tfrac{1}{2}\sigma(c^2-v^2)\, dx\, dy\, dz \qquad (18)$$

where σ stands for the mass of the Faraday tubes found above viz, E^2/c^2 or, in the case of radiation where electric and magnetic energies are equal to each other, L/c^2, L denoting the total energy per unit volume of radiation. The form (18) of the Lagrangian time-integral of the electromagnetic field may therefore be considered to be that governing the motion of the tubes.

Now since inertia and gravitation are co-existent according to the present theory, it is clear that the mass of the tubes must also be subject to the Newtonian force of gravitation.

There is also another important circumstance to consider. In the last section we saw that it is only the *scale* of the inertial phenomena that differs at different places, the other features being exactly the same; hence we have no reason to choose the scale at any particular place as the standard to which everything else is to be referred, since all regions are of equal gravitational importance. Therefore the only reasonable course open to measure inertial quantities such as energy is by means of instruments, which, when brought together and compared, are identical.

Consider two regions S_0 and S_1, the former being far from matter and the latter in its neighborhood, so that their respective potentials are c^2 and $c^2-\phi$; now, since the measurement of inertial quantities is based on the inertia of a given amount of matter called the mass-standard, and since, according to Eq. (14), the inertia of this mass-standard is lower at S_1 than at S_0 in the ratio $1-\phi/c^2$, it is clear that the *gauge* by which energy is measured is also smaller at S_1 than at S_0 in the same ratio. Hence if we suppose a given amount of radiation is sent from S_0 to S_1 and if L_0 and L_1 are the energies of this given amount of radiation, measured by the same means, at S_0 and S_1, respectively, then

$$L_1 = L_0/(1-\phi/c^2) = L_0(1+\phi/c^2) \text{ approx.}$$

Hence the excess of energy arriving at S_1 over that sent out from S_0 is $L\phi/c^2$ and a similar increase, namely, $L\phi/c^2$ also occurs owing to the fact that work is done on the mass L/c^2 of the radiation by the gravitational forces in its transit from S_0 to S_1; hence the total increase in energy during the process is $2L\phi/c^2$. It thus proves that, for the fulfilment of the principle of conservation of energy, we have to ascribe to the energy L before its emission in S_0 a potential energy due to gravity corresponding to a gravitational mass $2L/c^2$ or, in other words, the gravitational mass of the Faraday tubes in the radiation is double their inertial mass L/c^2. Introducing this value of the gravitational potential energy in (18), the Langrangian function for motion of the tubes in the gravitational field becomes

$$\int dt \iiint \sigma(2\phi+\tfrac{1}{2}v^2)\, dx\, dy\, dz$$

the electrical potential energy being omitted owing to its constancy over the path; since the integral is the same as for a material particle, whose gravitational mass is double its inertial and which is subject to Newtonian attraction, in ordinary dynamics, its variation, according to Lagrange's principle, may easily be seen to lead to the observed value 1.75″ of the deflection of light at the sun's limb; one half of this deflection is due to the Newtonian attraction and the other half to the modification of the medium round the sun as indicated above.

6 Problem of One Body in this Gravitational Theory.

To deal with this, we write the line-element ds in polar coordinates, in a plane as

$$ds^2 = -dr^2 - r^2 d\theta^2 + c^2 dt^2 \tag{19}$$

Then the equations of motion for the θ and t coordinates may, from (11), be easily seen to be

$$(c^2-\phi)\left\{\frac{d^2\theta}{ds^2} + \frac{2}{r}\frac{dr}{ds}\cdot\frac{d\theta}{ds}\right\} = \frac{d\phi}{ds}\cdot\frac{d\theta}{ds}$$

$$(c^2-\phi)\frac{d^2t}{ds^2} = \frac{d\phi}{ds}\cdot\frac{dt}{ds}$$

which readily yield the integrals

$$(c^2-\phi)r^2\, d\theta/ds = h_1\,; \qquad (c^2-\phi)\, dt/ds = h_2 \tag{20}$$

which, together with (19), may be shown to lead to the equation of the orbit

$$\frac{d^2u}{d\theta^2} + u = \frac{\gamma M c^2}{h_1^2} - \frac{\gamma^2 M^2}{h_1^2}u \tag{21}$$

The integrals (20) also yield

$$r^2\, d\theta/dt = h_1/h_2 \equiv h$$

so that Kepler's law of areas holds exactly; and it is also clear from Eq. (21) that the orbit is very nearly an ellipse and calculation shows that the small term $-\gamma^2 M^2 u/h_1^2$ causes a recession of Mercury's perihelion amounting to 7″ in a century. Although this result seems disappointing, it is not impossible that this difficulty might be ultimately cleared up when the problem of perturbations is considered as a whole in the light of the present law, especially as the outstanding discrepancy is not a directly observed quantity but is only a remainder term; perhaps in this connection, the calculations of the periodic perturbations by which the mass of Venus is inferred need looking into, owing to the possibility of fresh complications being introduced in them by the present law on account of the large masses of Sun and Jupiter. Further E. Grossmann[7] has shown, re-examining the observational evidence,

[7] E. Grossmann. Astron. Nachr. **219**, 41 and 195 (1921).

that Newcomb's value for the Mercurian anomaly, viz., 43″, is subject to a much greater range of uncertainty than 2″ and that it may lie between 29″ and 38″. In view of these facts and of the well-known practical difficulties attending the transit observations of Mercury, it seems necessary to re-examine this question thoroughly both from the theoretical and observational points of view. Apart from this question, the present law can be applied to the various other problems of perturbations, since it is much less complicated than Einstein's and, what is far more important, the significance to be attached to the coordinates is clear and definite.

MADRAS, INDIA.
February, 1927

THE RATES OF EVAPORATION AND THE VAPOR PRESSURES OF TUNGSTEN, MOLYBDENUM, PLATINUM, NICKEL, IRON, COPPER AND SILVER

By Howard A. Jones, Irving Langmuir and G. M. J. Mackay

Abstract

Langmuir and Mackay's data on the rates of evaporation of tungsten, molybdenum and platinum have been corrected to the tungsten temperature scale of Forsythe and Worthing. Similar data on nickel, iron, copper and silver are published for the first time on the same temperature scale. The third law of thermodynamics has been assumed in all calculations and the vapor pressures are calculated from the rates of evaporation. The experimental data check the third law as shown by the constancy of the calculated values of λ_o, the latent heat of evaporation at the absolute zero. Tables are given of the rates of evaporation and the vapor pressures up to the boiling points. The data are compared with those of other investigators. The evaporation of metals heated in an atomic hydrogen flame was very rapid and gave results which confirmed the data on evaporation in vacuum. The values of λ_o expressed in cal. gm. $(atom)^{-1}$ and the boiling points in degrees Kelvin are

	W	Mo	Pt	Ni	Fe	Cu	Ag
λ_o	191880	146000	127500	89440	89025	82060	71320
B.P.	6970	5960	4800	3650	3475	3110	2740

DATA have been published by Langmuir[1] on the rate of evaporation of tungsten as measured by the loss in weight of tungsten filaments. Langmuir and Mackay[2] have also published similar data for molybdenum and platinum. These measurements were based upon a temperature scale for tungsten filaments which has recently been revised.[3,4,5,6] For this reason we have recalculated the old measurements on the basis of the new temperature scale. We also have data taken in 1915, but not previously published, on the rate of evaporation of nickel, iron, copper and silver filaments. We now have recalculated all these data using the new temperature scale, assuming the validity of the third law of thermodynamics in all calculations.

A further discussion of the method which we have used will be given in a subsequent paper by S. Dushman and H. A. Jones in which also a comparison will be made with the results calculated by means of a semi-empirical equation developed by Dushman for the velocity of a unimolecular reaction.[7]

[1] Langmuir, Phys. Rev. **2**, 450 (1913).
[2] Langmuir and Mackay, Phys. Rev. **4**, 377 (1914).
[3] Forsythe and Worthing, Astrophys. J. **61**, 126 (1925).
[4] Zwikker, Physica. **5**, 249 (1925) and Proc. Roy. Acad. Amsterdam, **34**, No. 5.
[5] Jones, Phys. Rev. **28**, 202 (1926).
[6] Jones and Langmuir, G. E. Rev. **30**, 310 (1927).
[7] Dushman, Jour. Amer. Chem. Soc. **43**, 397 (1921).

Variation of the Rate of Evaporation with the Temperature. The relation between the vapor pressure, p, of any substance and the temperature is given by the Clausius-Clapeyron formula

$$\lambda_T = T(V - v_0)\, dp/dT \tag{1}$$

In general the volume of the metal is entirely negligible as compared with the volume of the vapor produced by its evaporation, so we may place $v_0 = 0$. If we consider λ to be the latent heat of evaporation per gram atom of metal, then since $pV = RT$, we have

$$d \ln p/dT = \lambda/RT^2 \tag{2}$$

which result can also be obtained directly from Van't Hoff's equation.

The latent heat of evaporation λ_T is a function of the temperature such that

$$\lambda_T = \lambda_0 + \int_0^T C_p dT - \int_0^T c_p dT \tag{3}$$

where λ_0 is the latent heat of evaporation per gram atom of metal at the absolute zero, C_p is the specific heat of the vapor, and c_p the specific heat of the solid metal, both measured at constant pressure.

The atomic heat of a metallic vapor, which obeys the gas law at constant pressure, is constant down to absolute zero and equal to $(5/2)R$ calories per gm atom.

Substituting in (3) we have

$$\lambda_T = \lambda_0 + (5/2)RT - \int_0^T c_p dT \tag{4}$$

Substituting (4) in (2) we obtain

$$d \ln p/dT = \lambda_0/RT^2 + (5/2)/T - (1/RT^2) \int_0^T c_p dT \tag{5}$$

and integration gives

$$\ln p = -\lambda_0/RT + (5/2) \ln T - H/R + i \tag{6}$$

where i is a constant of integration, the so-called "chemical constant," and

$$H = \int_0^T (dT/T^2) \int_0^T c_p dT$$

It has been shown by Sackur[8] and Tetrode[9] that for monatomic vapors

$$i = i_0 + (3/2) \ln M \tag{7}$$

[8] Sackur, Ann. d. Physik. **40**, 67 (1913).

[9] Tetrode, Ann. d. Physik. **38**, 434; **39**, 255 (1912).

where M is the atomic weight of the metal and i_0 is a universal constant given by

$$i_0 = \ln \left[(2\pi)^{3/2} k^{5/2} / N_0^{3/2} h^3\right] \tag{8}$$

where k is the molecular gas constant, N_0, is Avogadro's number and h is Planck's constant. Using the values for the constants adopted in the International Critical Tables, i.e., $k = 1.372 \times 10^{-16}$ erg deg.$^{-1}$; $N_0 = 6.061 \times 10^{23}$ mol.$^{-1}$; $h = 6.554 \times 10^{-27}$ erg sec. we find that

$$(2\pi)^{3/2} k^{5/2} / N_0^{3/2} h^3 = 26130 \text{ baryes} \cdot \text{deg.}^{-5/2} \text{ gm.}^{-3/2}$$

Substituting equation (7) in equation (6) and converting to common logs we have

$$\log_{10} p = -\lambda_0 / 2.303RT + (5/2)\log_{10} T - H/2.303R + 4.417 + (3/2)\log_{10} M \tag{9}$$

The pressure p being expressed in baryes.

Langmuir has shown[10] that on the basis of the kinetic theory the rate at which vapor comes into contact with the metal is given by

$$m = p(M/2\pi RT)^{1/2} \tag{10}$$

where m is the rate in gm cm^{-2} sec.$^{-1}$, and R is the molecular gas constant (83.15×10^6 erg. deg.$^{-1}$ mol.$^{-1}$) Expressing equation (10) logarithmically and expressing p in baryes, we obtain

$$\log_{10} p = \log_{10} m - (1/2)\log_{10} M + (1/2)\log_{10} T + 4.359 \tag{11}$$

If we assume that every atom of the vapor which strikes the metal condenses, then equation (10) gives the desired relation between the vapor pressure and the rate of evaporation in vacuum. If, however, a certain proportion r, of the atoms of the vapor is reflected from the surface, then the vapor pressure will be greater than that calculated from (10) in the ratio $1:(1-r)$.

Langmuir[11] has presented a great deal of evidence in support of the assumption that the reflection of molecules from the surface of the metal takes place to a negligible degree only. Hence we substitute equation (11) in equation (9) and obtain

$$\log_{10} m = 2\log_{10} M + 2\log_{10} T + 0.058 - H/4.577 - \lambda_0/4.577T \tag{12}$$

Transposing, we have

$$\lambda_0/T = 4.577(2\log_{10} M + 2\log_{10} T + 0.058 - \log_{10} m) - H \tag{13}$$

Hence, accepting the third law of thermodynamics, we are enabled by means of equation (13) to calculate the latent heat of evaporation per gm atom of solid metal at the absolute zero from a single measurement of the rate of evaporation of the metal at a known temperature T in vacuum. With the value λ_0 determined, we may then calculate the complete curve for the

[10] Langmuir, Phys. Rev. **2**, 331 (1913).

[11] Langmuir, Physical Review **2**, 332 (1913).

rate of evaporation as a function of temperature and may convert the rates of evaporation to vapor pressures by means of equation (10).

To evaluate the double integral, H, of equation (13) we proceed as follows: Debye's theory of the specific heat of solids at low temperatures gives us the curve for c_v, the specific heat of a solid at constant volume, as a function of θ/T, where θ is a characteristic temperature for the solid and is proportional to ν the vibrational frequency of the atoms of the solid. The values of θ for different elements are given by F. Simon[12] and the values of the Debye integral

$$F=\int_0^T (dT/T^2)\int_0^T c_v dT$$

are given as F/T in tables in volume 10 of the Handbuch der Physik by Julius Springer, Berlin (1926). Since we are interested, however, only in the value c_p, the atomic heat of the solid at constant pressure, we add a correction equal to the double integral of (c_p-c_v) which may be calculated from data on the linear expansion and the compressibility. It may be shown thermodynamically that

$$c_p-c_v=9\alpha^2VT/\beta \tag{14}$$

where α is the coefficient of linear expansion, V the atomic volume and β the compressibility. The quantities α and β have been measured for most substances at room temperature, but they are functions of the temperature and there is considerable uncertainty in making the calculation at low temperatures. Lindemann and Magnus[13] have proposed the empirical equation

$$c_p-c_v=aT^{3/2} \tag{15}$$

where a is calculated at ordinary temperatures from the measured values of α and β. Equation 15 is a very rough approximation, but the total value of the correction term is usually about one percent and is nearly negligible in all cases.

Hence we may write

$$H=F+(4/15)aT^{3/2} \tag{16}$$

The Debye theory leads to a limiting value of $c_v=3R$ cal. (gm. atom)$^{-1}$ degree^{-1}. It has been shown experimentally, however, that $c_p>3R$ for nearly all metals at high temperatures and is approximately a linear function of the temperature. We therefore plot all the experimental data on the specific heat c_p of the solid and obtain the equation of the straight line which best fits the data. The temperature at which c_v (Debye) plus (c_p-c_v) meets the curve through the experimental data on specific heats we call T_0. Values of the double integral, H, in equation (13) for temperatures less than T_0 are evaluated from the tables plus the double integral of the correction term (c_p-c_v).

[12] F. Simon, Zeits. f. Phys. Chem. **109**, 138 (1924).

[13] Lindemann and Magnus, Zeits. f. Electrochem. **16**, 269 (1910).

To obtain the value of H in equation (13) for temperatures greater than T_0, we add to the value determined up to T_0, i.e., $T=T_0$ in equation (16), the value of the double integral of the specific heat curve between the limits T_0 and T_2, i. e.,

$$\int_{T_0}^{T_2}(dT/T^2)\int_{0}^{T_2}c_p dT=G$$

Since all values of m, the rate of evaporation in gm cm^{-2} sec^{-1} have been measured at temperatures T_2 greater than T_0 in the cases which we are considering equation (13) may be written

$$(\lambda_0/T)=4.577(2\log_{10}M+2\log_{10}T+0.058-\log_{10}m)-F-(4/15)aT_0^{3/2}-G \quad (17)$$

Specific heats. The specific heats of solid tungsten,[14] molybdenum,[15] platinum,[16] nickel,[17] iron,[18] copper[19] and silver[20] at constant pressure have been measured by a number of investigators.

If we express the atomic heats of the solids by a general equation of the form

$$c_p=N+ZT \quad (18)$$

where T is the absolute temperature we find from the plots of the experimental data that the values of the constants for the various metals are those given in Table I.

For tungsten, the value of c_v (Debye) plus (c_p-c_v) equals 6.05 at 900°K and c_p calculated by equation (18) equals 6.05 at 900°K so that T_0 equals 900°K. For tungsten Simon gives $\theta=306$°K.

[14] Tungsten: Pirani, Verh. d. Phys. Ges. **14,** 1037 (1912); Corbino, Phys. Zeits. **13,** 375 (1912); Worthing, Phys. Rev. **12,** 199 (1918); Smith and Bigler, Phys. Rev. **19,** 268 (1922); Smith and Bockstahler, Proc. Nat. Acad. Sci. **10,** 386 (1914); Phys. Rev. **25,** 677 (1925); Gaehr, Phys. Rev. **12,** 396 (1918).

[15] Molybdenum: Stücker, Wien. Ber. **114** (2a) 657 (1905); Richards and Jackson, Zeits. f. Phys. Chem. **70,** 414 (1910); Wüst, Verh. Deutsch. Ing. Forschungsarb No. 204 (1918).

[16] Platinum: White, Phys. Rev. **12,** 438 (1918); see also Wüst, loc. cit. 15.

[17] Nickel: Wüst, loc. cit. 15; Schübel, Z. Anorg. Chem. **87,** 81 (1914); Schimpf, Z. Phys. Chem. **71,** 257 (1910); Weiss and Beck, J. Physique **7,** 299 (1908); Pionchon, Comptes rendus. **103,** 1122 (1886); **106,** 1344 (1888); Richards and Jackson: loc. cit. 15; Tilden, Proc. Roy. Soc. **71,** 220 (1903); Phil. Trans. **A201,** 37 (1903); Schlett, Ann. d. Physik. **26,** 201 (1908).

[18] Iron: Wüst, loc. cit. 15; Griffiths and Griffiths, Trans. Roy. Soc. London **214A,** 319 (1914); Schübel, loc. cit. 17; Weiss and Beck, J. Physique **7,** 299 (1908); Dürrer, 17 S. Diss. Aachen (1915).

[19] Copper: Wüst, loc. cit. 15; Griffiths and Griffiths, loc. cit. 18; Schübel, loc. cit. 18; Naccarri, Atti di Torino **23,** 107 (1887–8); Nernst and Lindemann, Berl. Sitzber 1160 (1912); J. W. Richards, Chem. New. **68,** 58, 69, 82, 93 (1893); Le Verrier, Comptes rendus. **114,** 907 (1892); Harper, Bull. Bur. Stds. **11,** 259 (1915); Magnus, Ann. d. Physik. (4) **31,** 597 (1910).

[20] Silver: Wüst, loc. cit. 15; Griffiths and Griffiths, Proc. Roy. Soc. **A88,** 549 (1913); Phil. Trans. **213A,** 119 (1913); Schübel, loc. cit. 17; Eastman, Williams and Young, J. Amer. Chem. Soc. **46,** 1178 (1924); Le Verrier, loc. cit. 19; Pionchon, Ann. Chim. Phys. (6) **11,** 33 (1887); Comptes rendus. **102,** 675, 1454 (1886); **103,** 1122 (1886); Tilden, loc. cit. 17; Nernst and Lindemann, loc. cit. 19.

The values of T_0 and θ for the other metals obtained in a similar manner are given in Table I.

TABLE I

Constants in Equation (18) for c_p.

	N	Z	T_0	θ
Tungsten	4.70	0.0015	900	306
Molybdenum	4.88	0.00248	360	360
Platinum	5.40	0.0017	220	220
Nickel	4.39	0.00411	300	375
Iron	4.39	0.00405	300	390
Copper	5.33	0.0016	300	315
Silver	5.44	0.00194	300	390

We may write equation (17) in the general form

$$\lambda_0/T = A - B\log_{10}T - C\log_{10}m - DT - E/T \tag{19}$$

Using the data from Table I, we have tabulated the values of the constants for the different metals in Table II.

TABLE II

Constants in Equation (19) for λ_0/T.

Metal	A	B	C	D	E	K	λ_0	λ_l	λ_F	T_m	B. P.
W	44.510	1.666	4.577	0.00075	80	3.227	191880	180680	11200	3655	6970
Mo	44.719	2.076	4.577	0.00124	457	3.368	146000	137620	8380	2895	5960
Pt	48.023	3.276	4.577	0.00085	340	3.214	124750	119490	5260	2045	4800
Ni	40.218	0.971	4.577	0.00206	400	3.475	89440	85100	4340	1725	3650
Fe	40.231	0.971	4.577	0.00203	240	3.486	89025	86350	2675	1808	3475
Cu	44.638	3.126	4.577	0.00080	370	3.458	82060	79310	2750	1356	3110
Ag	45.836	3.396	4.577	0.00097	382	3.343	71320	68690	2630	1234	2740

Langmuir[1] and Zwikker[4] have measured the rate of evaporation of tungsten filaments in vacuum.

Langmuir's temperature data were based upon the candle power relation previously given by him, i.e.,

$$T = \frac{11230}{7.029 - \log_{10}C'} \tag{20}$$

We find that these data come into agreement with Zwikker's more recent data when the Langmuir temperatures are corrected by means of the equation which expresses the latest data on the candle power of tungsten as a function of temperature,[6] i.e.,

$$T = \frac{10957}{6.797 - \log_{10}C'} \tag{21}$$

Langmuir and Mackay[2] have measured the rate of evaporation of molybdenum and platinum filaments in vacuum. The platinum temperatures

were based upon equation (20) so that these temperatures may be corrected by means of equation (21).

They actually photometered molybdenum filaments and multiplied the observed values by the ratio of the assumed emissivities (0.514/0.529) to obtain the candle power of tungsten, the curve of which furnished the temperature. Hence their temperatures are corrected by calculating the candle power for tungsten from Langmuir's old relation, i.e., equation (20) for the temperatures given in their paper. These calculated candle powers for tungsten are then multiplied by (0.529/0 514) to obtain the candle power of molybdenum actually observed. These observed values of candle power are then substituted in the equation expressing the candle power of molybdenum as a function of temperature which we have derived from Worthing's[21] measurements. The nickel and iron data are based solely upon the unpublished measurements made by Langmuir and Mackay on the rate of evaporation of filaments in vacuum.

They determined the temperatures of nickel and iron filaments by an optical pyrometer which was calibrated against a tungsten standard in the red ($\lambda = 0.665\mu$). The nickel and iron temperatures were calculated by means of Wien's equation from the known relation between the emissivities of the two metals for $\lambda = 0.665\mu$. They assumed the emissivities to be constant for $\lambda = 0.665\mu$ and equal to 0.46, 0.36, and 0.36 for tungsten, nickel and iron[22] respectively.

Worthing and Forsythe[3] have shown that the emissivity of tungsten is not constant in the red so that the temperatures calculated have been corrected for the latest data on the emissive power of tungsten in the red ($\lambda = 0.665\mu$).

TABLE III

Values of λ_0 calculated from the data for tungsten.

		Langmuir			Zwikker		
1	2	3	4	5	6	7	8
Old temp. of fil.	Corr. temp. of fil.	$m \times 10^6$	λ_0	Method	Temp. of fil.	$m \times 10^6$	λ_0
2440°K	2518°K	0.0020	193000	Weight	2389°K	0.000115	197200
2522	2610	0.0059	191900	"	2510	0.00099	196100
2800	2913	0.39	189000	Resistance	2614	0.00525	196400
3136	3300	30.0	187700	"	2637	0.00621	198700
2738	2852	0.151	193300	"	2657	0.00969	195200
2825	2950	0.52	192400	"	2759	0.0427	194300
2825	2950	0.59	191800	Weight	2887	0.293	192000
2875	3000	1.01	191800	Resistance	2889	0.275	192300
2875	3000	1.14	191000	Weight	3017	1.28	191400
2925	3060	1.73	191900	Resistance	3108	3.47	190700
2925	3060	2.33	190200	Weight	3124	3.82	190800
2930	3066	1.84	191900	Resistance	3129	4.69	189800
2930	3066	2.45	189800	Weight	3132	4.69	190000
					3137	4.95	190300
				Average = 191,880			

[21] Worthing, Phys. Rev. **28,** 190 (1926).

[22] Burgess and Waltenburg, Bul. Bur. Stds. **11,** 591 (1915).

The copper and silver data are based upon the measurements by Langmuir and Mackay together with several measurements by Rosenhain and Ewen[23] of the loss in weight of copper and silver rods in a high vacuum electric furnace. We have used the values given by Forsythe and Worthing for the emissivity of tungsten in the red and the values [24] $E_\lambda = 0.11$ and 0.07 for copper and silver respectively (for $\lambda = 0.665\mu$) to calculate the true temperatures. Rosenhain and Ewen used a platinum, platinum-rhodium thermocouple imbedded in the copper or silver rods for temperature determinations and in this way probably attained a high order of accuracy.

The values of λ_0 calculated from the data for tungsten are given in Table III. Col. 1 gives Langmuir's original temperatures calculated by equation (20); col. 2, the corrected temperatures calculated by equation (21); col. 3, the experimental rates of evaporation in gm cm^{-2} sec^{-1}; col. 4, the values of λ_0 calculated by means of equation (19) while col. 5 gives the method used in the determination of (m).

Column 6 and column 7 give Zwikker's experimental values of temperature and the rate of evaporation respectively, while column 8 gives the values of λ_0 which we have calculated from his data by means of equation (19).

The values of λ_0 calculated from the data of Langmuir and Mackay for molybdenum are given in Table IV. Column 1 gives their original temperatures; column 2, the temperatures corrected in the manner described above; column 3, the experimental rates of evaporation in gm cm^{-2} sec^{-1} while column 4 gives the values of λ_0 calculated by means of equation (19).

TABLE IV

Values of λ_0 calculated from the data for molybdenum and platinum.

Molybdenum				Platinum			
1	2	3	4	5	6	7	8
Old temp. of fil.	Corr. temp. of fil.	$m \times 10^6$	λ_0	Old temp. of fil.	Corr. temp. of fil.	$m \times 10^6$	λ_0
1994°K	2070°K	0.00766	149,200	1682°K	1697°K	0.00617	124,400
2040	2118	0.0305	146,700	1710	1728	0.0052	125,200
2112	2200	0.124	146,500	1800	1823	0.0695	124,500
2121	2215	0.111	146,400	1890	1918	0.373	124,500
2220	2325	0.630	146,600	1912	1942	0.503	124,700
2287	2388	1.74	145,500	1982	2016	1.32	125,200
2312	2430	3.29	145,000	2000	2035	1.88	124,800
2326	2455	3.65	145,800				
2350	2480	6.49	144,300			Average	124,750
2373	2504	8.47	144,200				
		Average	146,000				

The values of λ_0 calculated from the data of Langmuir and Mackay for platinum are also given in Table IV. Column 5 gives their original temperatures; column 6, the corrected temperatures; column 7, the experimental rates of evaporation in gm cm^{-2} sec^{-1} while column 8 gives the values of λ_0 calculated by means of equation (19).

[23] Rosenhain and Ewen, Journ. Inst. of Metals **2**, 8, 149 (1912).

[24] Foote and Fairchild, Trans. Amer. Inst. of Min. & Met. Engrs., pp. 1404 (1919).

The values of λ_0 calculated from the data of Langmuir and Mackay for nickel and iron are given in Table V. Column 1 gives the true temperature of the nickel in degrees Kelvin; column 2, the experimental rates of evaporation in gm cm^{-2} sec^{-1}, while column 3 gives the values of λ_0 for nickel calculated by means of equation (19). Column 4 gives the true temperature of the iron in degrees Kelvin; column 5 the experimental rates of evaporation in gm cm^{-2} sec^{-1}, while column 6 gives the values of λ_0 for iron calculated by means of equation (19). These data for nickel and iron were obtained by the loss in weight method only.

TABLE V

Values of λ_0 calculated from the data for nickel and iron.

Nickel			Iron		
1	2	3	4	5	6
True temp. of fil.	$m \times 10^6$	λ_0	True temp. of fil.	$m \times 10^6$	λ_0
1318°K	0.03	90,400	1270°K	0.013	89,800
1409	0.604	88,000	1438	0.852	89,100
1532	3.77	89,600	1562	9.66	88,600
1544	4.38	89,700	1580	13.4	88,600
1602	14.2	89,500			
	Average	89,440		Average	89,025

The values of λ_0 calculated from the data on copper and silver are given in Table VI. Column 1 gives the author; column 2, the true temperature of the copper in degrees Kelvin; column 3, the experimental rates of evaporation in gm cm^{-2} sec^{-1}, while col. 4 gives the values of λ_0 for copper calculated by means of equation (19). Column 5 gives the author; column 6 the true temperature of the silver in degrees Kelvin; column 7, the experimental rates

TABLE VI

Values of λ_0 calculated from the data for copper and silver.

Copper				Silver			
1	2	3	4	5	6	7	8
Author	True temp. of fil.	$m \times 10^6$	λ_0	Author	True temp. of fil.	$m \times 10^6$	λ_0
L and M	1186°K	0.0292	80900	L and M	1167°K	1.54	70600
"	1298	0.426	81600	"	1198	2.11	71800
Rosenhain	1288	0.236	82350	"	1234	3.81	72300
and Ewen	1288	0.293	81600	Rosenhain	1143	0.82	70750
"	1288	0.151	83500	and Ewen	1143	0.569	71600
"	1288	0.229	82400	"	1143	0.75	70900
				"	1143	0.639	71300
		Average	82060	"	1143	1.06	70200
				"	1143	0.472	72000
				"	1143	0.476	72000
				"	1143	0.60	71500
				"	1143	0.521	71750
				"	1143	0.919	70500
						Average	71320

of evaporation in gm cm^{-2} sec^{-1}; while column 8 gives the value of λ_0 for silver calculated by means of equation (19). These data for copper and silver were obtained by the loss in weight method only.

Substituting the average value of λ_0 for the metal in equation (19) the equation expressing the rate of evaporation of the solid in gm cm^{-2} sec^{-1} in vacuum becomes in general form

$$\log_{10} m = \frac{A}{C} - \frac{\lambda_0 + E}{CT} - \frac{B}{C} \log_{10} T - \frac{DT}{C} \tag{22}$$

From equation (10), it follows that

$$\log_{10} m = \log_{10} p - K - 0.5 \log_{10} T \tag{23}$$

where K is a constant depending on the metal and the units in which p is expressed. Expressing p in baryes, the values of K for the various metals are those given in Table II.

Substituting equation (23) in equation (22) we obtain for the equation expressing the vapor pressure of a metal in baryes

$$\log_{10} p = \frac{A}{C} + K - \frac{\lambda_0 + E}{CT} - \left(\frac{B}{C} - 0.5\right) \log_{10} T - \frac{DT}{C} \tag{24}$$

Tables, VII and VIII contain the calculated values of m, the rate of evaporation in gm cm^{-2} sec^{-1} and p, the vapor pressure of these metals in baryes at 100° intervals.

Since $\lambda_0 = \lambda_l + \lambda_F$ where λ_l is the latent heat of evaporation per gm atom of the liquid and assuming that the equation which expresses the atomic heat of the solid as a function of temperature applies also to the liquid, we may write the equation expressing the rate of evaporation of the liquid in gm cm^{-2} $sec.^{-1}$ in general form

$$\log_{10} m_l = \frac{A}{C} - \frac{\lambda_l + E}{CT} - \frac{B}{C} \log_{10} T - \frac{DT}{C} - \frac{\lambda_F}{CT_m} \tag{25}$$

Similarly we may write the equation expressing the vapor pressure of the metal over the liquid in baryes in the general form

$$\log_{10} p_l = \frac{A}{C} + K - \frac{\lambda_F}{CT_m} - \frac{\lambda_l + E}{CT} - (B - 0.5) \log_{10} T - \frac{DT}{C} \tag{26}$$

The values of λ_0, λ_l, λ_F and T_m used to calculate the rates of evaporation and the vapor pressures of the liquids are given in Table II.

It was found by plotting the latent heats of fusion λ_F of metals as given by the International Critical Tables against the melting point in degrees Kelvin that the heat of fusion is roughly proportional to the melting point. We have, therefore, used this method to estimate the heats of fusion for tungsten and molybdenum. Experimental data are lacking on these metals, but we believe that the values 11200 and 8380 cal. gm $atom^{-1}$ for tungsten and molybdenum are probably within ten percent of the true values.

TABLE VII

Values of the rate of evaporation m and the vapor pressure p of tungsten, molybdenum and platinum.

T°K	Tungsten m	Tungsten p	Molybdenum m	Molybdenum p	Platinum m	Platinum p
500						
600						
700						
800					1.29×10^{-26}	5.99×10^{-22}
900					7.21×10^{-23}	3.55×10^{-18}
1000			1.37×10^{-24}	1.01×10^{-19}	6.70×10^{-20}	3.47×10^{-15}
1100			9.77×10^{-22}	7.57×10^{-17}	1.81×10^{-17}	9.80×10^{-13}
1200	3.22×10^{-27}	1.88×10^{-22}	2.44×10^{-19}	1.97×10^{-14}	2.06×10^{-15}	1.17×10^{-10}
1300	1.34×10^{-24}	8.13×10^{-20}	2.53×10^{-17}	2.13×10^{-12}	9.73×10^{-14}	5.74×10^{-9}
1400	2.50×10^{-22}	1.57×10^{-17}	1.29×10^{-15}	1.13×10^{-10}	2.92×10^{-12}	1.79×10^{-7}
1500	2.36×10^{-20}	2.86×10^{-15}	3.81×10^{-14}	3.44×10^{-9}	5.23×10^{-11}	3.31×10^{-6}
1600	1.24×10^{-18}	8.61×10^{-14}	7.60×10^{-13}	7.09×10^{-8}	6.56×10^{-10}	4.24×10^{-5}
1700	4.16×10^{-17}	2.89×10^{-12}	1.05×10^{-11}	1.01×10^{-7}	6.18×10^{-9}	4.18×10^{-4}
1800	9.46×10^{-16}	6.75×10^{-11}	1.06×10^{-10}	1.05×10^{-6}	4.42×10^{-8}	3.07×10^{-3}
1900	1.47×10^{-14}	1.18×10^{-9}	7.52×10^{-10}	7.64×10^{-6}	2.57×10^{-7}	1.83×10^{-2}
2000	1.75×10^{-13}	1.32×10^{-8}	5.34×10^{-9}	5.58×10^{-4}	1.24×10^{-6}	9.07×10^{-2}
2100	1.58×10^{-12}	1.22×10^{-7}	2.82×10^{-8}	3.01×10^{-3}		
2200	1.25×10^{-11}	9.89×10^{-7}	1.30×10^{-7}	1.43×10^{-2}	1.7×10^{-5}	1.3
2300	7.82×10^{-11}	6.32×10^{-6}	5.00×10^{-7}	5.60×10^{-2}		
2400	4.36×10^{-10}	3.52×10^{-5}	1.80×10^{-6}	2.05×10^{-1}	1.5×10^{-4}	1.2×10^{1}
2500	2.03×10^{-9}	1.71×10^{-4}	5.62×10^{-6}	6.58×10^{-1}		
2600	8.79×10^{-9}	7.57×10^{-4}	1.57×10^{-5}	1.87	8.5×10^{-4}	7.1×10^{1}
2700	3.17×10^{-8}	2.77×10^{-3}	4.18×10^{-5}	5.07		
2800	1.12×10^{-7}	9.99×10^{-3}	1.04×10^{-4}	12.8	4.0×10^{-3}	3.4×10^{2}
2900	3.45×10^{-7}	3.18×10^{-2}	2.35×10^{-4}	29.5		
3000	9.69×10^{-7}	9.09×10^{-2}	5.0×10^{-4}	64.	1.5×10^{-2}	1.3×10^{3}
3100	2.66×10^{-6}	2.51×10^{-1}				
3200	6.67×10^{-6}	8.06×10^{-1}	1.8×10^{-3}	2.4×10^{2}	4.5×10^{-2}	4.2×10^{3}
3300	1.60×10^{-5}	1.55				
3400	3.55×10^{-5}	3.49	5.6×10^{-3}	7.7×10^{2}	1.2×10^{-1}	1.1×10^{4}
3500	7.57×10^{-5}	7.55				
3600	1.55×10^{-4}	15.7	1.5×10^{-2}	2.1×10^{3}	2.8×10^{-1}	2.7×10^{4}
3655	2.28×10^{-4}	23.3				
3800	5.6×10^{-4}	58.	3.5×10^{-2}	5.1×10^{3}	5.9×10^{-1}	5.9×10^{4}
4000	1.7×10^{-3}	1.8×10^{2}	7.7×10^{-2}	1.1×10^{4}	1.2	1.2×10^{5}
4200	4.7×10^{-3}	5.1×10^{2}	1.5×10^{-1}	2.3×10^{4}	2.1	2.2×10^{5}
4400	1.1×10^{-2}	1.3×10^{3}	2.8×10^{-1}	4.3×10^{4}	3.6	3.9×10^{5}
4600	2.6×10^{-2}	2.9×10^{3}	4.7×10^{-1}	7.5×10^{4}	5.8	6.4×10^{5}
4800	5.2×10^{-2}	6.1×10^{3}	7.7×10^{-1}	1.3×10^{5}	8.9B. P.	1.0×10^{6}
5000	1.0×10^{-1}	1.2×10^{4}	1.2	2.0×10^{5}	B. P. = 4800°K	
5200	1.8×10^{-1}	2.2×10^{4}	1.8	3.0×10^{5}		
5400	3.2×10^{-1}	3.9×10^{4}	2.5	4.3×10^{5}		
5600	5.4×10^{-1}	6.8×10^{4}	3.5	6.1×10^{5}		
5800	8.6×10^{-1}	1.1×10^{5}	4.6	8.2×10^{5}		
6000	1.3	1.7×10^{5}	5.6 B. P.	1.0×10^{6}		
6200	2.0	2.6×10^{5}	B. P. = 5960°K			
6400	2.8	3.8×10^{5}				
6600	4.0	5.5×10^{5}				
6800	5.6	8.8×10^{5}				
6970	7.1 B. P.	1.0×10^{6}				
	B. P. = 6970 °K					

For example, if the value chosen for the heat of fusion of tungsten is high by ten percent, the calculated values of m_l and p_l will be correct at the melting point, but would be high by about 8 percent at the boiling point.

In view of the assumption that the atomic heat of the liquid is the same function of the temperature as that of the solid, we have calculated the

possible error if the atomic heat of the liquid remains constant up to the boiling point. For example if the atomic heat of liquid tungsten remains constant between the melting and boiling points, the values of m_l and p_l which we have calculated would be low by about 13 percent at the boiling

TABLE VIII

Values of the rate of evaporation m and vapor pressure p for nickel, iron, copper and silver.

T°K	Nickel m	Nickel p	Iron m	Iron p	Copper m	Copper p	Silver m	Silver p
500					8.89×10^{-29}	5.71×10^{-24}	5.61×10^{-24}	2.77×10^{-19}
600	2.21×10^{-25}	1.62×10^{-20}	3.30×10^{-25}	2.48×10^{-20}	7.23×10^{-23}	5.08×10^{-18}	7.55×10^{-19}	4.07×10^{-14}
700	8.41×10^{-21}	6.65×10^{-16}	1.25×10^{-20}	1.01×10^{-15}	1.16×10^{-18}	8.81×10^{-14}	3.26×10^{-15}	1.90×10^{-10}
800	2.35×10^{-17}	1.99×10^{-12}	3.17×10^{-17}	2.75×10^{-12}	1.64×10^{-15}	1.33×10^{-10}	1.64×10^{-12}	1.03×10^{-7}
900	1.08×10^{-14}	9.68×10^{-9}	1.38×10^{-14}	1.27×10^{-9}	3.64×10^{-13}	3.13×10^{-8}	2.10×10^{-10}	1.39×10^{-5}
1000	1.42×10^{-12}	1.34×10^{-7}	1.82×10^{-12}	1.76×10^{-7}	3.96×10^{-11}	3.59×10^{-6}	9.97×10^{-9}	6.95×10^{-4}
1100	7.48×10^{-11}	7.41×10^{-6}	9.35×10^{-11}	9.48×10^{-6}	1.51×10^{-9}	1.44×10^{-4}	2.29×10^{-7}	1.67×10^{-3}
1200	2.00×10^{-9}	2.07×10^{-4}	2.43×10^{-9}	2.58×10^{-4}	3.11×10^{-8}	3.10×10^{-3}	3.13×10^{-6}	2.39×10^{-2}
1300	3.19×10^{-8}	3.43×10^{-3}	3.89×10^{-8}	4.29×10^{-3}	3.94×10^{-7}	4.08×10^{-2}		
1400	3.38×10^{-7}	3.77×10^{-2}	4.04×10^{-7}	4.63×10^{-2}	3.5×10^{-6}	3.6×10^{-1}	1.6×10^{-4}	1.3×10^{1}
1500	2.55×10^{-6}	2.94×10^{-1}	3.04×10^{-6}	3.60×10^{-1}				
1600	1.46×10^{-5}	1.74	1.74×10^{-5}	2.13	1.0×10^{-4}	1.2×10^{1}	2.9×10^{-3}	2.5×10^{2}
1700	6.82×10^{-5}	8.40	8.11×10^{-5}	1.02×10^{1}				
1800	2.5×10^{-4}	3.2×10^{1}	3.08×10^{-4}	4.00×10^{1}	1.4×10^{-3}	1.8×10^{2}	2.6×10^{-2}	2.5×10^{2}
2000	2.2×10^{-3}	2.9×10^{2}	2.9×10^{-3}	3.9×10^{2}	1.1×10^{-2}	1.4×10^{3}	1.5×10^{-1}	1.5×10^{4}
2200	1.2×10^{-2}	1.7×10^{3}	1.6×10^{-2}	2.4×10^{3}	5.9×10^{-1}	7.9×10^{3}	6.0×10^{-1}	6.2×10^{4}
2400	5.0×10^{-2}	7.3×10^{3}	6.9×10^{-2}	1.0×10^{4}	2.3×10^{-1}	3.2×10^{4}	1.9	2.1×10^{5}
2600	1.6×10^{-1}	2.4×10^{4}	2.2×10^{-1}	3.5×10^{4}	7.3×10^{-2}	1.1×10^{5}	5.0	5.6×10^{5}
2800	4.0×10^{-1}	6.3×10^{4}	6.5×10^{-1}	1.1×10^{5}	1.9	2.9×10^{5}	8.8 B. P.	1.0×10^{6}
3000	9.0×10^{-1}	1.6×10^{5}	1.3	2.2×10^{5}	4.3	6.8×10^{5}	B. P. = 2740°K	
3200	1.8	3.0×10^{5}	2.6	4.6×10^{5}	6.4 B. P.	1.0×10^{6}		
3400	3.1	5.4×10^{5}	4.7	8.4×10^{5}	B. P. = 3100°K			
3600	5.1	9.0×10^{5}	7.5 B. P.	1.0×10^{6}				
3650	5.5 B. P.	1.0×10^{6}	B. P. = 3475°K					
	B. P. = 3650°K.							

point (6970°K). Hence the data for the liquid metals are probably correct at the melting points and have a probable error of 10–15 percent at the boiling points. For this reason, the calculated values are tabulated at 200° intervals and are given to two significant figures. The differences between values of m_l or p_l for adjacent temperature points are usually known more accurately than the absolute value at one point.

Table IX contains data on the vapor pressure of metals which have been published by other investigators. Column 1 gives the metal; column 2, the absolute temperature; column 3, the vapor pressure of the metal; column 4, the calculated latent heat of evaporation of the liquid; while column 5 gives the calculated latent heat of evaporation of the solid at the absolute zero. These are both expressed in cal. (gm atom)$^{-1}$. Equation 2b which assumes the third law of thermodynamics was used to calculate the values λ_L and λ_0. The references to the original papers are given in column 6.

Except for the value given by Greenwood for the boiling point of iron, the values of λ_0 in Table IX for nickel and iron are seen to be in fair agreement with those in Table V.

There is, however, a large discrepancy between the values of λ_0 calculated for copper and silver in Table IX and those given in Table VI.

However, if we plot $\log_{10}p_{obs}+(B/C-0.5)\log_{10}T+DT/C$ against $1/T$ for the data on copper and silver in Table IX, we find that straight lines having the slopes that we have already used (i.e., 17330 and 15010 for copper and silver respectively) fit the data as well as any other straight line that

could be drawn. Thus the discrepancy between these data of Table IX and those of Tables VII and VIII represents a parallel displacement of the semi-

TABLE IX

Values of the vapor pressure and latent heat of evaporation of various metals.

Metal	$T°K$	P(baryes)	λ_L	λ_0	Ref.	Metal	$T°K$	P(baryes)	λ_L	λ_0	Ref.
Nickel	2789	5.1×10^{4}	86000	90340	25	Copper	2138	2.0×10^{4}	73000	75750	34
	2777	4.8×10^{4}	86100	90440	26		2328	1.4×10^{5}	70500	73250	34
	2895	7.4×10^{4}	86700	91040	26		2348	1.4×10^{5}	71000	73750	34
	2613*	4.0×10^{4}	82700	87043	26		2643	1.0×10^{6}	68700	71450	34
Iron	2925	4.0×10^{4}	94300	96975	27	Silver	1933	1.4×10^{5}	57600	60230	35
	2723*	4.0×10^{4}	88900	91575	27		2053	3.5×10^{5}	57000	59630	35
	2723	1.0×10^{3}	71400	74075	28		2228	1.0×10^{6}	56800	59430	35
Copper	810	6.7×10^{-4}		58200	29		1933	1.4×10^{5}	57650	60280	36
	2373	1.0×10^{6}	60300	63050	30		1953	1.6×10^{5}	56800	59430	36
	2253	1.3×10^{5}	68000	70750	31		2031	2.7×10^{5}	57600	59230	36
	2453	3.4×10^{5}	68800	71550	31		2083	4.0×10^{5}	57300	59930	36
	2583	1.0×10^{6}	66700	69450	31		2213	9.9×10^{5}	56400	59030	36
	2148	2.7×10^{4}	71900	74650	32		1000	1.5×10^{-1}		60600	37
	2378	1.7×10^{5}	70600	73350	33		1453	1.9×10^{2}	63100	65730	38
	2443	2.8×10^{5}	69700	72450	33		1589	1.1×10^{3}	63200	65830	38
	2488	4.0×10^{5}	69000	71750	33		1708	5.2×10^{3}	62400	65030	38
	2518	5.4×10^{5}	68300	71050	33		2373†	1.0×10^{6}	60100	62730	38
	2573	1.0×10^{6}	66600	69350	33						

* Estimated by the authors for the pure metals as they believe the first results are in error due to a small amount of carbon being present.

† Estimated by von Wartenburg.

log plot against $1/T$. An error of the temperature obtained by optical pyrometers, such as would be caused by a wrong value for the emissivity, would produce this kind of parallel displacement.

We have recently performed several experiments in which nickel, copper and silver were caused to evaporate rapidly when heated by an atomic hydrogen flame[38] from a 60 ampere arc between tungsten electrodes. A known weight of nickel was melted in a magnesia cupel and heated rapidly to 2869°K by holding the atomic hydrogen flame on a portion of the melted surface. The temperatures were measured by an optical pyrometer with a red screen ($\lambda=0.665\mu$). After a measured interval of time, the sample was

[25] Ruff and Bormann, Zeits. f. Anorg. Chemie **88,** 386 (1914).

[26] Ruff and Bormann, Zeits. f. Anorg. Chemie **88,** 397 (1914).

[27] Greenwood, Proc. Roy. Soc. (London) **82,** 396 (1909).

[28] Mack, Osterhof and Kraner, J. Amer. Chem. Soc. **45,** 617 (1923).

[29] Fery, Ann. chim. phys. (7) **28,** 428 (1903).

[30] Greenwood, see ref. (3) also Zeits. f. Phys. Chemie **76,** 484 (1911) and Zeits. f. Electrochemie **18,** 319 (1912).

[31] Ruff and Mugdan, Zeits. f. Anorg. Chemie **117,** 157 (1921).

[32] Ruff and Bergdahl, Zeits. f. Anorg. Chemie **106,** 76 (1919).

[33] Ruff and Konschak, Zeits. f. Electrochemie **32,** 515 (1926).

[34] See Ref. 27 and 30.

[35] See Ref. 32.

[36] Piersol, Phys. Rev. **23,** 785 (1924).

[37] H. Von Wartenburg, Zeits. für. Electrochemie **19,** 482 (1913).

[38] Langmuir, Gen. Elec. Rev. **29,** 153 (1926) also Jour. Ind. Eng Chem. **19,** 667 (1927).

cooled quickly and the rate of loss in weight per unit area determined. The emissivity of liquid nickel was assumed to be $E_\lambda = 0.36$ for $\lambda = 0.665\mu$.

The rate of evaporation of nickel heated to 2869°K in hydrogen was found to be 0.0188 as great as the rate of evaporation in vacuum as given in Table VIII. This *evaporation factor* is of the same order of magnitude as has been found for the evaporation of tungsten filaments in gas filled lamps, as compared with evaporation of similar filaments in vacuum.[39] A filament 0.0254 cm diameter in nitrogen at about atmospheric pressure evaporated 0.023 as fast as in vacuum. An equation given by Fonda indicates that this evaporation factor would approach 0.0018 for wires or rods of very large diameter. The higher diffusion coefficient in hydrogen and the effect of the blast of hydrogen seem adequate to explain the fact that our evaporation factor is ten times as great.

Copper and silver were evaporated in a similar manner, and, using the values $E_\lambda = 0.11$ and 0.07 for liquid copper and silver respectively with the evaporation factor 0.0188 obtained from the experiments on nickel, we obtained rates of evaporation of these metals which agreed well with the rates calculated from the measurements obtained on the evaporation of filaments and rods. The accuracy of our temperature data is supported by the work of Rosenhain and Ewen who used thermocouples for temperature measurements.

The data from the rather crude experiments using the atomic hydrogen flame are summarized in Table X. Column 1 gives the metal; column 2, the

TABLE X

Values of the energy losses by radiation and evaporation from nickel, copper and silver surfaces.

1 Metal	2 B. P. °K.	3 Max. Temp. °K	4 W (rad.)	5 W (evap.)	6 $\frac{W \text{ (evap.)}}{W \text{ (total)}}$
Nickel	3650	2869	140	60	0.30
Copper	3110	2838	37	300	0.865
Silver	2740	2665	20	328	0.943

calculated boiling point of the metal; column 3, the maximum surface temperature which we succeeded in obtaining; column 4, the energy loss by radiation in watts per cm; column 5, the energy loss by evaporation in the same units; while column 6 gives the ratio of the energy loss by evaporation to the total energy loss.

The writers take pleasure in extending their thanks to Dr. S. Dushman for many helpful suggestions.

RESEARCH LABORATORY,
GENERAL ELECTRIC COMPANY.
April 11, 1927.

[39] G. R. Fonda, Phys. Rev. **21**, 343 (1923).

SOME CURRENT-TIME RELATIONS IN THE ALUMINUM CELL

By W. E. Meserve

Abstract

The relation between current and time in an aluminum cell with the aluminum as anode and with d.c. applied voltage has been investigated. Apparatus and methods for obtaining data are described whereby many of the difficulties which have in the past hindered observers in obtaining consistent results have been overcome. The results obtained are in agreement with the theory of Guthe as modified by Fitch. After the lapse of a certain time (t_0), which was found to be about 300 seconds, from the moment of applying the voltage, the dependence of current on voltage conforms to the relation $E/i^2 = Ct + D$. From this is deduced a linear relationship between E/i and quantity of electricity passing through the cell, $(E/i - E/i_0 = Cq/2)$. The slope, $Cq/2$, is in the nature of a resistance and assuming that it represents the resistance of the oxide layer, the thickness and resistivity (3.403×10^{12} ohm cm) of the layer are computed. The data obtained show that the slopes of these lines vary inversely with the square of the anode area, which checks with the theory. Results obtained by Günther-Schulze with tantalum are compared and are shown to check the theory. After a short time of closed circuit the opposition to the flow of current when the aluminum is the anode is shown to be due primarily to the ohmic resistance of the solid layer which increases in value with time of closed circuit.

Introduction

As A result of his work with the aluminum cell in an attempt to explain its rectifying action, Guthe[1] proposed the oxide-gasfilm theory. According to this theory a solid oxide or hydroxide film is formed on the anode which increases in thickness with the passage of current, and a thin film of gas is formed on this solid layer which further increases the resistance of the cell. The action of rectification is attributed to the ease with which free electrons which are present on the surface of the anode can penetrate the oxide and gas layer and traverse the electrolyte to the cathode, whereas the heavier cations are more or less completely held up by the film.

On the basis of this theory, Fitch,[2] while investigating the counter-electromotive force of the cell, showed that some permanent change must take place in the cell, for the current does not attain a steady minimum value but constantly drops lower and lower. His experimental results agreed very closely with a formula derived on the assumption that the thickness of the gas layer decreases with the time of open circuit. The increase in thickness of the solid layer results in an increase in the resistance of the combined layer and after a comparatively short time this is by far the predominating effect, thus explaining the slow diminution of current with time. As a result of this work it was concluded that any cell will function as a rectifier if a passage of current will cause a stable oxide film of high resistance

[1] Guthe, Phys. Rev. **15**, 327 (1902).
[2] A. L. Fitch, Phys. Rev. **9**, 15 (1917).

to be formed on the anode and if the electrolyte is such as to liberate oxygen on electrolysis. This is in accord with the results of Graetz and Pollak[3] and also with the results of Günther-Schulze.

Günther-Schulze[4] has proposed a modification of the above theory in which he ascribes the valve effect to the gas film only. Smits,[5] after discussing the assumptions made in the theories advanced, arrived at the conclusion that the explanations are not sufficient to meet all the facts; such as for instance that amalgamated aluminum shows no rectifying effect.

Various metals have been used, aluminum probably being the most common, but later investigation has shown that many other metals possess the same property to a greater or less degree, notably tantalum. Electrolytes most commonly employed are the alums, carbonates, and phosphates. In view of the importance of the problem it seemed desirable to repeat and extend the measurements, and, by more refined methods of procedure, to determine if a careful study of the cell with the aluminum as the anode will not throw some additional light on the theory of its rectifying action.

Apparatus and Method

The cell employed for making the tests consisted of two electrodes, one of aluminum and the other of platinum, immersed in a 20% solution of

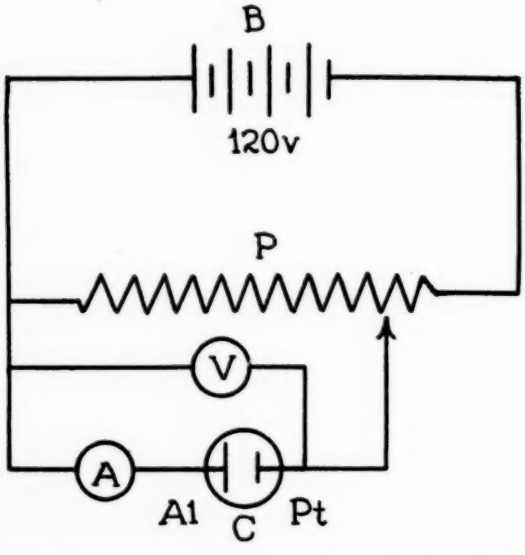

Fig. 1. Diagram of connections; *A*, Rawson multimeter; *C*, aluminum cell; *V*, Weston voltmeter; *P*, potentiometer rheostat.

sodium bicarbonate. The aluminum electrode was in the form of 99.8% pure, 0.102 cm diam. wire cut to the desired length. The cathode consisted of platinum foil of about 1 sq cm area, welded to a platinum wire which was

[3] Pollak, Elec. Zeits. **25**, 359.
[4] A. Günther-Schulze, Phys. Zeits. **22**, 146 (1921).
[5] A. Smits, Adak. Amst. 876 (1921).

sealed through the end of a glass tube. Platinum was chosen for this electrode in order to eliminate any reaction with the gas evolved at its surface. Changes in effective area due to the electrolyte's creeping up on the platinum wire were prevented by keeping the platinum-glass seal below the surface of the electrolyte at all times. For a variable source of voltage, a 3000 ohm potentiometer rheostat was connected across the terminals of a storage battery of 120 volts. A Rawson Multimeter was connected in series with the cell and a Weston voltmeter was connected in parallel with the cell and Multimeter.

Because of two factors, namely, the effect of surface tension in varying the effective area of the aluminum electrode, and second, the exposing of new areas to the action of the electrolyte by the breaking off of large bubbles of gas which form and adhere to the surface of the aluminum, considerable difficulty was at first experienced in obtaining consistent results. A coating of shellac was applied to the electrode where it entered the electrolyte but it was observed that after a time the liquid attacked the coating thereby rendering it ineffective. A black enamel such as is used for enamelling metal articles, which adheres very closely and which presents a very hard surface when dry, proved entirely satisfactory if two coats were applied. The resistance of this coating was sufficiently high so that any current which might pass through it was so small as to cause no deflection of the meter at 120 volts. To overcome the second difficulty, the bubbles were kept wiped off the aluminum by means of two camel's hair brushes so placed that they completely surrounded it. These brushes were driven by a small adjustable speed motor through a cam and vertical shaft. With this arrangement the brushes could be made to move up and down over the electrode at any desired speed and thus kept bubbles of gas from collecting on its surface.

Results

Observations were made of the relation between current i and time t of closed circuit for different areas of aluminum anode and for different values of applied potential E. The results indicate that a relation of the form

$$E/i^2 = Ct + D. \tag{1}$$

correlates the data fairly well provided t is not less than about 300 sec. In this expression the slope C depends on the area of the anode. The extent to which this relation is satisfied is illustrated in Figs. 2 and 3. In Fig. 2 is plotted the variation of E/i^2 with time for a constant potential of 60 volts and for various areas of aluminum anode. It will be noted that the points lie nearly on straight lines whose slopes vary with the anode area. In Fig. 3 the anode area is constant (0.652 sq cm) while the potential is given values of 20, 60, 100, and 120 volts. The points lie fairly well on a single straight line.

The significance of Eq. (1) is most clearly brought out as follows. Transposing

$$i = (E/C)^{1/2}(t+a)^{-1/2}$$

where $a = D/C$. Multiplying this expression by dt and integrating between two instants t_0 and t (over range of time for which (1) is valid), gives the

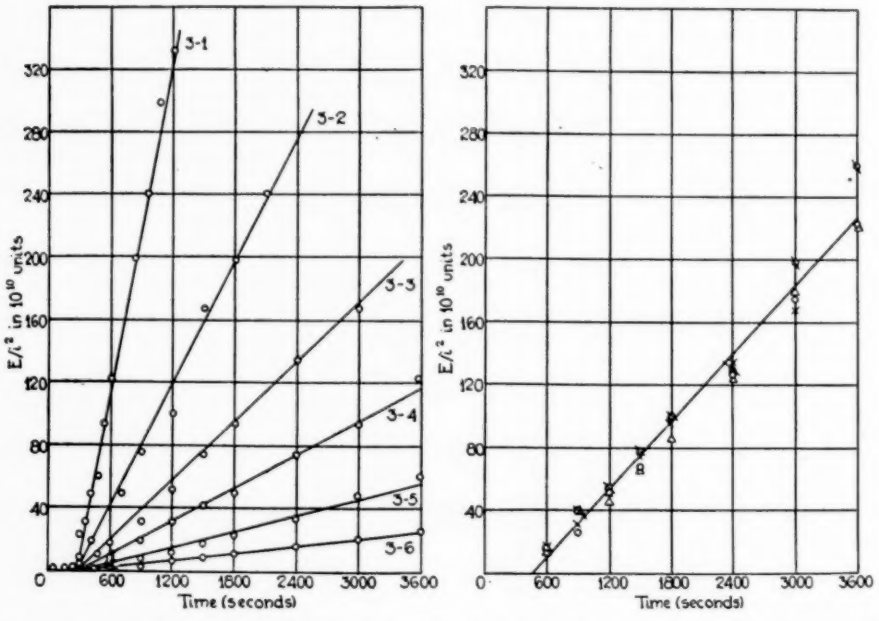

Fig. 2. E/i^2 plotted against time of closed circuit for different areas of aluminum anode. Numbers refer to those of column 2, Table I. 20% N sodium bicarbonate solution. 60 volts between electrodes. Temperature, 20°C.

Fig. 3. E/i^2 plotted against time of closed circuit to show the effect of various impressed voltages with a constant anode area. 20% N solution of sodium bicarbonate and anode area of 0.652 sq cm. Temperature, 20°C.

quantity of electricity q which has passed through the cell between these instants.

$$q = \int_{t_0}^{t} i\,dt = \frac{2E}{C}\left(\frac{1}{i} - \frac{1}{i_0}\right)$$

Rearranging, this becomes

$$E/i - E/i_0 = Cq/2 \qquad (2)$$

We may regard E/i as the resistance of the cell at any instant. Hence (2) becomes

$$R - R_0 = Cq/2$$

This indicates that the resistance of the cell, after a time of about 300 sec, increases linearly with the quantity of electricity which has passed through it.

If this increase in resistance $Cq/2$ be assumed to be due to a solid layer of uniform thickness it may be written as $\rho T/A$ where ρ is the specific resistance of the solid, T its thickness and A its area. If this layer is formed by electrolytic action its mass M may be expressed as Kq where K is the

electrochemical equivalent of the substance formed. Its mass is also ATd where d is its density. We thus find that the constant C of Eq. (1) has the value given by

$$C=2\rho K/A^2d,$$

which indicates that the slopes of the lines in Fig. 2 should vary inversely as A^2. To see how nearly this prediction is satisfied, we multiply the slopes in each case by the square of the corresponding areas. The results are presented in Table I. It will be noted that the products are reasonably constant.

TABLE I

Area aluminum (sq cm)	Line of Fig. 2	Slope $\left(\frac{\text{volts}}{\text{amp}^2\ \text{sec}}\right)$	Area^2×Slope $\left(\frac{\text{volts cm}^4}{\text{amp}^2\ \text{sec}}\right)$
.330	3–1	35.3×10^8	3.85×10^8
.491	3–2	12.8	3.08
.652	3–3	6.6	2.81
.973	3–4	3.5	3.32
1.293	3–5	1.7	2.88
1.940	3–6	0.76	2.86
			Mean 3.13×10^8

The E/i^2 intercepts of the lines in Fig. 2 also vary inversely as A^2, however the reason for their negative value is not apparent.

The complete equation for the lines of Fig. 2 becomes on using the mean values of slope and intercept as obtained from all the data,

$$E/i^2=3.02\times10^8t/A^2-11.49\times10^{10}/A^2. \tag{3}$$

Likewise Eq. (2) becomes

$$E/i-2.09\times10^8=1.51\times10^8q/A^2 \tag{4}$$

If the solid layer formed on the anode be aluminum oxide, Al_2O_3, its resistivity may be computed and its thickness for various times of closed circuit may be determined from the relation $r=\rho T/A$. The mass of oxygen liberated at the anode is given by $(.829\times10^{-4})q$ grams. If the liberated oxygen all unites with aluminum to form oxide, the mass of oxide will be given by $1.77\times10^{-4}q$ grams. Using this value for K in the expression for the slope and solving for ρ, its value is found to be 3.403×10^{12} ohm-cm. For sake of comparison it may be noted that the resistivity of glass is 9×10^{13} at 20°C and that the value for varnish is 2×10^{12}. This shows that the resistivity of the assumed oxide layer is of the same order of magnitude as that of some of the best dielectrics. The thickness of the layer for various times of closed circuit are plotted in Fig. 4.

In the computation of the specific resistance of the oxide layer it was assumed that all of the oxygen liberated at the anode combined with aluminum to form oxide. To obtain some idea as to the amount of gas which

actually does combine with aluminum, the following test was made. Two cells were made up using U tubes having side tube connections near the top. In one of these cells two platinum electrodes were placed in a sodium bicarbonate solution of the same concentration as that used in the previous work while in the other tube an aluminum and a platinum electrode were placed in the same kind of electrolyte. These two cells were connected in series electrically with the aluminum as anode in the second cell. With this arrangement the same volume of gas is formed at each anode. Connection was made to the side tube above each anode by means of rubber tubing

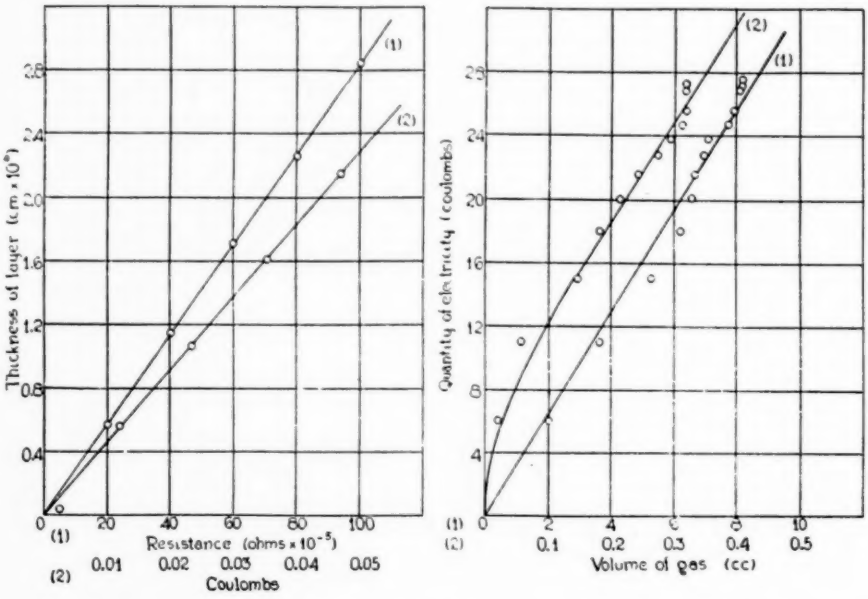

Fig. 4. Linear variation of thickness of solid layer with quantity of electricity which has passed through the cell, and with resistance of the cell.

Fig. 5. Quantity of electricity plotted against volume of gas given off at the anode to show relative magnitude for aluminum and platinum anodes. (1), platinum, diam. of measuring tube .34 cm (2), aluminum, diam of measuring tube, .0767 cm. Temperature 20°C. 20% N solution of sodium bicarbonate.

to two long horizontal glass tubes which were fastened to the tops of two meter sticks. These two tubes, when containing a drop of water served to measure the volume of gas given off at the two anodes. The results when using an aluminum anode of 32.6 sq cm on closed circuit for 900 seconds are shown in Fig. 5. The curvature in the line for aluminum is probably due to the time lag of the gas because of the small diameter of the measuring tube. These results show that about 96% of the liberated oxygen combines with aluminum.

The results obtained by Günther-Schulze[4] with tantalum were plotted in accordance with the theory given in this paper in Fig. 6. It is interesting to note that the results obtained with tantalum are in agreement with this

theory, but one outstanding difference is that the $\frac{E}{i^2}$ intercept is positive instead of negative.

The results of this investigation seem to indicate that after a rather definite time of closed circuit the opposition to the flow of current when the aluminum is the anode is due primarily to the ohmic resistance of the solid layer, which increases in value with time of closed circuit. The current

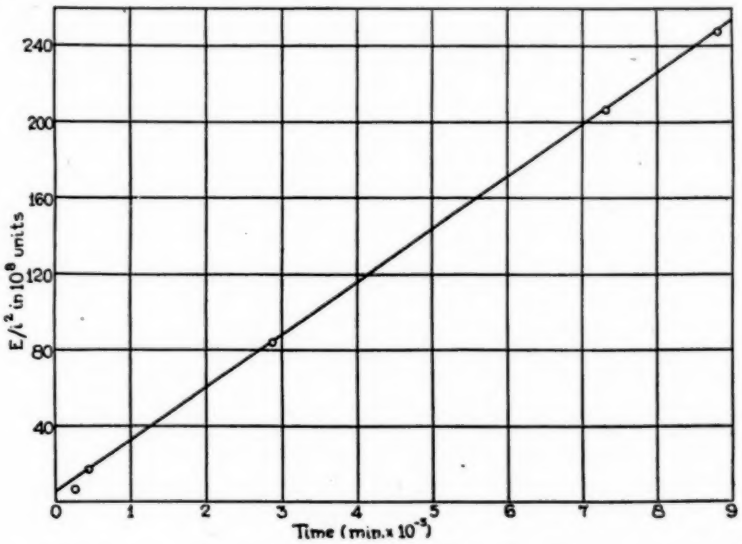

Fig. 6. E/i^2 plotted against time of closed circuit for a tantalum anode having an area of 12.5 sq cm in a 5 % N solution of potassium nitrate with impressed voltage of 100. Temperature, 20°C.

does not attain a steady minimum value but constantly drops at a diminishing rate with time of closed circuit. Tests carried over a period of several days showed this to be true. It has been shown that nearly all of the gas liberated at the anode combines with aluminum to form the solid layer. Consequently if the substance formed is aluminum oxide, the computed value of the specific resistance and the thickness of the solid layer are reasonably correct. The results are in agreement with the theory of Guthe as modified by Fitch.

In conclusion the writer wishes to express his thanks to Professor A. L. Fitch, at whose suggestion the problem was undertaken, for his kindly interest and helpful counsel during the progress of the work; and to Professor Ernest Merritt of Cornell University for aid in the arrangement of the material for publication.

PHYSICAL LABORATORY,
UNIVERSITY OF MAINE,
June, 1926.*

* Received March 14, 1927.—Ed.

BOOK REVIEWS

Eminent Chemists of our Time. BENJAMIN HARROW, PH. D. This useful and interesting volume has been extended and made more useful and interesting by the addition of fuller bibliographies and descriptions of the chief researches of each of the chemists considered, with quotations in many cases from the original papers. It is hard to get biographical information as to living and recently living chemists so this volume is convenient. There are eleven biographical sketches dealing with: Perkin and Coal-Tar Dyes; Mendelejeff and the Periodic Law; Ramsay and the Gases of the Atmosphere; Richards and Atomic Weights; van't Hoff and Physical Chemistry; Arrhenius and the Theory of Electrolytic Dissociation; Moissan and the Electric Furnace; Madame Curie and Radium; Victor Meyer and the Rise of Organic Chemistry; Remsen and the Rise of Chemistry in America; Fischer and the Chemistry of Foods. Pp. 471+xx. 2nd ed., D. Van Nostrand Company, New York, 1927. $3.00.

EDWIN E. SLOSSON

Science and Life. FREDERICK SODDY, M.A., F.R.S. These Aberdeen Addresses of 1915–1919 are well worth reprinting for they are not yet out of date. Many advances have been made in the knowledge of radio-activity since then but his criticisms of government, education and industrial waste are unfortunately still pertinent. The book bears the bitterness born of the war, when science was being employed for the destruction of life, because, in Professor Soddy's opinion, the appliances of science were controlled by men in authority incapable of appreciating its ideals, since they had been educated in a classical and anti-scientific atmosphere. He complains that the million pounds given by Carnegie twenty-five years before for making the Scottish universities real homes of research, have been mostly absorbed in routine teaching of the old-fashioned sort. Speaking to the University Christian Union he said: "We hear from well-meaning, but rather unpractical, people that the evils the world suffers are due to its neglect of God, but surely the worst of them are directly traceable to the enthronement of God in the wrong place." Pp. 229. E. P. Dutton and Company, New York, 1926. $4.00.

EDWIN E. SLOSSON

Chemistry in the World's Work. HARRISON E. HOWE. There have been many books of late designed to enlighten the layman about the progress of industrial chemistry but this has some points of superiority over its predecessors. It is, in the first place, wide in its scope and cautious in its statements. The author's position as editor of the official periodical of the American Chemical Society, "Industrial and Engineering Chemistry," gives him a point of vantage from which he can survey the entire field, and being in constant touch with the men engaged in such work he knows more than can be obtained from books. He indulges in no rhetorical writing and tells no fairy stories to entice unwilling readers, but makes the facts speak for themselves. Further he has adopted a rather novel arrangement of material. He groups his data, for the most part, according to human needs, instead of by chemical composition or by factory production. For instance, Chapter I is entitled "Solitude" and deals with railroads, electric lines and automobiles. Chapter II, "Mental Isolation," treats of paper making, optical glass, radio tubes and the transmission of pictures by telephone. "Permanency of Possessions" gives him a chance to explain what the chemist has done to protect metals against rust, timber against decay, cloth against fire, and paper against water.

Mr. Howe avoids the common fault of writers on technological topics, which is to take up too much time in describing methods and machinery. He deals with products, not processes. He has, therefore, brought out a book readable to the unscientific and useful as well to the physicist or other scientist who feels the need of catching up in this subject where the applications of science have been exceptionally numerous and rapid. Few persons are so well informed as not

to find something novel and interesting in every chapter; say in power development, new metals and medicines, food and sanitation, synthetic textiles or the arts. Pp. 244+vi. 25 figs. D. Van Nostrand Company, New York, 1926. $3.00.

EDWIN E. SLOSSON

Clinical Application of Sunlight and Artificial Radiation. EDGAR MAYER, M.D.—The general scope of the subject matter discussed in the present volume may, perhaps, be best inferred from a statement of the table of contents: Chapter I, Introduction and Historical; Chapter II, The Nature of Radiation; Chapter III, Some Fundamental Considerations on the Action of Light in Animal and Plant Life; Chapter IV, The Action of Light on Growth and Nutrition; Chapter V, The Effect of Radiant Energy Upon Bacteria and Related Biological Products; Chapter VI, Physiological Action of Light; Chapter VII, The Skin as an Organ; Chapter VIII, The Sensitization of Tissues to Light; Chapter IX, Some Experimental Studies; Chapter X, The Influence of Climate on Solar Radiation; Chapter XI, The Clinical Application of Solar and Aerotherapy; Chapter XII, The Sources of Light Used in Therapy; Chapter XIII, Clinical Studies with Artificial Light; Chapter XIV, The Dosage and Technique in the Clinical Use of Artificial Light; Chapter XV, Indications and Contraindications for Irradiation (Sunlight, Artificial Light and X-Ray Therapy); Chapter XVI, The X-Ray Treatment of Tuberculosis; Appendix, Influence of Light on Biochemical Reactions; Bibliography; Author Index; Subject Index. This index may be classified, roughly under two headings: (1) the physics of therapeutic light sources and radiations; (2) biological effects of these radiations. As for the first, it is much the less satisfactory. A mass of observations and results from a variety of sources is presented without critical comment. Frequently the results appear contradictory—as, for example, in the discussion of the effect of radiant energy upon bacteria and in consequence, it is difficult to draw definite conclusions. Ever since the appearance of Kayser's Handbuch der Spectroskopie one looks instinctively for a word of criticism, favorable or adverse, on the results obtained by others than the author.

The second part of the book, dealing with biological effects, assumes an authoritative tone. The author, having devoted many years to the study of the effect of ultra-violet radiations on tuberculosis and allied ailments, is undoubtedly in a position to draw definite conclusions relative to the efficacy of heliotherapy.

Among the most valuable features of the book is the very extensive and complete bibliography which covers all phases of the subject. The book, in its entirety, is commended as an important contribution to the subject of heliotherapy. Pp. 468, 70 figs. Williams & Wilkins, Baltimore, 1926. $10.00.

A. F. PFUND

Physics for Colleges. H. HORTON SHELDON, C. V. KENT, CARL W. MILLER, AND ROBERT F. PATON.—This book has several notable features. One is the praiseworthy attempt to weave "modern Physics" into the body of the text. The attempt is for the most part successful; only the danger has not always been avoided, of casually assuming, in earlier passages, a knowledge of terms or concepts that are explained on a much later page. Just how far the writer of an introductory text ought to go in making his language conform at all points to the latest hypotheses is a matter of opinion. The research worker, no less than the engineer, must have a thorough grounding in classical physics, that is, in the physics of statistical phenomena and of first-order effects. Yet it becomes more and more the duty of the modern textbook to present also an account of the newer points of view and their startling consequences. The blending of the new with the old in the text before us is especially evident in the section on heat and molecular physics, in which the kinetic theory is prominent, and in that on electricity and magnetism, where we find fundamental phenomena explained in terms of electrons.

A second noteworthy feature is the frequent departure from the usual order of topics. For example, after a short historical introduction, the book begins boldly with kinematics, the subject of statics not being reached until the seventh chapter. This rather unconventional order is skillfully developed. But just why throughout the book (with one or two exceptions) trigonometry is avoided, considering the quite advanced character of some of the paragraphs, is not apparent.

Two further characteristics of the book are less admirable. One is the circumstance, mentioned almost boastfully in the preface, that no attempt has been made to coordinate closely the contributions of the four authors. The unfortunate results of this cannot but make the text less satisfactory to teachers and students alike. The other characteristic is the rather hasty, almost haphazard manner in which much of the text seems to have been written. At times this betrays itself by carelessness or inaccuracy in style, and at times by misstatements. Surely such remarks as that the electron has "little or no mass," or that "this $0.4\pi I$ is equal to one ampere-turn," or that beta rays "penetrate through sheets of metal as if nothing were there," or that Edison storage cells are more efficient than lead cells, should never have crept in! Loose language never helps clear thinking. Some of the diagrams, especially those bearing on the applications of electricity, indicate hasty preparation.

The book closes with excellent chapters on sound and light, including brief accounts of such topics as the Michelson-Morley effect, relativity, and the Compton effect.

Historical references are of frequent and welcome occurrence throughout the book; yet why, in a text emphasizing modern developments, should we have to look in vain for the names of Bohr and of the Braggs? Pp. 655+vi, numerous figures. D. Van Nostrand Company, New York, 1926. $3.75.

W. G. CADY

A Treatise on Light. R. A. HOUSTOUN.—This deservedly popular book is so well known that but few words need be said about this latest edition, the fifth. It differs only slightly from the previous editions, there being merely minor changes in a few places throughout the book. Modern spectroscopic theories, x-rays, and relativity are just briefly mentioned, but the reviewer is inclined to agree with the author that little space should be devoted to these modern advances in a book of this scope. Spectral series and quantum theory should perhaps be treated more fully, however, in order to serve as an introduction to more advanced work.

The book meets satisfactorily the needs of students "who have been through a first year's physics course and who are proceeding further with the study of light." It is an admirable text for a senior college course in optics, and well merits the good reception it has had. Pp. 489+xi, 2 plates. Longmans, Green and Co., 1927. $4.00.

WILLIAM W. WATSON

History of the Sciences in Greco-Roman Antiquity. ARNOLD REYMOND. Translated by R. G. de Bray.—The book begins with a laudatory preface by León Brunschvicg. After fifteen pages descriptive of science in Egypt and Chaldea, come three chapters devoted respectively to the Hellenic period (650–300 B.C.), the Alexandrian period (300 B.C.–100 A.D.), and the Greco-Roman period. The last four chapters are devoted to the ancient principles and methods in mathematics, astronomy, mechanics. physics, chemistry and the natural sciences. Some interesting philosophical points are touched upon in the "Conclusion."

Reymond's history is written in a pleasing style and will be enjoyed by readers who desire to secure a general survey of Greek and Roman science without being very particular with regard to the extreme accuracy of details and the latest results of historical research. The book is not the outgrowth of painstaking study of original sources, nor even of a full survey of present-day literature on the subject. Not only does the author ignore some half dozen American writers who have made critical studies of particular fields of ancient science, but he overlooks also some recent European critics, for example, the late G. Eneström of Stockholm. Pp. 245+vii, 40 figs. E. P. Dutton and Company, New York, 1927. $2.50.

FLORIAN CAJORI

Ergebnisse der exakten Naturwissenschaften, volume 5. Probably no one in the world will read all of this highly diversified potpourri, but almost any physicist will be interested in some of it. The contents are: Radiation of the planets (E. Schoenberg); "Photogrammetrie" (P. Seliger); Dynamic meteorology (A. Wegener); Electric forces between electrolytic ions (N. Bjerrum); Photoelectric ionization of gases (P. Pringsheim); Disintegration of atom-nuclei (G. Kirsch); Evidence for the random distribution of disintegrations of radioactive atoms

(K. W. F. Kohlrausch); "Clean up" in discharge tubes (E. Pietsch); Compton effect (H. Kallmann & H. Mark). Most of the articles have rich bibliographies.

Pringsheim's contribution is a timely and excellent discussion of the ionization of gases by visible and ultra-violet light, with an additional section concerning Auger's recent important experiments on multiple ionization by X-rays. The article by Kallmann and Mark is a simple and lucid exposition of the data and theories of the Compton effect; I found their account of the "semi-classical" theories (those in which the velocity imparted to the electron by the electric and magnetic fields of the light-ray is evaluated from the classical electromagnetic theory) particularly interesting. They enrich the German language with the words *comptonmässig* and *comptonartig*. In both of these articles it is pleasant to observe how largely the development of the subjects is due to the work of Americans. The 54-page paper by Pietsch leaves a less favourable impression. With remarkable industry he has abstracted or used abstracts of some 170 articles in the journal literature; but he has failed to digest, unify and criticize them sufficiently, and his review seems to be a succession of abstracts strung end to end, section after section containing conflicting conclusions quoted from different authorities without even a conjecture as to the reasons for the diversity or a recommendation as to which should be preferred. This makes the paper tiresome reading, although it should be valuable to experts who wish to be reminded of prior work and are capable of judging it for themselves. Pietsch uses "clean up" as a German noun, with droll results ("*das clean up setzte aus*," etc.) Kirsch gives a well-written brief account of the properties of protons and the disintegration of atom-nuclei by alpha-particle-bombardment. Kohlrausch writes a welcome review of a subject seldom discussed; he went to the trouble of shuffling and drawing from an aggregate of 100 dice (or something of the kind) no fewer than five thousand times to provide himself with an illustration. I do not feel competent to comment on the other articles. The book abounds with misprints. Pp. 329, 103 figures. Julius Springer, Berlin, 1926. 21.00 R.M.

KARL K. DARROW

The General Theory of Thermodynamics. J. E. TREVOR. In this little book the author has endeavored "to develop the general laws of thermodynamics with logical consecutiveness and mathematical clarity. In the pursuit of cogency much care has been taken to leave no gaps in the chain of reasoning by which the results of the theory are obtained. The text deals exclusively with general principles; no applications are considered." These excerpts from the preface will indicate the purpose and scope of this valuable exposition of thermodynamic concepts. The reviewer is of the opinion that the lack of applications and of a treatment of the Third Law of Thermodynamics will detract from its value in the class-room. No student, however, of the subject can fail to be benefited by a study of this precise and logical treatment. Pp. 104+x. 34 figs. Ginn and Co., New York, 1927. $1.60.

F. H. MACDOUGALL

Physico-Chemical Metamorphosis and Some Problems in Piezochemistry. ERNST COHEN. In this book the genial professor from the University of Utrecht presents twenty-one lectures delivered at Cornell University under the Non-Resident Lectureship in Chemistry. The first ten lectures deal in a highly illuminating way with the subject of polymorphism; the remaining lectures discuss the effect of pressure on reaction velocity, on solubility, on transition-temperatures, and on diffusion. The experimental material used to illustrate the lectures is taken chiefly from the monumental researches of the author himself. Chemists who are interested in these fields will find in this book much that is interesting, instructive and suggestive. Pp. 190, 58 figs. McGraw-Hill Book Co., New York. 1926. $2.50.

F. H. MACDOUGALL

The Evolution and Development of the Quantum Theory. N. M. BLIGH. This book is intended to be something more than a popular account of the theory without being a detailed textbook. It presents in some detail the blackbody radiation and spectroscopic reasons for introducing quanta. The Balmer formula and the fine-structure formula of Sommerfeld, Planck's formula, Debye's specific heats, Einstein's fluctuation formula, and other standard

facts are given. The difficulties of the quantum theory are not emphasized. The spinning electron is only mentioned. The Stern-Gerlach effect is mentioned but only for silver. Relativity doublet difficulties, the helium atom, half-quantum numbers, the dispersion difficulty are not discussed. The Compton effect is mentioned but evidence for simultaneity of recoil and scattering is not presented. New statistics is not considered. The presentation is clear. Mathematics is not avoided and not over-emphasized. Pp. 112, 6 figs. Longmans Green and Company New York, 1926. $3.00.

G. BREIT